# REACTIVITY OF RHODIUM-HETEROATOM BONDS: FROM CATALYTIC BOND ACTIVATION TO NEW STRATEGIES FOR OLEFIN FUNCTIONALIZATION

by

SARA EMILY VAN ROOY

B.Sc., Dalhousie University, 2003

A THESIS SUBMITTED IN PARTIAL FULFILMENT OF
THE REQUIREMENTS FOR THE DEGREE OF

MASTER OF SCIENCE

in

THE FACULTY OF GRADUATE STUDIES

(Chemistry)

THE UNIVERSITY OF BRITISH COLUMBIA

October 2007

# Abstract

Rhodium complexes bearing multidentate nitrogen donor ligands were investigated for their ability to promote alkyne and olefin functionalization reactions. This thesis work is comprised of two projects in which rhodium-heteroatom reactivity is investigated: P-H bond activation reactions and olefin functionalizations via rhodaoxetane intermediates.

[Tp*Rh($PPh_3$)$_2$] [Tp* = hydrotris(3,5-dimethylpyrazolyl)borate] and [Tp*Rh(cod)]$_2$ (cod = cyclooctadiene) were evaluated for their activity in alkyne hydrophosphinylation in comparison to known catalysts for this reaction. [Tp*Rh($PPh_3$)$_2$] and [Tp*Rh(cod)]$_2$ were both shown to effect hydrophosphinylation of 1-octyne with diphenylphosphine oxide with high regioselectivity but moderate yields in comparison with Wilkinson's catalyst [ClRh($PPh_3$)$_3$]. [Tp*Rh($PPh_3$)$_2$] was further shown to effect hydrophosphinylation of a range of aromatic and aliphatic alkynes with diphenylphosphine oxide, in each case exclusively providing the *E*-linear vinylphosphine oxide product. $^1$H and $^{31}$P NMR spectroscopy provided evidence that alkyne hydrophosphinylation in the presence of pyrazolylborate rhodium complexes follows an analogous mechanism to that proposed for this reaction catalyzed by [ClRh($PPh_3$)$_3$] or [ClRh(cod)]$_2$.

The 2-rhodaoxetane [(TPA)Rh$^{III}$($\kappa^2$-C,O-2-oxyethyl)]$^+$ $BPh_4^-$ (TPA = tris[(2-pyridal)methyl]amine) was investigated for its potential as an intermediate in proposed functionalization reactions of olefins. [(TPA)Rh$^{III}$($\kappa^2$-C,O-2-oxyethyl)]$^+$ $BPh_4^-$ was prepared by two published methods with limited success. A third method involved the use of nitrous oxide to oxygenate [($\eta^2$-ethene)($\kappa^4$-TPA)Rh$^I$]$^+$ to [(TPA)Rh$^{III}$($\kappa^2$-C,O-2-

oxyethyl)]$^{+}$. Only a trace amount of [(TPA)Rh$^{III}$($\kappa^2$-C,O-2-oxyethyl)]$^{+}$ was observed in the $^{1}$H NMR spectrum of this reaction mixture. Initial test reactions of [(TPA)Rh$^{III}$($\kappa^2$-C,O-2-oxyethyl)]$^{+}$ combined with substrates (aniline, toluenesulfonamide, phenylboronic acid, or benzaldehyde) were inconclusive since the results were obscured by the impurity of the samples.

# Table of contents

# List of tables

# List of figures

# List of schemes

# List of symbols and abbreviations

| | |
|---|---|
| Å | angstroms ($10^{-10}$ meters) |
| ° or deg | degrees |
| °C | degrees Celsius |
| δ | chemical shift |
| μL | microliter |
| ν | frequency |
| acac | acetylacetonato |
| Ar | aryl |
| Bp* | dihydrobis(3,5-dimethylpyrazolyl)borate |
| br | broad |
| Bu | butyl |
| Bz | benzyl |
| Bzbpa | *N*-benzyl-*N,N*-di(pyridylmethyl)amine |
| calcd | calculated |
| cm | centimeters |
| cod | cyclooctadiene |
| COSY | correlation spectroscopy |
| Cp | cyclopentadienyl |
| Cp* | pentamethylcyclopentadienyl |
| D, *d* | deuterium |
| 2D | two-dimensional |
| d | doublet |
| DCE | 1,2-dichloroethane |
| DCM | dichloromethane |
| dd | doublet of doublets |
| ddd | doublet of double doublets |
| ddq | doublet of double quartets |
| DFT | density functional theory |
| *E* | entgegen |
| EI | electron impact |
| Eq. | equation |
| equiv. | equivalents |
| Et | ethyl |
| g | gram |
| GC | gas chromatography |

| | |
|---|---|
| GCMS | gas chromatography-mass spectroscopy |
| h | hours, Planck's constant |
| HRMS | high resolution mass spectroscopy |
| Hz | hertz |
| *i*-Pr | isopropyl |
| IR | infrared |
| *J* | coupling constant |
| kcal | kilocalorie |
| L | liter, ligand |
| M | molar (mol $L^{-1}$) |
| m | multiplet |
| Me | methyl |
| mg | milligram |
| MHz | mega hertz |
| min | minutes |
| mL | milliliter |
| mmol | millimole |
| mol | mole |
| m/z | mass/charge |
| *n* | normal |
| nbd | norbornadienyl |
| NMR | nuclear magnetic resonance |
| Ph | phenyl |
| ppm | parts per million |
| pz | pyrazolyl |
| pz* | 3,5-dimethylpyrazolyl |
| q | quartet |
| rt | room temperature |
| s | singlet |
| *t* | tertiary |
| t | triplet |
| TfO | trifluoromethanesulfonate |
| THF | tetrahydrofuran |
| TLC | thin layer chromatography |
| Tp | hydrotris(pyrazolyl)borate |
| Tp* | hydrotris(3,5-dimethylpyrazolyl)borate |
| TPA | tris[(2-pyridyl)methyl]amine |
| UV | ultra violet |
| VT | variable temperature |
| *Z* | zusammen |

# Acknowledgements

Many people have been generous with their expertise, time, advice and encouragement. I could not have completed this project without their support, for which I am truly grateful.

First of all, I would like to thank my supervisor, Dr. Jennifer A. Love. Her ideas and her wealth of knowledge are ever-inspiring. She is a kind, patient and supportive leader to our group and has been a mentor to me throughout my graduate studies. It has been a great experience participating in the launch of her research program.

I would like to thank the members of the Love research group: Paul Bichler, Jeffery Bird, Heather Buckley, Changsheng Cao, Alex Dauth, Lauren Fraser, Bal Kang, Anthony Sabarre, Shiva Shoai, Alex Sun, Tongen Wang and Jun Yang. They have provided valuable feedback, encouragement and camaraderie, which has greatly enhanced my experience at UBC. I have really appreciated all the advice and assistance from Lauren Fraser, our group's first graduate (and a great friend). I especially want to thank Shiva Shoai for being such a great friend and being the person above all who really welcomed me to the UBC Chemistry crowd and to Vancouver in general.

Thank you to all of the UBC Chemistry department's faculty, support staff and administrative staff. In particular, the NMR staff have been an invaluable resource. Thanks as well to the UBC librarians, especially Kevin Lindstrom.

Many thanks go to my neighbors, friends, and family, who have given me so much support: Caroline, Jason and Milan Crowe (and Papi); Tabea and Paulina Dauth; Sandy and Micha Hamouz; Claire and Mila Plumb; Amanda and Larry Richer; Emily Simpson and Robyn Williams; Brian Rempel and Daria Kotovych; Shiva Shoai and Rob

Thomson; Lauren Fraser; Kim Van Rooy; and Joshua Knauer. Hundreds of hours of entertainment were provided to my daughter Maggie, enabling me to spend precious time writing this thesis.

Thanks to my long-distance family and friends who have provided lots of support and encouragement over the phone and by email. I especially want to mention my parents, Kim and Bill, my sister Naomi, and my best friend Tara.

Most importantly I want to thank my life partner, Joshua Knauer, and my daughter Maggie. I dedicate this work to you both.

# 1 Introduction

## 1.1 Metal-mediated olefin and alkyne functionalization

Simple olefins and alkynes are inexpensive and readily available as products of the petroleum industry. The development of reactions that transform simple olefins and alkynes into functionalized products is of fundamental importance to synthetic chemistry. The most straightforward approach for preparing these functionalized products involves the introduction of functional groups directly to unactivated carbon-carbon $\pi$-bonds. Metal catalysts have been used to achieve this goal in research laboratories and in industry.[1-11]

Olefins and alkynes can be converted to ketones, aldehydes, and many other products, which can be further functionalized to a broad array of useful small molecules to be used as building blocks in synthesis. Figure 1-1 shows a variety of available products from functionalization reactions of terminal olefins or alkynes.[9-12]

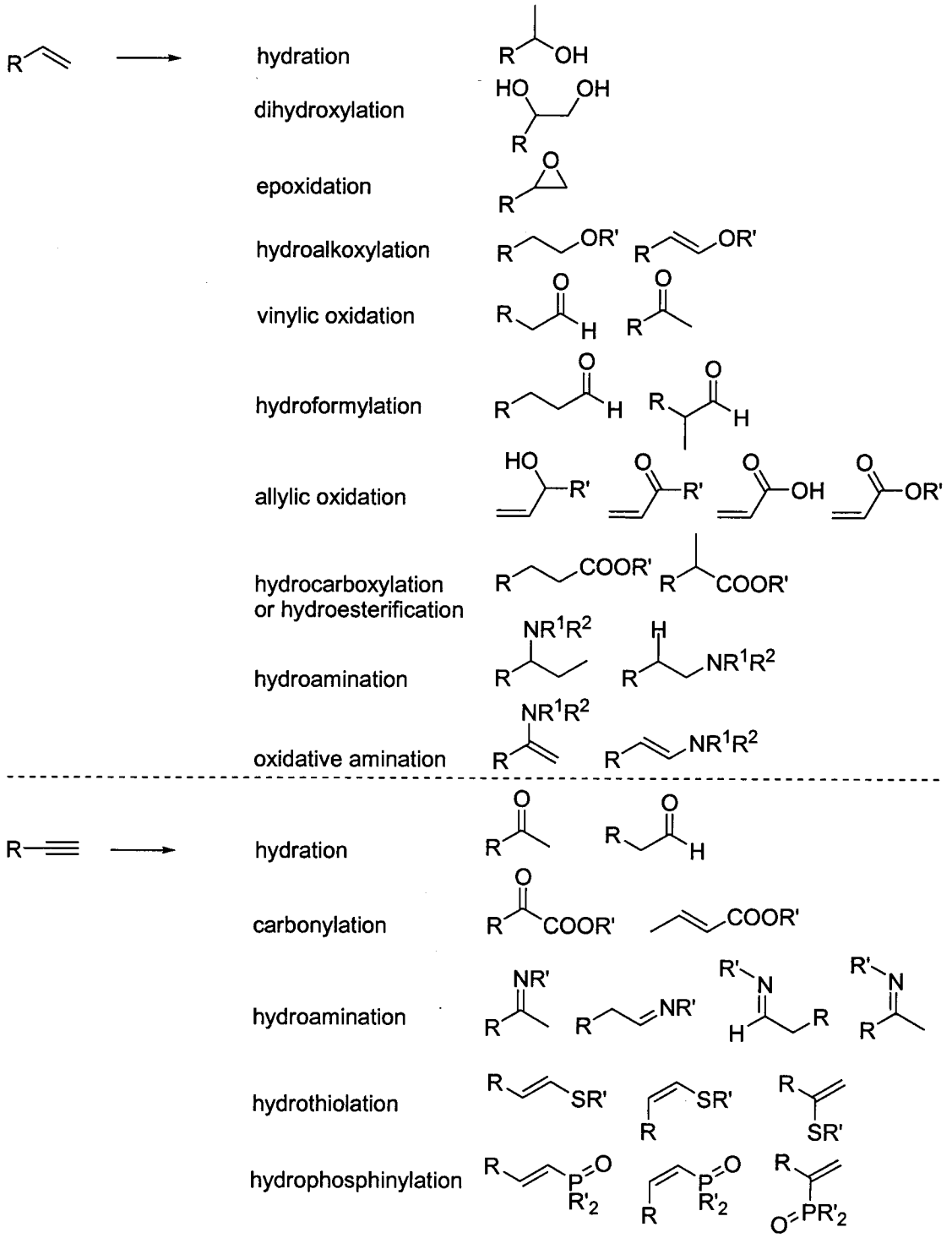


**Figure 1-1** Functionalized products derived from terminal olefins and alkynes

The study of these known processes as well as the development of new coupling reactions remains a highly active research area. The development of new, catalytic

methods for the selective functionalization of olefins and alkynes is a focus for the Love group. The approach taken in this thesis work involves studying the reactivity of Rh-P and Rh-O bonds for two classes of carbon-carbon π-bond functionalization reactions: P-H bond activation reactions and olefin functionalizations via rhodaoxetane intermediates. These reaction classes both involve rhodium complexes with multidentate nitrogen donor ligands; however, they are mechanistically distinct. The research presented in this thesis on Rh-P and Rh-O reactivity will thus be addressed in two separate chapters. This chapter provides the background information for these two subprojects.

## 1.2 Background of P-H bond activation reactions

### 1.2.1 Scorpionate ligands

The hydrotris(pyrazolyl)borate anion (Tp) and its use in coordination chemistry were first introduced by Trofimenko in 1966.[13] Since that time Tp and many of its derivatives ($Tp^R$, R = H, alkyl, aryl, substituted aryl, halide, etc.) have been utilized as ligands for numerous coordination complexes.[14] $Tp^R$, shown in Figure 1-2, is an example of a scorpionate ligand; it is a tripodal donor where two of the binding groups are firmly bound to the metal center and the third binding group is more labile, like the claws and stinger of a scorpion. The stinger can be identical to the claws (*i.e.* homoscorpionate) or different (*i.e.* heteroscorpionate). Many other scorpionate ligand derivatives are known with various substituents at the 3, 4, and 5 positions on the pyrazolyl groups.[15]

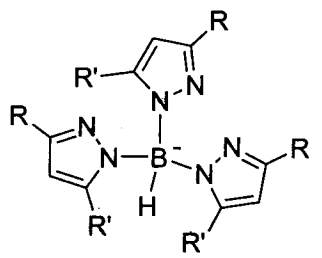


Tp : R = R' = H
Tp* : R = R' = Me
$Tp^{Me}$ : R = Me, R' = H

**Figure 1-2** General scorpionate ligand structure

## 1.2.2 Scorpionate complexes

Most $Tp^R$-metal complexes are either octahedral, trigonal bipyramidal or square planar in geometry. The octahedral and trigonal bipyramidal complexes have $Tp^R$ bound facially (i.e. $\kappa^3$) to the metal whereas in the square planar complexes, the $Tp^R$ ligand binds with only its pincers (i.e. $\kappa^2$), and the stinger is uncoordinated. Some examples of $\kappa^2$- and $\kappa^3$-$Tp^RRh^IL_n$ complexes are shown in Figure 1-3.

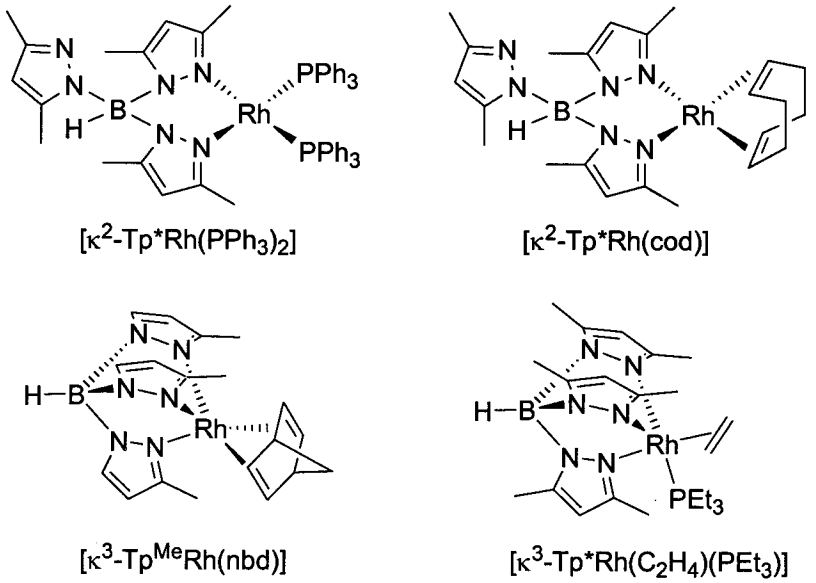


**Figure 1-3** Examples of $\kappa^2$- and $\kappa^3$-$Tp^RRh^IL_n$ complexes

The Tp ligand has been compared to the cyclopentadienyl ligand (Cp) since they are isoelectronic structures. Both Tp and Cp are monoanionic and are 6-electron donors when facially bound to a metal. However, Tp is far bulkier than Cp (cone angle of 211° versus 140°)[16] and Tp is a hard N donor, whereas Cp is soft. In solution, $Tp^R$-metal complexes usually exhibit rapid exchange between coordinated and uncoordinated pyrazolyl groups, observed in their nuclear magnetic resonance (NMR) spectra as an averaging of these $^1H$ signals.[17] This lability makes square planar $Tp^R$-metal complexes ideal as catalyst candidates since the stinger group can assist in converting the complex

from square planar to octahedral, then readily fall off again as the complex reverts back to the active catalyst. Scorpionate complexes are known for many elements, including most of those in groups 1 to 13, phosphorus, most lanthanides, and some actinides.[14] Reactivity of $Tp^R$-metal complexes includes photochemical and thermal stoichiometric transformations as well as catalytic reactions.[18]

### 1.2.3 Isomerism of scorpionate complexes

The lability of the stinger group in $Tp^R$-metal complexes has been demonstrated in the NMR spectroscopy of these complexes. Chauby *et al.* obtained crystal structures of complexes [Tp*Rh(CN-neopentyl)$_2$] (Tp* = hydrotris(3,5-dimethylpyrazolyl)borate) and [Tp'Rh(nbd)$_2$] (Tp' = HB(3-Mepz)$_3$) that show $\kappa^2$- and $\kappa^3$-binding, respectively.[17] However, in solution both of these complexes show an equivalence of their three pyrazolyl groups in their $^1$H NMR spectra, suggesting a rapid exchange between pyrazolyl groups, as shown for a general TpRhL$_n$ complex in Scheme 1-1.


**Scheme 1-1** Isomerism of a tris(pyrazolyl)borate rhodium complex

Jones and Hessel report that complexes of the type Tp*Rh(CNR)$_2$ (R = neopentyl, 2,6-xylyl, methyl) show fluxional behavior in their IR spectra as well as $^1$H and $^{13}$C NMR spectra.[19] They suggest that NMR spectroscopic evidence showing equivalence of the pyrazolyl signals is not sufficient to conclude that isomerism of $\kappa^2$ and $\kappa^3$ forms is occurring. An alternative explanation could be that the $\kappa^3$ isomer is the dominant form in solution and the observed equivalence of the pyrazolyl groups is due to rotation about the

Rh-B axis that is rapid on the NMR timescale. A comparison of the IR spectroscopy of these complexes in the solid state and in solution shows the isonitrile stretching frequencies to be identical. They also report that in the PhD dissertation of Ghosh, the IR spectra of an isomeric mixture of $\kappa^2$- and $\kappa^3$-Tp*Rh(CO)$_2$ in $CH_2Cl_2$ solution was reported to have a 20-30 $cm^{-1}$ difference in the carbonyl stretching frequencies which corresponds to a similar difference of 20-30 $cm^{-1}$ in the carbonyl stretching frequencies of solutions of $\kappa^3$-Tp*Rh(CO)$_2$ and $\kappa^2$-($H_2B(pz^*)_2$Rh(CO)$_2$.[20,21] These findings support the hypothesis that these complexes remain as the $\kappa^2$-isomer in solution but with a rapid interchange of pyrazolyl groups via isomerism to the $\kappa^3$ form.

Bucher *et al.* details the fluxional behavior of complexes of the type TpRh(LL) (LL = 2CO, cod, nbd).[22] The substituents at the 3 and 5 positions on the pyrazolyl groups affected interconversion rates between $\kappa^2$ and $\kappa^3$ forms such that the larger substituents disfavored the formation of the $\kappa^3$ isomer. Other factors that were shown to affect the rate of isomerism included the ancillary ligands on rhodium as well as solvent polarity.

Energies of activation for the isomerism of $\kappa^2$ and $\kappa^3$ forms of $Tp^RRhL_n$ complexes have been estimated based on their observed coalescence temperatures in variable-temperature $^1H$ NMR studies.[23] For [TpRh($C_2H_4$)($PPh_3$)], $\Delta G^{\ddagger}_{\kappa 2 \kappa 3}$ = 60 kJ/mol.[24] For [Tp*Rh(CO)($PMe_3$)], $\Delta G^{\ddagger}_{\kappa 2 \kappa 3}$ = 63 kJ/mol.[17]

Scorpionate rhodium complexes of the type [$Tp^RRh^ILL'$] can adopt up to four conformational isomers, as evidenced by IR and NMR spectroscopy as well as X-ray crystallography of a number complexes of this type.[25] These four isomers are shown in Figure 1-4.[26,27]

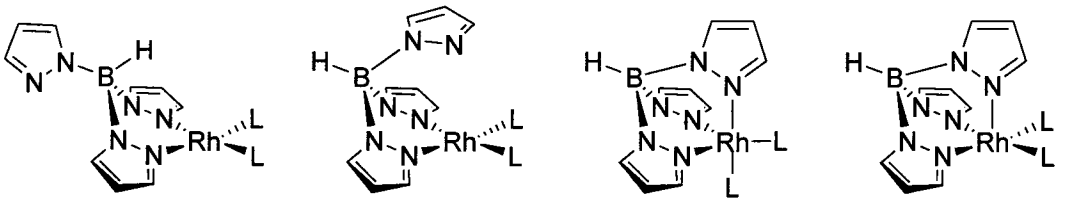


**Figure 1-4** Conformational isomers of tris(pyrazolyl)borate rhodium complexes

Connelly *et al.* reported solution and solid state structural data for $[Tp^*Rh(PPh_3)_2]$.[28] Their study included analysis of room temperature and -80 °C NMR spectroscopic experiments ($^1H$ NMR and $^{31}P\{^1H\}$ in $CD_2Cl_2$), IR spectroscopic data, and the crystal structure of this complex. The X-ray crystal structure of $[Tp^*Rh(PPh_3)_2]$ shows $\kappa^2$-coordination of Tp* to rhodium, as in conformation B. The solid state IR spectrum shows a B-H stretching frequency of 2467 $cm^{-1}$, which also indicates $\kappa^2$-binding of Tp*. At room temperature the $^1H$ and $^{31}P\{^1H\}$ NMR spectroscopic evidence suggests that $[Tp^*Rh(PPh_3)_2]$ exists in the $\kappa^2$ conformation in solution, with free rotation about the B-N bond of the uncoordinated pyrazole group. The $^1H$ NMR signals for the pyrazole rings appear in a 2:1 ratio, indicating the equivalence of two of these groups. As well, both phosphines are equivalent in the $^{31}P\{^1H\}$ NMR spectrum at this temperature. At -80 °C, three sets of pyrazole ring signals are seen in the $^1H$ NMR spectrum and the phosphines are no longer equivalent in the $^{31}P\{^1H\}$ NMR spectrum. They suggest that the low temperature inequivalence of these signals is due to restricted rotation of the unbound pyrazolyl ring.

Connelly *et al.* also studied $[TpRh(PPh_3)_2]$. They do not report a solid state structure for this complex; however, IR spectroscopy of the solid complex shows two B-H stretching frequencies that are both indicative of $\kappa^2$-coordination of Tp (2414 and 2394

$cm^{-1}$).[28] They attribute the two signals to the presence of both $\kappa^2$ conformers, A and B. $^1H$ NMR spectroscopy was not informative for this complex since even at low temperature, the spectra could not be resolved. The room temperature $^{31}P\{^1H\}$ NMR shows a broad doublet that splits into two signals as the temperature lowers to -80 °C. For this complex, they attribute the two signals to the presence of the two conformers, A and B, in approximately equal abundance. The two signals could not be attributed to a single isomer with inequivalent phosphines since the signals would then have appeared as doublets of doublets.

Fraser *et al.* compared a series of pyrazolylborate rhodium complexes for their solid state and solution structures as well as their catalytic activity in alkyne hydrothiolation reactions.[26,27] Five complexes were examined in this study: $[Tp^RRh(PPh_3)_2]$, where $Tp^R$ = $HBR'_3$ (R' = 3,5-dimethylpyrazolyl (**1**), pyrazolyl (**3**), 3-phenylpyrazolyl (**4**), or 3-phenyl-5-methylpyrazolyl (**5**)) and $[Bp^RRh(PPh_3)_2]$ ($Bp^R$ = $H_2BR'_2$, R' = 3,5-dimethylpyrazolyl) (**2**). These complexes are shown in Figure 1-5. These complexes were chosen to determine what effect varying the size and number of substituents on the pyrazolyl groups might have on their solution geometry and also what impact this may have on their catalytic activity in alkyne hydrothiolation reactions.

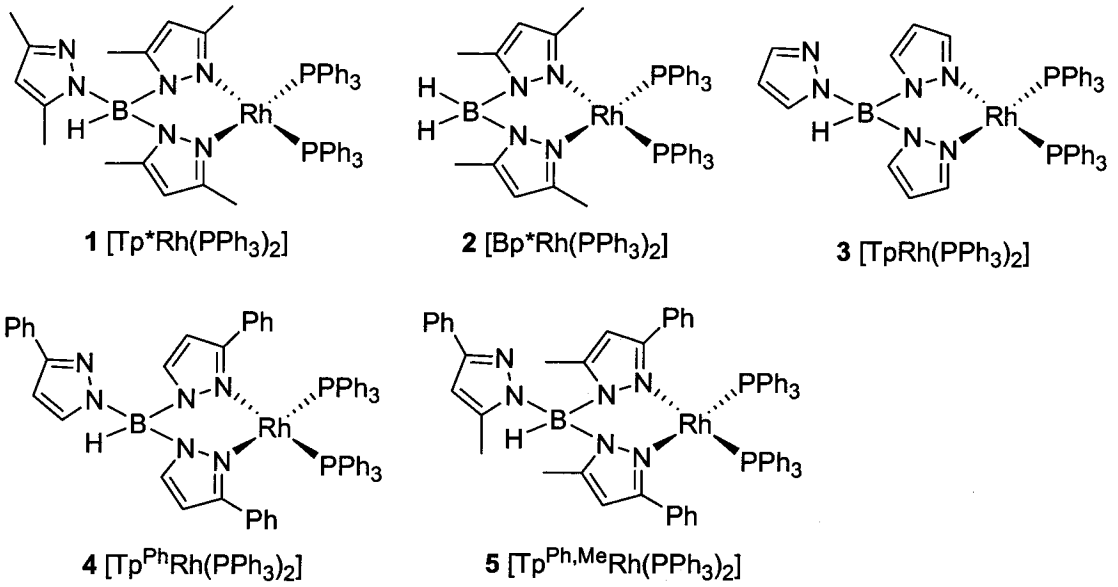


**Figure 1-5** Polypyrazolylborate rhodium complexes with varied substituents at positions 3 and 5 on the pyrazolyl rings

The X-ray crystal structures of complexes **2-5** were characterized[26,27] and compared to the reported structure of $[Tp^*Rh(PPh_3)_2]$.[28] In the solid state, all five complexes show $\kappa^2$-coordination. IR spectroscopic evidence for complexes **1** and **3-5** also corresponds to $\kappa^2$-coordination.[26-28] Specifically, complexes **1** and **5** have substituents at the 3- and 5-positions on their pyrazolyl groups and they exist in the B form with the uncoordinated pyrazolyl group pseudo parallel to the Rh square plane. Complexes **3** and **4** have no substituents at the 5-position and they exist in the A form with the uncoordinated pyrazolyl group perpendicular to the Rh square plane.

For the room temperature $^1H$ and $^{31}P\{^1H\}$ NMR spectroscopic studies on $[Tp^*Rh(PPh_3)_2]$ **1**, Fraser *et al.* obtain results that are consistent with those reported by Connelly *et al.* showing equivalence of the signals for two of the pyrazolyl rings and the phosphines.[26-28] At -80 °C, the results of these two studies differ. Fraser *et al.* do not see inequivalence of the pyrazolyl groups or phosphines. Presumably, rotation of the free

pyrazolyl ring about the B-N bond is not sufficiently slow for the NMR time-scale of their study. Between the two studies, the evidence suggests that [Tp*Rh($PPh_3$)$_2$] exists in solution with $\kappa^2$-coordination over a range of temperatures.

The $^1$H and $^{31}$P{$^1$H} NMR spectroscopic data for [Tp$^{Ph}$Rh($PPh_3$)$_2$] **4** at room temperature and -85 °C shows equivalence of the signals for the pyrazolyl rings and phosphines, indicating $\kappa^2$ coordination in solution.[26,27]

For [Tp$^{Ph,Me}$Rh($PPh_3$)$_2$] **5**, the room temperature $^1$H NMR spectroscopic signals for the pyrazolyl rings are equivalent. At -85 °C these signals become inequivalent, suggesting restricted rotation of the free pyrazolyl ring about the B-N bond. The room temperature $^{31}$P{$^1$H} NMR spectrum shows a 1:5 ratio of phosphine signals at δ 48.12 (d, $J_{Rh-P}$ = 182 Hz) and δ 43.44-39.33 (m), respectively. A variable temperature $^{31}$P{$^1$H} NMR spectroscopy experiment was performed for this complex. As the temperature decreased, the doublet signal disappeared and the multiplet signal resolved into two doublets of doublets (δ 42.60, dd, $J_{Rh-P}$ = 178 Hz, $J_{PP'}$ = 50 Hz; δ 39.42, dd, $J_{Rh-P'}$ = 172 Hz, $J_{PP'}$ = 51 Hz). The authors suggest that there are two species present at room temperature. At lower temperatures it may be that one isomer predominates the solution. Since coalescence of the phosphine signals was not observed, the authors suggest it is more likely that both are present in the low temperature solution but that the minor isomer is not seen due to broadening of the peaks from restricted rotation of the free pyrazolyl ring. As the temperature was raised, the doublet peak remained the same but the multiplet coalesced into a doublet. This observation is consistent with the free rotation of the unbound pyrazolyl group in the major isomer at higher temperatures but restricted rotation just under room temperature. The two species could be conformational isomers

A and B, or they could be regioisomers resulting from rearrangement by a 1,2-borotropic shift.

Complexes **1-5** were compared for their catalytic activity and selectivity in hydrothiolation reactions involving a range of alkynes and thiols with varying levels of steric bulk and functionality. Complexes with substituents at both the 3 and 5 positions on the pyrazolyl groups (**1** and **5**) provided the best yields and selectivities for these reactions. Complexes **1** and **5** also happened to exist in form B in the solid state and maintained $\kappa^2$-coordination in solution, showing evidence that restricted rotation of the free pyrazolyl group was occurring at lower temperatures. These results suggest that an ability to adopt $\kappa^3$-coordination in solution greatly enhances catalytic activity and selectivity for pyrazolylborate rhodium complexes in alkyne hydrothiolation reactions.

## 1.2.4 Reactivity of $Tp^RRh^IL_n$ complexes

Since $Tp^R$ ligands are hard N donors, the reactivity of $Tp^RRh^IL_n$ complexes for oxidative addition reactions is thought to be enhanced by the relative stability that $Tp^R$ affords to the $Rh^{III}$ product. This feature has made $Tp^RRhL_n$ complexes appealing candidates for their potential use in catalytic reactions. To date there are a number of stoichiometric and catalytic reactions known for these complexes and potential for much more investigation.

### 1.2.4.1 Stoichiometric reactions

The complex $[Tp^*Rh(CO)_2]$ has been shown to photochemically activate C-H bonds in aromatic and saturated hydrocarbons at room temperature.[29] Lian *et al.* later observed a reactive intermediate for this reaction in their femtosecond time-resolved IR spectroscopy study.[30] The observed reactive intermediate is a solvated monocarbonyl

complex.

The thermal activation of C-H bonds by [Tp*Rh(CO)$_2$] in benzene at 140 °C was achieved but with low yield and many decomposition products.[31] An attempt to improve the yield involved tailoring the Tp*RhL$_n$ complex with more labile ligands. Complexes of the type [Tp*Rh(CO)($\eta^2$-alkene)], where alkenes include ethylene, propylene and cyclooctene were prepared. These complexes were then used to thermally activate benzene in the range of 70 – 100 °C, forming [Tp*Rh(H)(CO)(Ph)] in 90% yield.

Hessel and Jones heated [Tp*Rh(CN-neopentyl)($\eta^2$-PhN=C=N-neopentyl)] in benzene to 100 °C and achieved C-H bond activation of benzene to form [Tp*Rh(H)(Ph)(CN-neopentyl)].[32] The same treatment of the analogous Cp* complex yielded no C-H activation product. They were also able to achieve reductive elimination of benzene by the thermolysis of [Tp*Rh(H)(Ph)(CN-neopentyl)].[33]

Cîrcu *et al.* prepared [Tp*Rh(PPh$_3$)$_2$] and [Tp*Rh{P(4-C$_6$H$_4$F)$_3$}$_2$]. Reaction of these two complexes with both phenylacetylene and *para*-nitrobenzaldehyde yielded C-H activation products. Reaction of the same two complexes with triphenyltin hydride also yielded the Sn-H activation product.[34]

Our group recently found that when [Tp*Rh(PPh$_3$)$_2$] is left in 1,2-dichloroethane (DCE) or tetrahydrofuran (THF), orthometalation of one of the phenyl rings on PPh$_3$ occurs.[35] This reaction is shown in Scheme 1-2. This does not occur in toluene and the reaction is suppressed in a 1:1 mixture of DCE and toluene. The oxidative addition of both ethylpropiolate and benzaldehyde to [Tp*Rh(PPh$_3$)$_2$] occurs with a loss of PPh$_3$, consistent with the findings of Cîrcu *et al.* These products are shown in Figure 1-6. If left in DCE or THF, these oxidative addition products undergo orthometalation of a

phosphine phenyl group to yield the same product as in the previous example, with loss of ethylpropiolate or benzaldehyde.

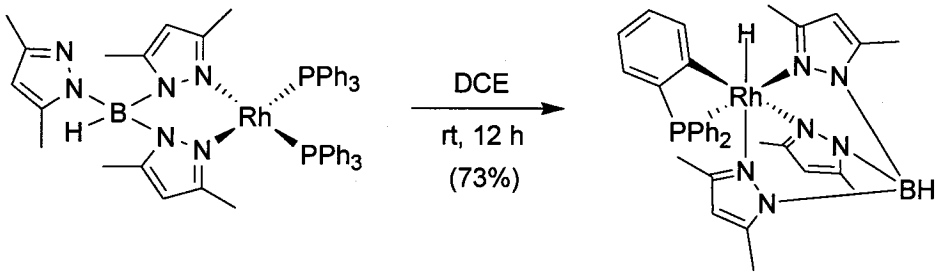


**Scheme 1-2** Orthometalation of [Tp*Rh(PPh$_3$)$_2$]

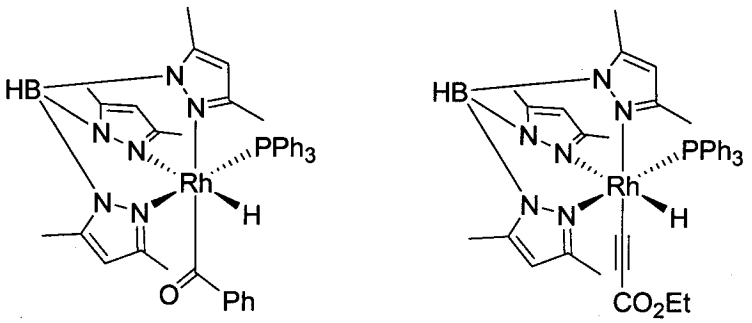

**Figure 1-6** Oxidative addition products of ethylpropiolate and benzaldehyde to [Tp*Rh(PPh$_3$)$_2$]

Cîrcu *et al.* report that reaction of [Tp*Rh(PPh$_3$)$_2$] with $C_6F_5SH$ gives the stoichiometric S-H activation product and the Tp* ligand fragments to give a 3,5-dimethylpyrazolyl (pz*) ligand.[36] They also report that $Ph_3SiH$ in $CH_2Cl_2$ reacts with [Tp*Rh(PPh$_3$)$_2$], fragmenting Tp* and $CH_2Cl_2$ to give pz*, Cl, and H ligands. Reaction of [Tp*Rh(PPh$_3$)$_2$] with $HgCl_2$ leads to the complete loss of Tp* ligand and the formation of a Hg-bridged dirhodium complex with $PPh_3$ and Cl ligands.

### 1.2.4.2 Catalytic reactions

Stereoregular polymerization of phenylacetylenes was achieved using [Tp*Rh(cod)], [Tp$^{Ph2}$Rh(cod)] and [Tp$^{i\text{-}Pr2}$Rh(cod)].[37] Catalysis was achieved using 1 mol% catalyst in $CH_2Cl_2$ solvent at 40 °C for 24 h and only worked for para substituted

phenylacetylenes. Generally yields were higher with bulkier $Tp^R$ ligands.

The regioselective, homogeneous hydrogenation of quinoline was achieved using [TpRh(cod)] prepared *in situ*.[38] [TpRh(cod)] was compared to related complexes of other metal centers including Ir and Ru. The catalytically active species is presumed to be [TpRh(quinoline)$_2$].

Trujillo reported the results of a preliminary study in which the dimerization of terminal alkynes was achieved using [Tp*Rh($C_2H_4$)($PEt_3$)] as a catalyst. In the same doctoral thesis work, [Tp*Rh($C_2H_4$)$_2$] was shown to catalyze the hydrosilylation of ethylene.[39]

Hydrothiolation is the addition of a thiol S-H bond to a double or triple C-C bond, as shown in Scheme 1-3.[40,41] The products can be branched (B or C)[40,42] or linear (A).[43-45] The third product type (C) forms from a double bond isomerization that occurs either before or after reductive elimination of the branched internal vinyl sulfide product (B) from the metal catalyst.[40,43] The regioselectivity of the reaction is highly tunable in that product distribution is strongly affected by the choice of catalyst and conditions. For instance, Wilkinson's catalyst provides stereoselective and regioselective addition of arylthiols to alkynes such that only the *E*-linear vinyl sulfide forms.[40]

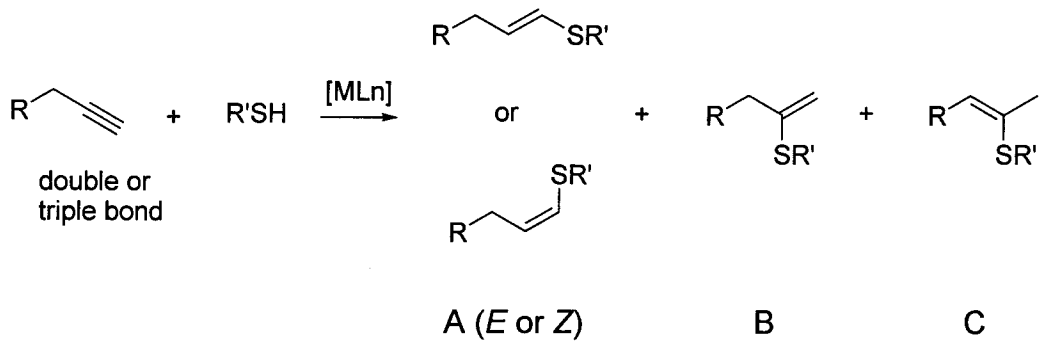


**Scheme 1-3** Alkyne hydrothiolation

The mechanism of hydrothiolation using Wilkinson's catalyst is believed to

proceed via *trans*-RhH(SPh)Cl($PPh_3$)$_2$ as the active catalyst.[40,46] The alkyne is thought to insert stereoselectively into the Rh-H bond, forming a *trans*-vinylrhodium intermediate, which then reductively eliminates the linear adduct in the presence of thiol.

Pd and Ni catalysts typically provide the branched products (B and C) when used with aryl thiols but no analogous reaction occurs with alkyl thiols.[40,42] In our lab, catalytic hydrothiolation of alkyl and aryl thiols was achieved using [Tp*Rh($PPh_3$)$_2$] catalyst with a range of alkynes in high yield and regioselectivity for the branched product.[41] It was thought that rhodium complexes bearing the Tp* ligand might be able to effect catalytic alkyl hydrothiolation because they have shown an ability to promote stoichiometric and catalytic bond activation.[18,36-39,47] Hydrothiolation using [Tp*Rh($PPh_3$)$_2$] with alkyl thiols forms the branched product exclusively and with aryl thiols a mixture of branched and linear products forms. In related work our group has also found that Wilkinson's catalyst, in contrast to published accounts which are limited to aryl thiols,[40] affords the *E*-linear isomer preferentially when used with alkyl thiols.

The activation of phosphorus-hydrogen bonds by metals can lead to many highly useful compounds containing phosphorus-carbon bonds.[48] Some of the products of P-H bond activation reactions include alkenylphosphine oxides, alkenylphosphines, alkenylphosphonates, and α-amino phosphonic acids, as shown in Figure 1-7. Organophosphorus compounds have found uses as ligands[49,50] for transition metals and are useful reagents in organic transformations.[50-52] A number of P-H bond activation reactions are known and will be briefly defined here. Additional emphasis will be given to hydrophosphinylation, which is the focus of the research presented in the next chapter. Hydrophosphination is the addition of a phosphine P-H bond to a C-C multiple bond to

form an organophosphine. Hydrophosphorylation is the addition of a phosphite P-H bond to an alkene to yield alkenylphosphonates. Hydrophosphonylation is the addition of a phosphite P-H bond to an imine to form α-amino phosphonic acids. Finally, hydrophosphinylation is the addition of a phosphine oxide P-H bond to an alkyne to form alkenylphosphine oxides as shown in Scheme 1-4.[48]

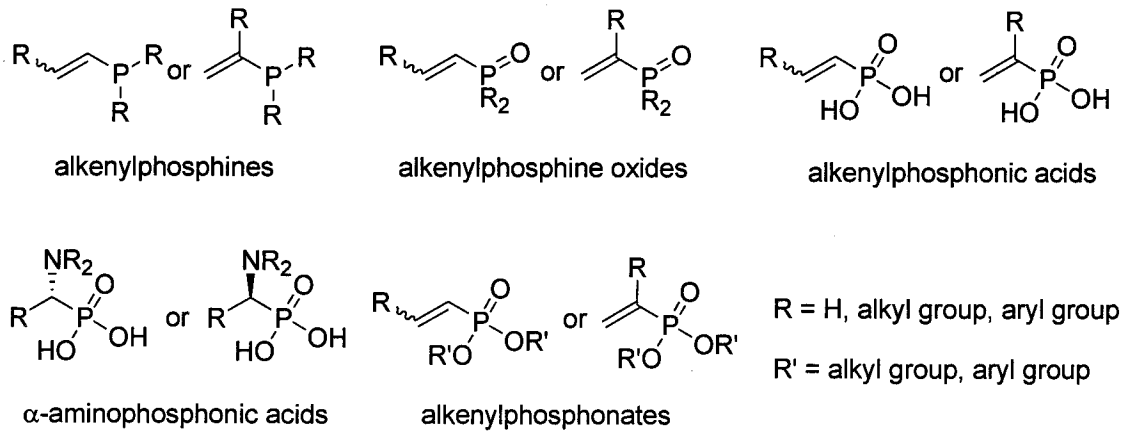


**Figure 1-7** Products of P-H bond activation reactions

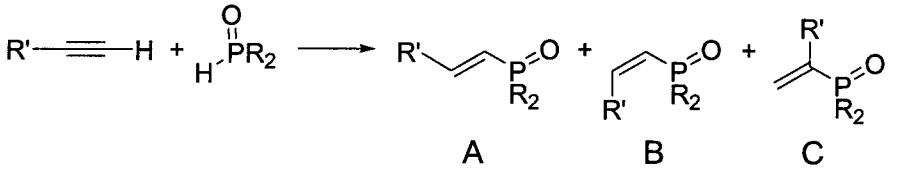


**Scheme 1-4** Alkyne hydrophosphinylation

When starting from terminal alkynes, hydrophosphinylation is a means of preparing vinylphosphine oxides, which are important starting materials in organic synthesis.[53,54] Vinylphosphine oxides can be selectively reduced[55] and they can be transformed into a variety of bifunctional reagents by addition of alcohols, thiols, amines and phosphines to the olefinic bond.[48] They are also used more directly in the Horner-Wadsworth-Emmons olefination reaction, Scheme 1-5.[56]

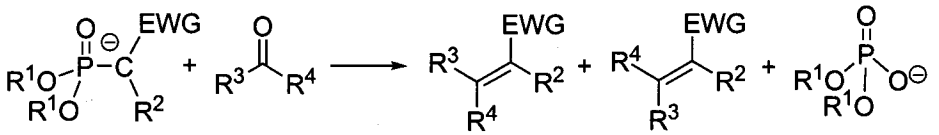

**Scheme 1-5** Horner-Wadsworth-Emmons olefination reaction

The first Pd-catalyzed regio- and stereoselective hydrophosphinylation of alkynes yielding alkenylphosphine oxides was developed by Han *et al.*[57] The reaction involves $Ph_2P(O)H$ and catalytic amounts of *cis*-$[Me_2Pd(PPhMe_2)_2]$ combined with a wide range of alkynes to generate a mixture of branched and linear products. In general, the *E*-linear product is favored. They later discovered that a minute quantity of phosphinic acid added to the reaction mixture with resulted in higher yields and a reversal of regiochemistry, favoring the branched product.[58]

A number of effective Rh catalysts were determined for the hydrophosphinylation of alkynes.[59] Among them, $BrRh(PPh_3)_3$ was an effective catalyst for a wide range of alkyne substrates. For all of the alkyne substrate and Rh catalyst combinations, (*E*)-alkenylphosphine oxides were produced exclusively.

It was later found that Ni was an effective metal for catalysis of hydrophosphinylation of a variety of alkyne and phosphine oxide substrates.[45] By changing the ligands on Ni as well as the reaction conditions, the regioselectivity of the reaction is reversed to favor either the branched or linear product in excellent yield.

### 1.2.4.3 Mechanistic studies on hydrophosphinylation

Han *et al.* propose a mechanism for hydrophosphinylation of alkynes catalyzed by either Wilkinson's catalyst or $[Rh(cod)Cl]_2$, shown in Scheme 1-6.[59] They propose that the mechanism is initiated by oxidative addition of P-H to the Rh complex, forming a Rh-H species. Han and coworkers combined $Ph_2P(O)H$ and $[ClRh(cod)]_2$ in $CD_2Cl_2$. NMR

spectroscopy of this solution showed $^1$H signals that appeared at -8.1 ppm (ddq, $J$ = 8.2, 15.5, 186.4 Hz) and -12.4 ppm (doublet of quintets, $J$ = 13.7, 21.0 Hz). In comparison, a mixture of excess $Ph_2P(O)H$ with $ClRh(PPh_3)_3$ in $CD_2Cl_2$ resulted in identical $^1$H NMR signals at -8.1 and -12.4 ppm. However, when a 1:1 mixture of $Ph_2P(O)H$ and $ClRh(PPh_3)_3$ was combined in $CD_2Cl_2$, the $^1$H NMR spectrum of this solution showed only the formation of a broad singlet at -16.2 ppm. Han suggests that in the equimolar mixture of $Ph_2P(O)H$ and $ClRh(PPh_3)_3$, a Rh-H species likely forms that includes at least one $PPh_3$ ligand. When excess $Ph_2P(O)H$ is present, as would be the case for catalytic conditions, both complexes $ClRh(PPh_3)_3$ and $[ClRh(cod)]_2$ form identical $Ph_2P(O)H$-ligated rhodium hydrides. Since there is no $PPh_3$ present in the $[ClRh(cod)]_2$ and $Ph_2P(O)H$ mixture, there can be no $PPh_3$ ligands on this Rh-H species, common to both mixtures. Furthermore, Han suggests that since both $[ClRh(cod)]_2$ and $ClRh(PPh_3)_3$ show similar catalytic activity in the hydrophosphinylation reaction, the $PPh_3$-free Rh-H complex is the active species for both of these catalytic reactions.

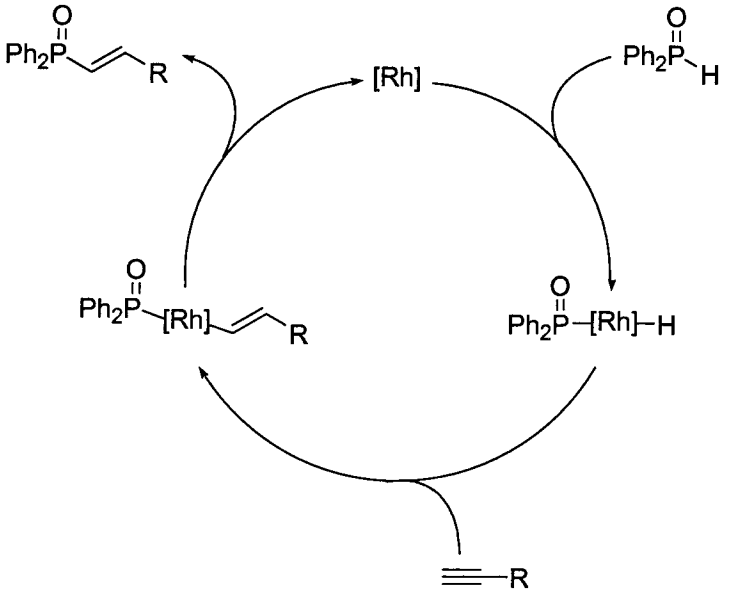


**Scheme 1-6** Mechanism of hydrophosphinylation catalyzed by either $[ClRh(cod)]_2$ or $ClRh(PPh_3)_3$, as proposed by Han

### 1.2.5 Conclusion

Pyrazolylborate rhodium complexes are known to promote stoichiometric bond activations but their catalytic activity is less well known. Based on their successful application as hydrothiolation catalysts,[26,27,41] we anticipated that $Tp^{R}RhL_n$ complexes would be useful in P-H bond activation reactions. Details of this work are presented in Chapter 2.

## 1.3 Background of olefin functionalization reactions via rhodaoxetane intermediates

### 1.3.1 Metallaoxetanes

A metallaoxetane is a 4-membered ring structure with a metal and an oxygen, shown in Figure 1-8.

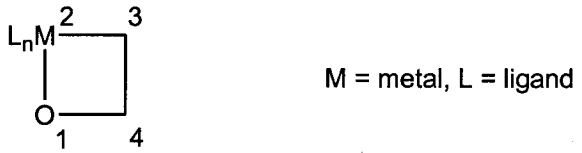


**Figure 1-8** General 2-metallaoxetane structure

Metals known to form metallaoxetanes include Pd, Pt, Re, Ni, Ag, Ir and Zr.[60-62] Metallaoxetanes are most well known for being invoked in some controversial mechanisms[61,63-66] and often have not been isolated or even observed. Examples of metal-mediated reactions for which metallaoxetanes have been invoked as intermediates include dihydroxylation of olefins catalyzed by osmium, manganese and chromium oxides,[64,67-71] catalytic epoxidation of olefins,[60,72] catalytic rearrangement of epoxides to ketones,[73] Ni-catalyzed reductive cyclization,[61] Ag-catalyzed epoxidation of ethylene,[62,74] and $Rh^{I}$-catalyzed asymmetric hydrogenolysis of epoxides.[75] However, the invocation of metallaoxetanes as intermediates has been controversial[65] and until recently few relevant

examples[76,77] were isolable or otherwise available for study. Certain metallaoxetanes can be generated by oxidation of olefin-ligated metal complexes.[78-80]

## 1.3.2 Oxidation of olefins

Periodate, permanganate, chromate and other traditional oxidizing agents have great chemical utility but cause a detrimental environmental impact and tend to be quite expensive, especially when used stoichiometrically.[81,82] Furthermore, these traditional oxidizing agents often lack functional group compatibility, limiting their application. Molecular oxygen and hydrogen peroxide are less environmentally harmful oxidants but their reactions can be difficult to control.[83] In the presence of certain metal complexes, oxidation of olefins by $O_2$, or $H_2O_2$ becomes more manageable. Metal-mediated oxidation processes that are in use on a massive scale include Wacker oxidation and hydroformylation.[84] These reactions are typified as being relatively environmentally benign since they each use molecular oxygen as the oxidizing agent and therefore produce minimal by-products.

## 1.3.3 Oxidation reactions with $H_2O_2$ as oxidant

### 1.3.3.1 Rhodaoxetanes

The first isolated rhodaoxetane was prepared by researchers in the Milstein group.[85] The structure of this complex is shown in Scheme 1-7, prepared by the method shown in path a.

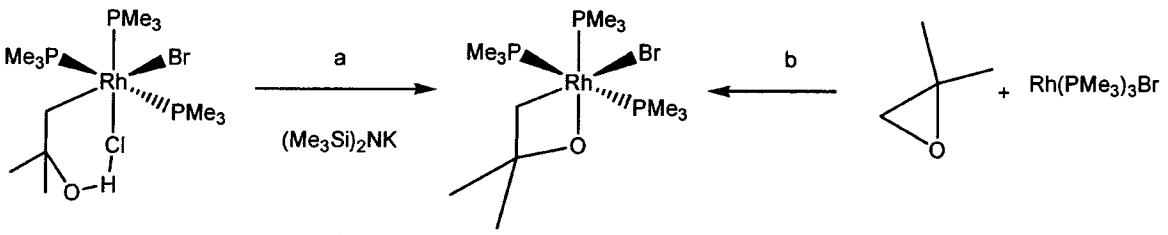


**Scheme 1-7** Preparation of the first isolable rhodaoxetane

An X-ray crystal structure of this complex showed a planar ring structure. The Rh-C and C-O bond distances suggest that the ring has partial carbene and ketone character, similar to the intermediate in the Tebbe olefination reaction with ketones.[86] Calhorda *et al.* report the first direct oxidative addition of a metal complex to a simple epoxide to yield a rhodaoxetane, shown above in Scheme 1-7, path b.[87]

The specific rhodaoxetane studied in this thesis work is $[(TPA)Rh^{III}(\kappa^2\text{-C,O-2-oxyethyl})]^+ BPh_4^-$ (TPA = tris[(2-pyridal)methyl]amine), shown in Figure 1-9, referred to herein as TPA-rhodaoxetane. TPA-rhodaoxetane was first prepared by the Gal research group from $[\{Rh(\mu\text{-Cl})(C_2H_4)_2\}_2]$ via $[(\eta^2\text{-ethene})(\kappa^4\text{-TPA})Rh^I]^+$ oxidized by hydrogen peroxide, shown in Scheme 1-8.[78]

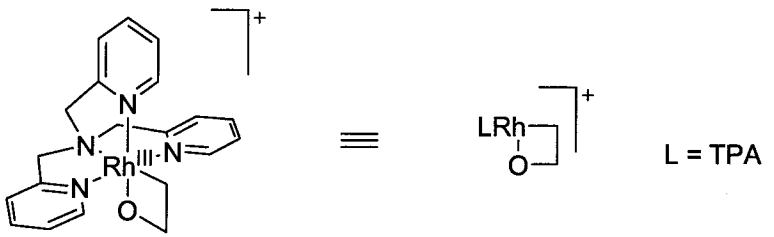


**Figure 1-9** TPA-rhodaoxetane

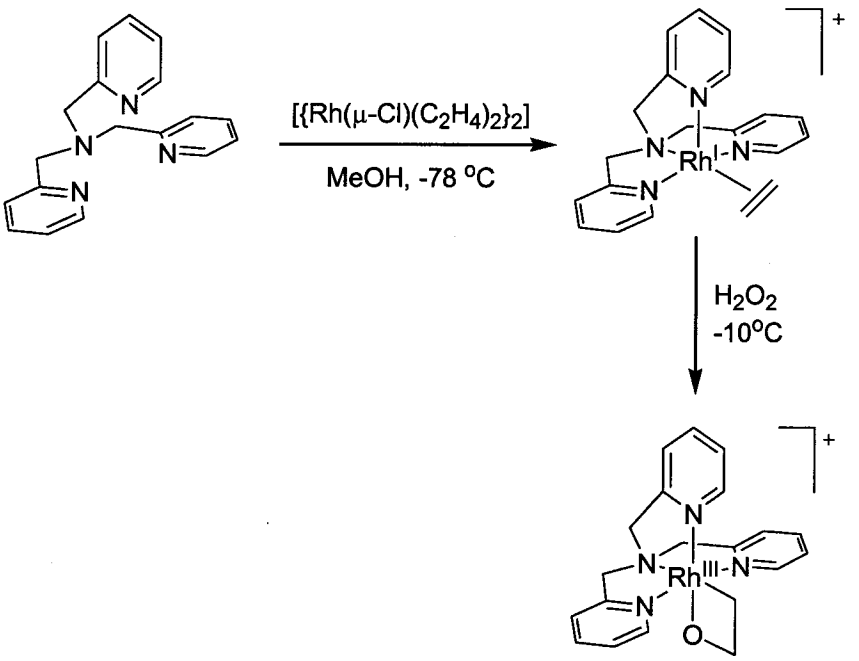


**Scheme 1-8** Preparation of $[(TPA)Rh^{III}(\kappa^2\text{-C,O-2-oxyethyl})]^+$, TPA-rhodaoxetane

Tris[(2-pyridal)methyl]amine (TPA), shown in Figure 1-10, was first prepared by Anderegg *et al.* in 1967.[88] TPA is an '$N_4$'-tripodal amine ligand, so-named because it contains a central donor nitrogen atom bonded to three arms, each containing a donor nitrogen atom. It most often coordinates to a metal using all four donor nitrogen atoms. Since its creation, TPA has been used to form complexes with all of the first row metals except for Ti, as well as most of the second and third row metals and lanthanides.[89]

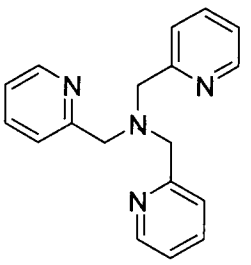

**Figure 1-10** Tris[(2-pyridal)methyl]amine (TPA)

### 1.3.3.2 Mechanism of rhodaoxetane formation

Budzelaar and Blok investigated the mechanism of oxidation of (olefin)$Rh^I$ and $Ir^I$

complexes to metallaoxetanes by $H_2O_2$ in a DFT study.[90] Their result, shown in Scheme 1-9, substantiates the suggested mechanism put forth by Gal and coworkers.[79] Heterolytic O-O cleavage occurs first, perhaps assisted by hydrogen bonding to the nascent hydroxide ion. A concerted mechanism for this initial step was also considered and determined not to occur since after extensive searching they could not locate a transition state for such an approach. In the next steps, intermolecular attack of coordinated $HO^-$ on coordinated olefin forms a zwitterionic intermediate, which then loses a proton to yield the rhodaoxetane. A comparison was made between the calculated energies for this transformation and one in which an oxo intermediate forms and rapidly cyclizes to the rhodaoxetane. The energy associated with the oxo species was calculated to be very high, making the first path much more likely. The stereochemistry of the $H_2O_2$ attack was analyzed and the cis approach of $H_2O_2$ with respect to the amine group was found to be slightly more favorable than the trans approach. The two possible approaches of $H_2O_2$ are illustrated in Scheme 1-10. The authors suggest that the energy difference between these two approaches is much higher than their calculations (0.2 kcal/mol) would indicate since in fact, no trans product is observed empirically.

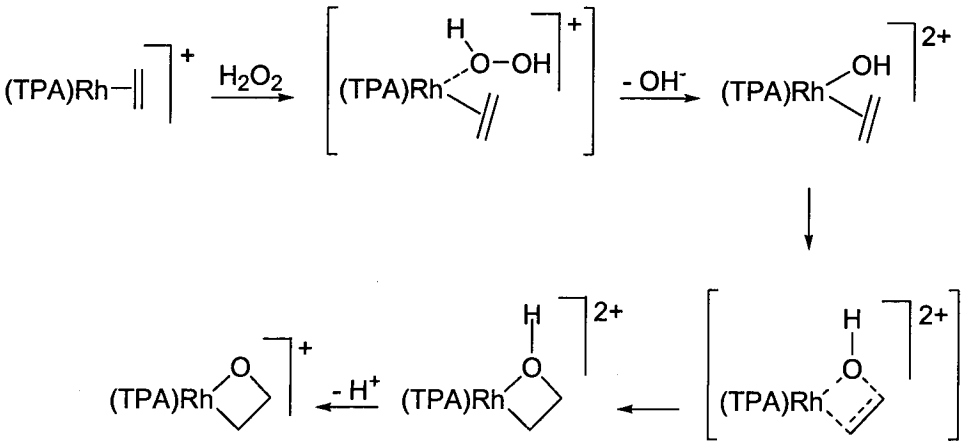


**Scheme 1-9** Mechanism of oxidation of [(TPA)Rh$^I$(ethene)] by $H_2O_2$

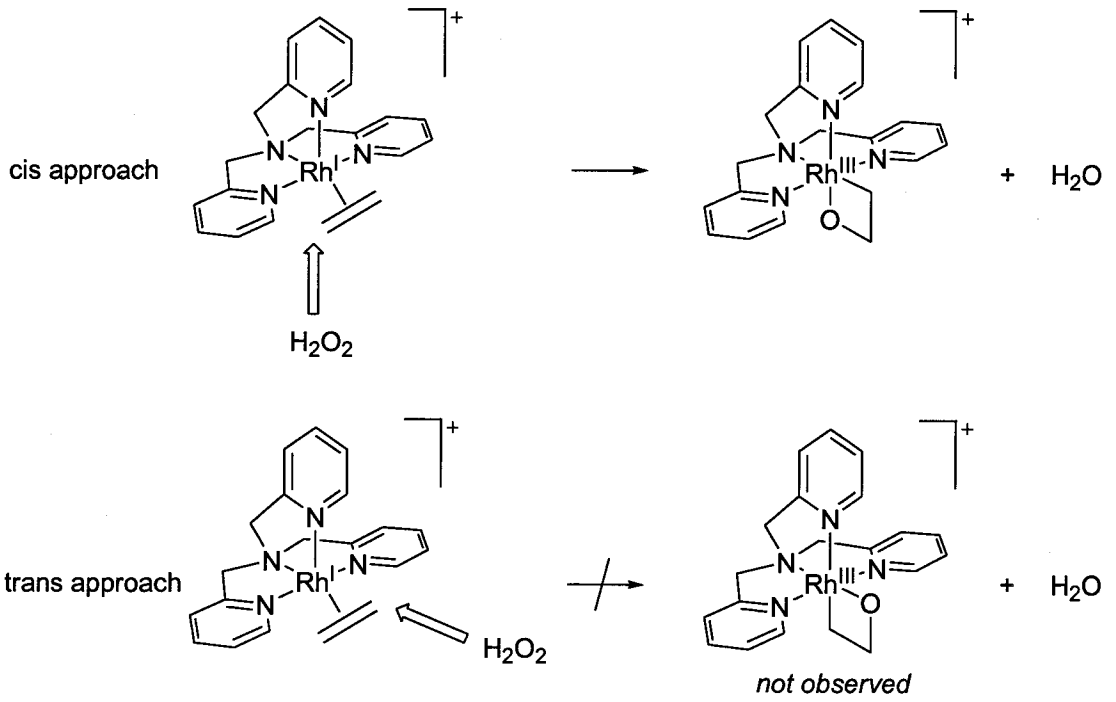


**Scheme 1-10** Cis and trans approaches of $H_2O_2$ attack

### 1.3.3.3 Reactivity of TPA-rhodaoxetane

TPA-rhodaoxetane has been shown to react with electrophiles including acids, MeI and acetone. TPA-rhodaoxetane will undergo ring-opening by electrophiles. Protonated TPA-rhodaoxetane generates acetaldehyde by β-H elimination at elevated temperatures or when activated by acid. These reactions are summarized in Scheme 1-11.[79] Contrary to what was expected,[85,87] at room temperature TPA-rhodaoxetane is stable to β-hydride elimination. However, in acidic conditions or at elevated temperatures β-H elimination occurs to yield acetaldehyde shown in Scheme 1-11, Eq. 1.[79] TPA-rhodaoxetane is stable to treatment of strong bases. Gal and coworkers also found that TPA-rhodaoxetane reacted readily with electrophiles such as $H^+$, $NH_4Cl$, MeI and $H^+/CH_3CN$, leading to ring-opened products (Scheme 1-11, Eq. 2).[79,91] It was discovered that TPA-rhodaoxetane slowly reacts with acetone (Scheme 1-11, Eq. 3) to form a six-

membered metallacyclic ketal, indicating an ability to react with less electrophilic substrates.[79]

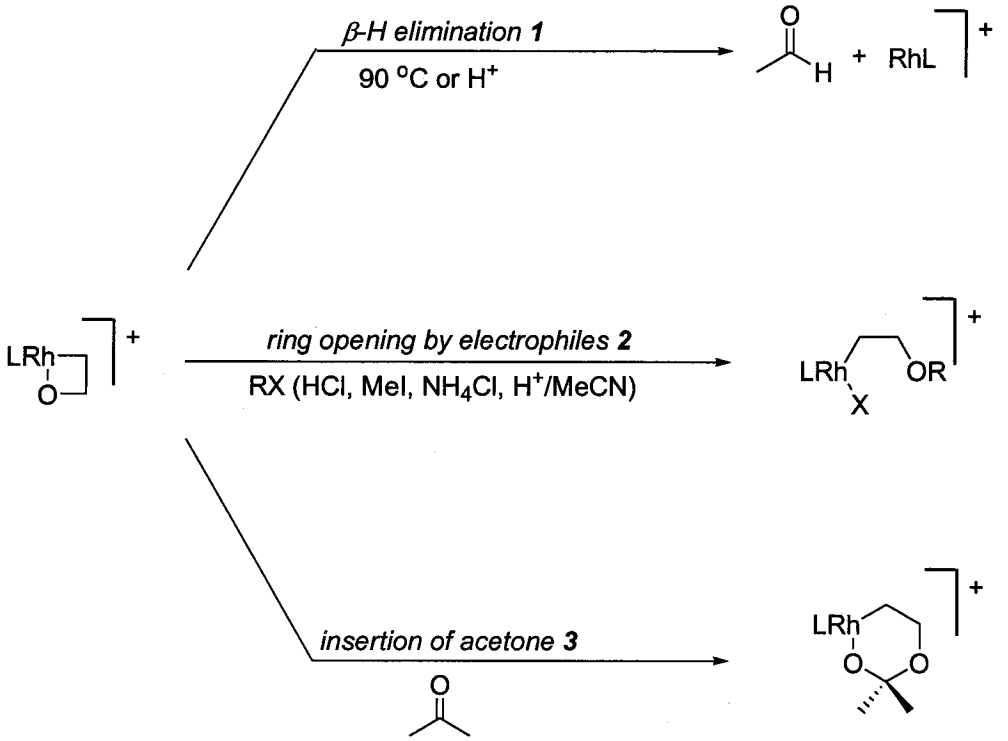


**Scheme 1-11** Reactivity of TPA-rhodaoxetane

Acetonitrile inserts into the protonated TPA-rhodaoxetane to form the ring-opened product, which readily rearranges to a metallacyclic imino-ester. The imino-ester can then rearrange upon heating to a metallacyclic amide.[91] These transformations are shown in Scheme 1-12.

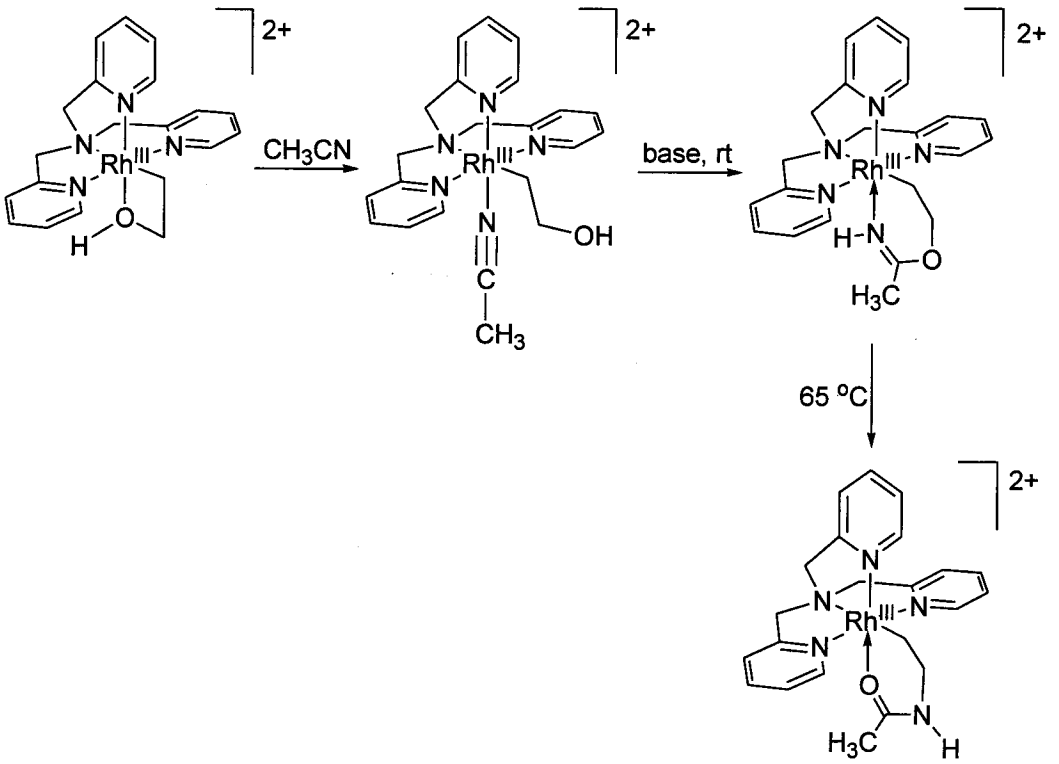


**Scheme 1-12** Acetonitrile insertion of TPA-rhodaoxetane and subsequent rearrangements

Theoretically, rhodaoxetanes should be able to reductively eliminate an epoxide but this has never been observed.[79] Reductive elimination is likely not seen because the formation of a strained epoxide from a less strained rhodaoxetane is not thermodynamically favorable.

### 1.3.3.4 '$N_3$'-rhodaoxetanes

In an effort to develop the reactive potential of this series of unsubstituted 2-rhodaoxetanes, the analogous '$N_3$' complexes were prepared, as shown in Figure 1-11.[80]

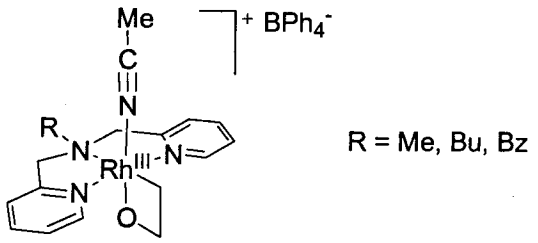


**Figure 1-11** Structure of '$N_3$'-rhodaoxetanes

The 'N$_3$' ligands make more reactive, less rigid complexes. 'N$_3$'-Rhodaoxetanes were shown to eliminate acetaldehyde at room temperature. Acetaldehyde also readily eliminates from these complexes when they are exposed to ethene or cod to form an ethene or cod complex in near quantitative yield.

Gal and co-workers attempted to produce a catalytic reaction that would prepare acetaldehyde from ethylene in the presence of 'N$_3$'-rhodaoxetanes. They achieved all of the individual steps that in theory complete the catalytic cycle, however they did not achieve catalytic turnover when the reagents were combined in one pot. The theoretical catalytic pathway is shown in Scheme 1-13.

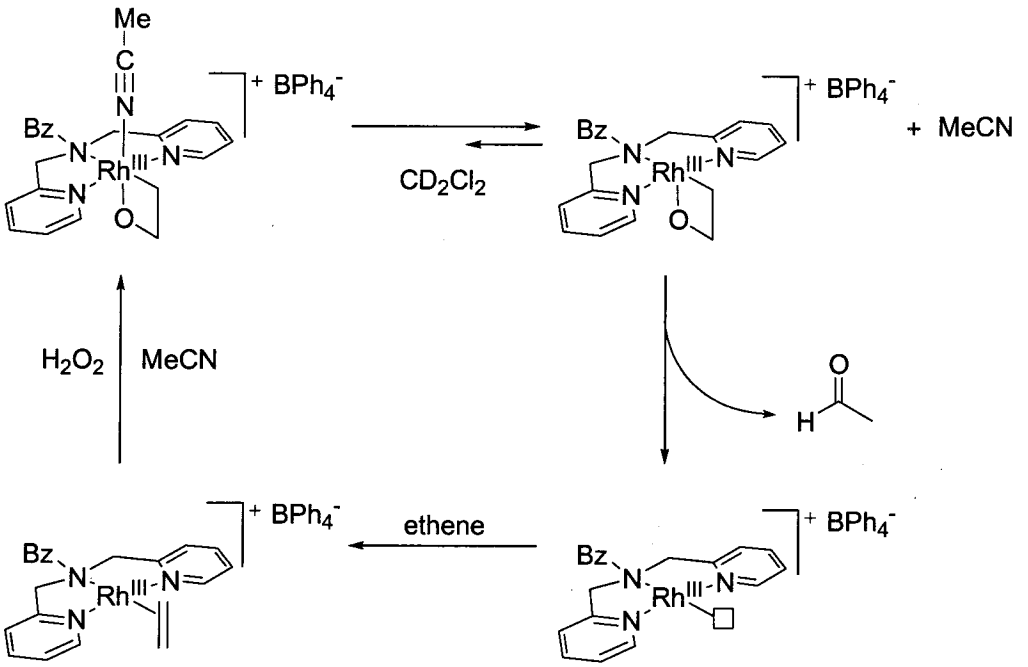


**Scheme 1-13** Theoretical catalysis of acetaldehyde from ethene via 'N$_3$'-rhodaoxetane

The authors suggest two possible explanations for why catalysis is not achieved for this series of reactions. First they suggest that [(Bzbpa)Rh$^{I}$]$^+$, which results from the reductive elimination step may react faster with hydrogen peroxide than with ethylene,

leading to the poisoning of the active catalyst. Alternatively, perhaps further oxidation occurs to form a formylmethyl-hydroxy complex, shown in Scheme 1-14.

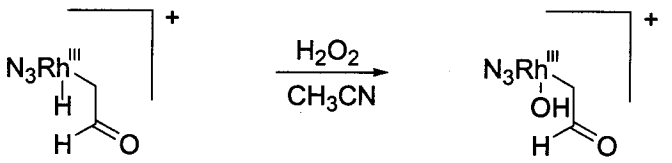


**Scheme 1-14** Formation of a formylmethyl-hydroxide rhodium complex

## 1.3.4 Oxidation reactions with $O_2$ as oxidant

Rhodium complexes have been shown to be active catalysts for the selective oxygenation of terminal alkenes to methyl ketones.[83] For example, Read and coworkers used rhodium catalysts to facilitate the conversions of hex-1-ene, hept-1-ene and oct-1-ene to methylketones with dioxygen. The catalysts studied were $RhH(CO)(PPh_3)_3$ and $RhCl(PPh_3)_3$, the latter complex providing the best yields.[92, 93] They were likewise able to oxidize oct-1-ene and triphenylphosphine to octan-2-one and triphenylphosphine oxide with $RhCl(PPh_3)_3$. These catalytic oxygenation reactions are shown below in Scheme 1-15. For the most part, reactions of this type incorporate only one of the two atoms of dioxygen into the substrate and the second oxygen atom is quenched by a sacrificial hydrogen donor or a phosphine.[83]

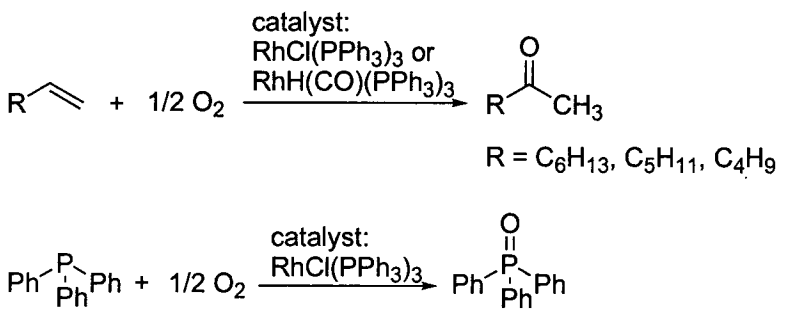


**Scheme 1-15** Catalytic oxygenation reactions

### 1.3.4.1 The Wacker reaction

Acetaldehyde is commercially prepared by the catalytic oxidation of ethene by

molecular oxygen in water, known as the Wacker process. It is a relatively environmentally benign reaction catalyzed by palladium, shown summarized in Scheme 1-16.[94] This process has a low impact on the environment because it is 100% atom efficient and does not involve the use of highly toxic solvents or reagents.

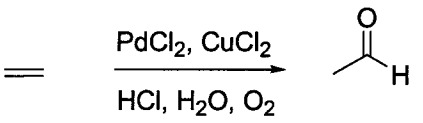


**Scheme 1-16** The Wacker reaction

Wacker-type oxidation is also possible for higher molecular weight terminal alkenes. This variation is often referred to as Wacker-Tsuji oxidation (Scheme 1-17).[95] The Wacker reaction involves oxypalladation, which is the net addition of oxygen and palladium atoms across the ethene π-bond, followed by β-elimination to yield acetaldehyde. In the case of higher alkenes, oxypalladation (*vida infra*) can occur in Markovnikov or *anti*-Markovnikov fashion to yield either a methyl ketone or an aldehyde product. Markovnikov addition is by far the more typical regioselectivity for this reaction. The products are often low-boiling compared to the solvent (*i.e.*, water), so they can be easily distilled, leaving the catalysts behind in solution for further reaction. For some higher molecular weight alkene oxidations the products do not boil at a low enough temperature to be removed by distillation. Instead the catalyst can be recovered by treating the reaction mixture with HCl and $PPh_3$ to make the $PdCl_2(PPh_3)_2$ complex which is insoluble. The products can then be extracted into an organic solvent.

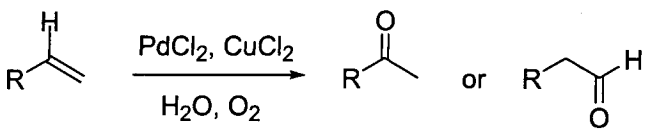


**Scheme 1-17** Wacker-Tsuji oxidation

The widely accepted mechanism for the Wacker reaction is shown in Scheme 1-18.[96-98] In solution, free chloride ions coordinate to $PdCl_2$ to form $[PdCl_4]^{2-}$. In the first two steps, water and ethene exchange with two of the chloride ions, forming a π-complex. The key step of this catalysis is nucleophilic attack of a second water molecule or hydroxide ion to the coordinated ethene in an anti fashion, forming a (β-hydroxyalkyl)palladium complex.[99] This step is routinely referred to as oxypalladation since addition of the water nucleophile is facilitated by the lowered electron density of the alkene when it is in the π-complex with electrophilic palladium. The nucleophilic addition of water is definitive of all Wacker-type oxidation reactions. Finally, a rapid succession of steps involving rearrangement and β-elimination yields the product acetaldehyde and reduced palladium. Deuterium labelling experiments have conclusively shown that all four hydrogen atoms in the product acetaldehyde are from ethene as opposed to solvent.[99] The Cu(II) co-catalyst reoxidizes Pd(0) to Pd(II). The reduced copper is reoxidized by molecular oxygen, a stoichiometric oxidant, which is both inexpensive and readily available.

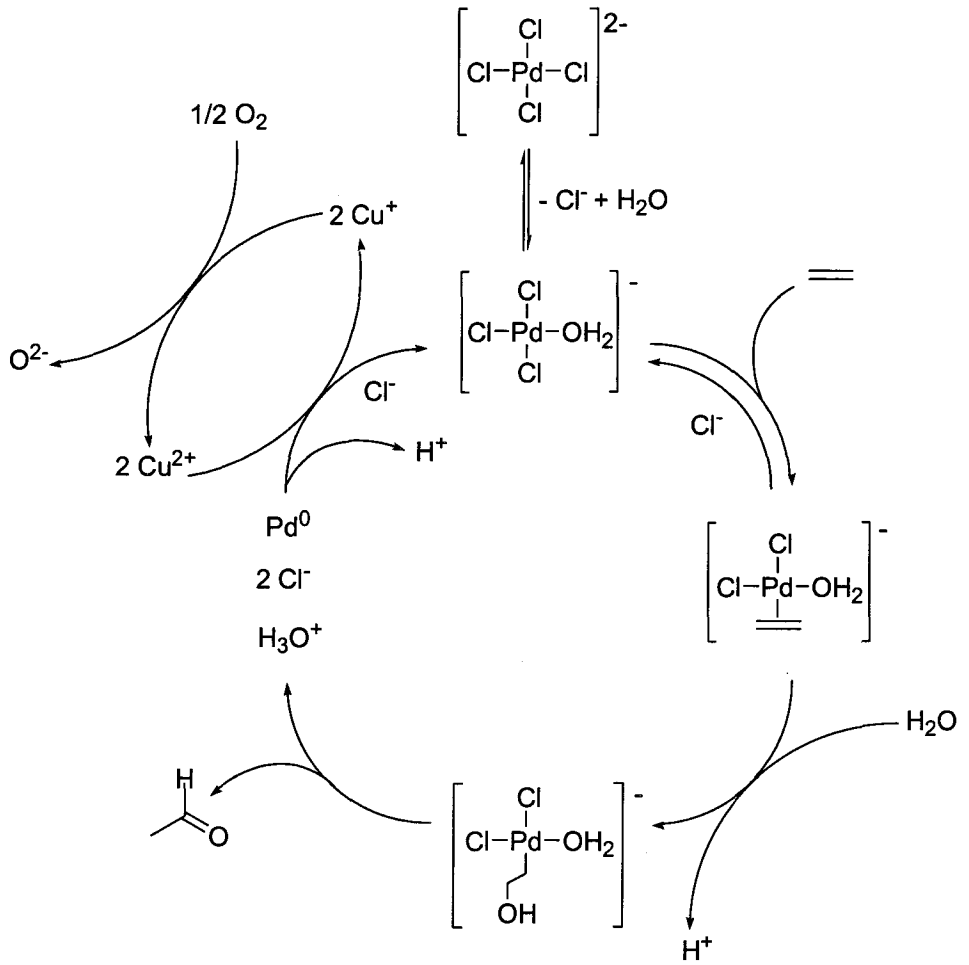


**Scheme 1-18** Mechanism of the Wacker reaction

Wacker-Tsuji oxidations are believed to follow an analogous mechanism involving the same key steps, with the exception that the nucleophilic addition of water or hydroxyl ion can sometimes occur in a syn or an anti fashion, leading to a mixture of products.[95,98]

### 1.3.4.2 Rhodadioxolane chemistry

3-Metalla-1,2-dioxolanes have been invoked as intermediates in groups 6 and 8-10 metal-catalyzed olefin oxygenation reactions, including epoxidation and oxidation to ketones.[100] However, these mechanistic details could not previously be readily evaluated

because of a lack of isolable complexes available for study.

Gal and coworkers prepared 3-rhoda-1,2-dioxolanes from $[(tpa)Rh(CH_2CH_2)]PF_6$ following their successful preparation of a 2-rhodaoxetane by oxidation of this same complex with $H_2O_2$. These 3-rhoda-1,2-dioxolanes contain an unsubstituted 3-metalla-1,2-dioxolane fragment, which was unprecedented. A solid-gas reaction of the ethylene complex in air provided a 1:1 mixture of regioisomers, shown in Scheme 1-19.[101] They were also able to selectively prepare regioisomer **b**, by substituting the $BPh_4^-$ counterion for $PF_6^-$. They later prepared analogous 3-irida-1,2-dioxolanes.[100]

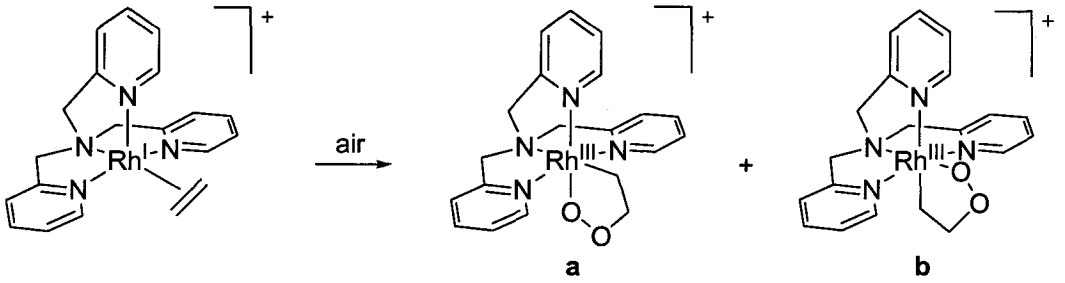


**Scheme 1-19** Preparation of a 3-rhoda-1,2-dioxolane

3-Rhoda-1,2-dioxolanes were shown to rearrange to rhodium formyl methyl hydroxy complexes upon exposure to light or acid, shown in Scheme 1-20.[102]

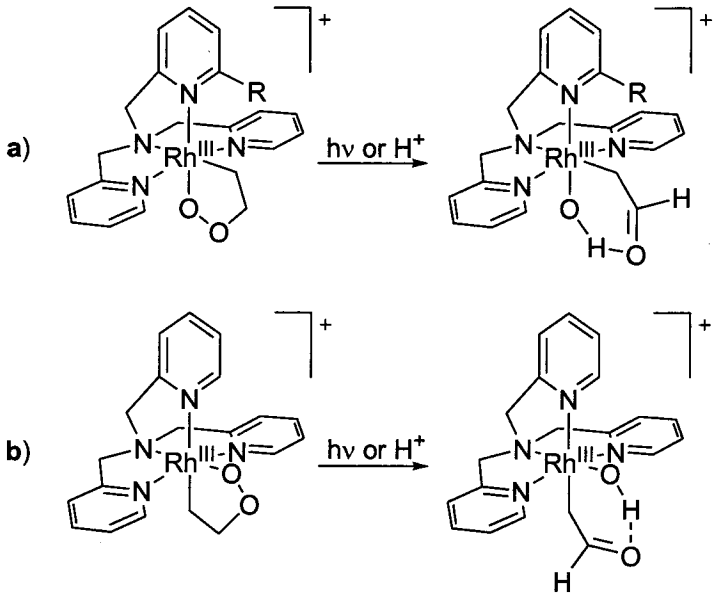


**Scheme 1-20** Rearrangement of 3-rhoda-1,2-dioxolanes

## 1.3.5 Oxidation of organometallics with $N_2O$ as oxidant

The reaction of nitrous oxide with hydride, aryl and alkyl ligands in certain metal complexes results in oxygen insertion into the metal-ligand bond, shown in Scheme 1-21.[103-110]

$$N_2O + L{-}M^{n+} \longrightarrow L{-}O{-}M^{n+} + N_2$$

L = hydride, aryl, alkyl

M = Mo, Ni, Zr, Hf

**Scheme 1-21** Oxygen insertion into metal complexes by $N_2O$

Matsunaga *et al.* prepared an oxanickelacycle by oxygen insertion into a nickelacyclopentane ring using nitrous oxide.[108] This reaction is shown in Scheme 1-22. They did not observe any intermediates but they suggest the mechanism likely involves coordination of nitrous oxide to the nickel center followed by oxygen transfer and loss of dinitrogen. Previous findings in the Hillhouse group support this proposed mechanism.[111, 112]

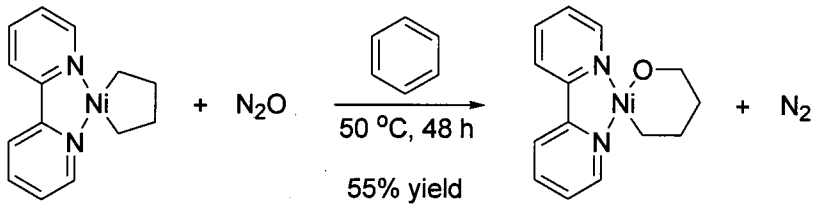


**Scheme 1-22** Oxygen insertion into an organonickel complex by $N_2O$

## 1.3.6 Conclusion

TPA-rhodaoxetane can be readily prepared and isolated[78] and has shown interesting reactivity[79] that could be exploited for the development of new methods for olefin functionalizations. We anticipated that TPA-rhodaoxetane could be utilized as a common reactive intermediate for several potentially catalytic olefin functionalization reactions. Details of this work are presented in Chapter 3.

# 2 Hydrophosphinylation catalyzed by pyrazolylborate rhodium complexes

## 2.1 Introduction

Pyrazolylborate rhodium complexes are known for their ability to enable stoichiometric bond activation reactions but their catalytic activity has been less studied.[18] In a recent study, we postulated that rhodium pyrazolylborates might be sufficiently electron-rich to catalyze hydrothiolation of alkynes with alkyl thiols.[41] Indeed, we found that [Tp*Rh($PPh_3$)$_2$] catalyzed hydrothiolation with high regioselectivity for branched alkyl vinyl sulfides. [Tp*Rh($PPh_3$)$_2$] was found to be an effective hydrothiolation catalyst for both aryl and alkyl thiols and a range of alkynes. Based on this success we chose to further explore the potential of [Tp*Rh($PPh_3$)$_2$] to catalyze reactions involving H-X bond activation as a key step (X = C, heteroatom).

## 2.2 Research hypotheses and goals

We hypothesized that [Tp*Rh($PPh_3$)$_2$] could catalyze the hydrophosphinylation of alkynes; a reaction that is believed to involve P-H bond activation as a fundamental step.[59] We further hypothesized that the regioselectivity of this reaction would be similar to that which we observed for hydrothiolation catalyzed by [Tp*Rh($PPh_3$)$_2$], which results in a preference for the formation of the branched regioisomer.[41] We set out to compare a series of known hydrophosphinylation catalysts with [Tp*Rh($PPh_3$)$_2$] and related [Tp*Rh$L_n$] complexes for their efficacy in the hydrophosphinylation of 1-octyne with diphenylphosphine oxide. We further planned to investigate the scope of possible substrates for hydrophosphinylation with [Tp*Rh($PPh_3$)$_2$]. Auxiliary experiments were performed to investigate the mechanism of hydrophosphinylation and related P-H bond

activation reactions catalyzed by [Tp*Rh($PPh_3$)$_2$].

Sections 2.2.1 and 2.2.2 of this chapter are based on a published account of the research conducted in our group by me and my colleague, Changsheng Cao.[113] More specifically, all of the catalytic experiments in Section 2.2.1 were performed by me and the experiments discussed in Section 2.2.2 were performed by C. Cao. The experiments performed by C. Cao are not part of any other thesis and are included here in order to provide a complete account of our findings. All other research presented in the results and discussion section 2.2 as well as the experimental section 2.3 were conducted by me.

# 2.3 Results and Discussion

## 2.3.1 Catalytic hydrophosphinylation of alkynes

### 2.3.1.1 Catalyst comparison

A comparison was made of known catalysts with their analogous pyrazolylborate complexes for the hydrophosphinylation reaction of diphenylphosphine oxide with 1-octyne. The complexes for comparison included Wilkinson's catalyst [ClRh($PPh_3$)$_2$] **I**, [ClRh(cod)]$_2$ **II**, [(OTf)Rh($PPh_3$)$_3$] **V**, [Tp*Rh($PPh_3$)$_2$] **III**, and [Tp*Rh(cod)] **IV**. Both Wilkinson's catalyst **I** and [ClRh(cod)]$_2$ **II**, are known hydrophosphinylation catalysts.[59] [(OTf)Rh($PPh_3$)$_3$] **V**, which was prepared *in situ* by adding silver triflate to Wilkinson's catalyst **I**, was included to see what effect a more weakly coordinating counter ion would have. It was thought that the use of a more weakly coordinating anion, i.e. triflate,[114] may provide a Wilkinson's catalyst analog with more cationic character. The catalyst loading for all reactions was 3 mol% Rh and all reactions were performed on a 1 mmol scale. The results are presented in Table 2-1. The isolated yields are reported for the linear product only, as no branched product was observed.

**Table 2-1** Catalyst comparison

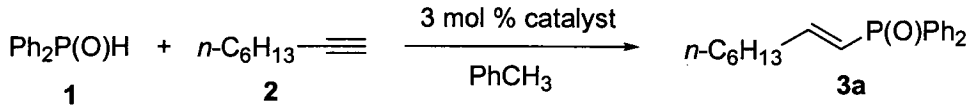


| Entry[a] | Catalyst | Temp, time | Isolated yield (%) |
|---|---|---|---|
| 1 | none | 110 °C, 1 h | trace[b] |
| 2 | $ClRh(PPh_3)_3$ **I** | 110 °C, 1 h | 80 |
| 3[c] | $[ClRh(cod)]_2$ **II** | 110 °C, 1 h | 55 |
| 4[d] | $[(OTf)Rh(PPh_3)_3]$ **V** | 110 °C, 1 h | 74 |
| 5 | $Tp^*Rh(PPh_3)_2$ **III** | 110 °C, 1 h | 51 |
| 6 | $Tp^*Rh(cod)$ **IV** | 110 °C, 1 h | 35 |
| 7 | $ClRh(PPh_3)_3$ **I** | rt, 18 h | 84 |
| 8 | $Tp^*Rh(PPh_3)_2$ **III** | rt, 18 h | 51 |
| 9 | $Tp^*Rh(cod)$ **IV** | rt, 18 h | 25 |

[a] Reactions conducted with 1.0 equiv diphenylphosphine oxide, 1.0 equiv alkyne, 3 mol % catalyst. [b] Trace product observed by $^1H$ NMR spectroscopy. [c] 1.5 mol % catalyst used. [d] 3 mol % AgOTf.

The reactions were run for durations of either 1 or 18 h, depending on the chosen temperature. The reactions could have been run just to completion or they could be evaluated at a certain point in time. The latter option was chosen since it is operationally simpler and gives a good snapshot of the efficiency of each catalyst system. With the exception of entry 1 for which negligible product formed, all of the products were then isolated by column chromatography. Attempts were made to monitor the reactions over time using various methods including thin layer chromatography (TLC), $^1H$ NMR spectroscopy and gas chromatography (GC) to determine when the reaction was completed. TLC was of limited use; since none of the reactions went to 100% completion, the technique would only show that some amount of product had formed and

some of the starting material remained. If an internal standard was added to the reaction mixture, $^1$H NMR spectroscopy could be reliably used to measure the progress of the longer reactions. For the faster reactions the reaction would continue in the NMR tube and travel time from the laboratory to the spectrometer made this type of monitoring somewhat less precise. GC-MS was used to monitor a test reaction with the conditions of 110 °C in toluene. In this case, the samples were filtered through a plug of silica gel to remove the metal complex before injection onto the column. Again there were difficulties in accurately monitoring the faster reactions since the gas chromatograph required a long run time to separate this mixture and the reaction would have long been completed by the time the analysis of the first sample was available. There was also some concern that filtration through silica may have altered the ratio of materials in the mixture. The results of the GC analysis showed that nearly all of the $Ph_2P(O)H$ starting material was gone by 15 minutes, so a set reaction time of 1 hour was chosen to ensure ample time to reach completion. Similarly for test reactions done at room temperature, 18 h was determined to be more than sufficient.

Wilkinson's catalyst **I** (entry 2) was found to be a more effective catalyst than $[ClRh(cod)]_2$ **II** (entry 3) for this reaction, as is consistent with the results reported by Han *et al.*[59] The addition of silver triflate to Wilkinson's catalyst for this reaction (entry 4) lowered the yield modestly. Han *et al.* report results for a series of Wilkinson's catalyst analogs in which the chloride ligand is replaced by another halide. Their results show that the effectiveness of these catalysts for hydrophosphinylation follows the order of I > Br > Cl. The result reported here that the triflate ion makes for a weaker catalyst than chloride follows the trend first established by Han *et al.,* that more weakly

coordinating ligands on Rh in Wilkinson's catalyst analogs made for less effective catalysts for this reaction. The effectiveness of Wilkinson's catalyst analogs for hydrophosphinylation follows the order of I > Br > Cl > OTf.

Replacing chloride with Tp* in both Wilkinson's catalyst **I** and $[ClRh(cod)]_2$ **II** to form $[Tp^*Rh(PPh_3)_2]$ **III** (entry 5) and [Tp*Rh(cod)] **IV** (entry 6), respectively, resulted in viable catalysts for hydrophosphinylation. In both cases, yields were moderate but not as high as for their chloride ligand counterparts. Interestingly, with these catalysts the linear product formed exclusively. We did not know what regioselectivity to expect for this reaction but we had reason to suspect the opposite result, that in the case of $[Tp^*Rh(PPh_3)_2]$ **III**, the branched regioisomer may form preferentially as it does in hydrothiolation reactions with this catalyst[41] since similar mechanisms have been proposed for both hydrothiolation and hydrophosphinylation.

There were two sets of reaction conditions used for this comparison. Entries 7, 8 and 9 were performed at room temperature for 18 h, in toluene. Entries 2, 5 and 6 were performed at 110 °C for 1 h in toluene. For the most part, both sets of conditions produced similar yields for this hydrophosphinylation reaction. The reaction with [Tp*Rh(cod)] **IV** catalyst was more efficient by a difference of 10% when done at 110 °C as opposed to room temperature, in toluene.

#### 2.3.1.2 $[Tp^*Rh(PPh_3)_2]$ catalyzed alkyne hydrophosphinylation - substrate scope

$[Tp^*Rh(PPh_3)_2]$ **III** was chosen to explore the scope of hydrophosphinylation using a rhodium pyrazolylborate catalyst since it was found to be more effective than [Tp*Rh(cod)] **IV** in the preceding catalyst comparison. The results of this analysis are presented in Table 2-2.

**Table 2-2** Alkyne substrate scope for hydrophosphinylation catalyzed by [Tp*Rh(PPh$_3$)$_2$]

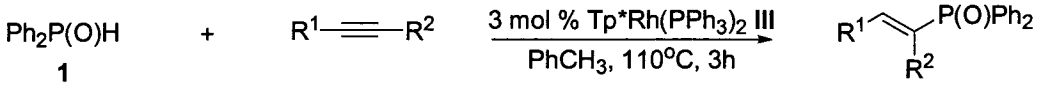


| Entry[a] | Alkyne | Product | Isolated yield (%)[b] |
|---|---|---|---|
| 1 | *n*-$C_6H_{13}$—≡ **2** | *n*-$C_6H_{13}$ P(O)$Ph_2$ **3a** | 51 |
| 2 | *t*-Bu—≡ **4** | *t*-Bu P(O)$Ph_2$ **8** | 41 |
| 3 | Ph—≡ **5** | Ph P(O)$Ph_2$ **9** | 17[c] |
| 4 | $CH_3O$— —≡ **6** | $CH_3O$ P(O)$Ph_2$ **10** | 28[c] |
| 5 | ≡ **7** | P(O)$Ph_2$ **11** | 61 |

[a] Reactions conducted with 1.0 equiv diphenylphosphine oxide, 1.0 equiv alkyne, 3 mol % catalyst. [b] Complete consumption of starting materials. [c] Additional unidentified precipitate formed.

All of the reactions in this comparison were done in toluene at 110 °C as these conditions were found to be generally more successful in the previous study. The reaction time was extended to 3 h to ensure completion and the results of NMR spectroscopy analysis showed no remaining starting material for these reactions. The reactions were done on a 1 mmol scale with 3 mol% catalyst. The selection of alkynes included terminal aliphatic and aromatic examples, as well as an internal aliphatic alkyne.

Products **3a**, **8**, and **9** (entries 1 – 3) have been prepared previously by the same reaction but with a different catalyst and different conditions.[59] Han *et al.* used [BrRh(PPh$_3$)$_3$] as the catalyst for this reaction in toluene for 40 min at rt to provide isolated yields of 91% for **3a** (entry 1) and 93% for **8** (entry 2). The same catalyst and

conditions but a longer reaction time of 2 h provided 89% isolated yield for **9** (entry 3). Product **10** (entry 4) was previously prepared in 98% isolated yield by a non-catalytic 2-step process involving nucleophilic substitution reactions by Bartels *et al.*[115] Product **11** (entry 5) has no literature precedent for comparison. The use of [Tp*Rh(PPh$_3$)$_2$] **III** does not provide an improvement on existing known yields for catalytic hydrophosphinylation of the alkynes in entries 1 – 3; however, the catalytic potential of [Tp*Rh(PPh$_3$)$_2$] **III** has been demonstrated.

All of the substrates exclusively provided the vinylphosphine oxide product that would be expected from *syn*-addition of the P-H bond across the alkyne. The terminal alkynes (entries 1 – 4) exclusively provided linear vinylphosphine oxide products. The aliphatic alkyne substrates (entries 1, 2 and 5) had better yields than the aromatic alkyne substrates (entries 3 and 4). Of the terminal aliphatic alkynes, a straight chain alkyne (entry 1) produced a better yield than the bulkier branched alkyne (entry 2). The highest yield was obtained for 3-hexyne **7** (entry 5), a straight-chain and internal alkyne. One might expect that crowding around the metal center of the active catalyst would reduce the efficiency of this reaction.

The reactions with aromatic alkyne substrates produced an additional unidentified precipitate, which presumably reduced the amount of available starting material for the formation of the desired product, effectively limiting these yields. This byproduct does not appear to be formed by oligomerization or polymerization, as has been seen for similar reactions using the [Tp*Rh(cod)] complex **IV**.[37] Cyclotrimerization could also potentially account for this byproduct, which nevertheless remains unidentified. There may be a competitive reaction that occurs only with aromatic alkynes in the presence of

[Tp*Rh($PPh_3$)$_2$] **III**.

### 2.3.1.3 Hydrophosphinylation in the absence of catalyst

In order to determine the extent of any background reaction, diphenylphosphine oxide **1** and 1-octyne **2** were combined with no catalyst present in toluene-$d_8$ for 1 h at room temperature. The reaction mixture was monitored by $^1$H NMR spectroscopy and no product was observed in the spectrum. This experiment was repeated as described above, but the mixture was heated to 110 °C for 1 h. $^1$H NMR spectroscopy of the heated mixture showed a trace of hydrophosphinylation product had formed. For this reaction both the linear **3a** and branched **3b** isomers were observed in a 1:1 ratio. Integration of these peaks indicated a yield of less than 1% for each isomer, an amount that is lower than can be reliably measured for this technique. It was concluded that any background hydrophosphinylation reaction for these conditions was not significant and could be disregarded as a contributing source of product in all other hydrophosphinylation reactions in this study.

### 2.3.1.4 Background reaction of diphenylphosphine oxide with triphenylphosphine

It was thought that a ligand exchange reaction involving diphenylphosphine oxide **1** and triphenylphosphine **12** might occur to form triphenylphoshine oxide **13**. Such a reaction could facilitate the breakdown of any catalyst containing labile triphenylphosphine ligands, resulting in an inactive complex. A mixture of triphenylphosphine **12** and diphenylphosphine oxide **1** in $CDCl_3$ was monitored by $^{31}$P NMR in comparison to standards of the two reagents made up to the same concentration in separate NMR tubes. The concentration of the two reagents did not change and no new peaks formed as monitored by $^{31}$P NMR spectroscopy over several hours. The absence of

any change in these spectra suggests that no competing reaction between diphenylphosphine oxide **1** and triphenylphosphine **12** occurs during the relevant timescale and conditions for the reaction of interest.

### 2.3.2 Crystallographic studies

The mechanism of catalytic hydrophosphinylation by $[ClRh(cod)]_2$ **II** is thought to proceed via a Rh-H intermediate formed by a P-H activation step. Trzeciak *et al.* have observed such a species by $^1H$ and $^{31}P$ NMR spectroscopy as a product of the reaction of diphenylphosphine oxide **1** and $[ClRh(cod)]_2$ **II**.[116] This species likely forms by oxidative addition of P-H to $Rh^I$. Based on this finding it is reasonable to presume that a Rh-H species may also be an intermediate in catalytic hydrophosphinylation using phosphine-bound rhodium complexes.

To test this, another member of the Love research group (C. Cao) prepared X-ray quality crystals from reactions of $[ClRh(cod)]_2$ **II** or $[Tp^*Rh(PPh_3)_2]$ **III** with excess diphenylphosphine oxide **1**.[113] These reactions were intended to mimic catalytic conditions in the absence of any alkyne. One equivalent of either $[ClRh(cod)]_2$ **II** or $[Tp^*Rh(PPh_3)_2]$ **III** was combined with 10 equivalents diphenylphosphine oxide **1** in toluene for 12 h at rt. The reaction of $[ClRh(cod)]_2$ **II** with excess diphenylphosphine oxide **1** is shown in Scheme 2-1. The X-ray diffraction analysis of the crystalline product reveals a distorted trigonal bipyramidal structure, shown in Figure 2-1.

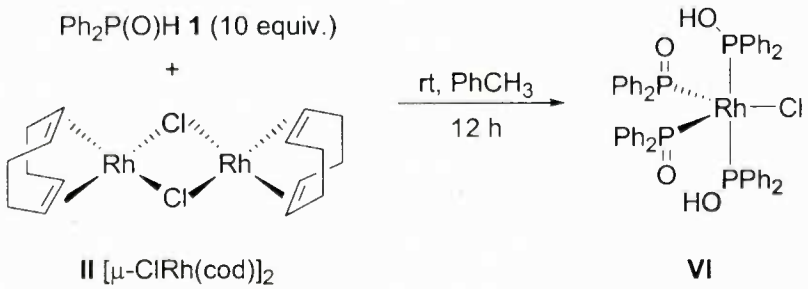


**Scheme 2-1** Synthesis of complex **VI**

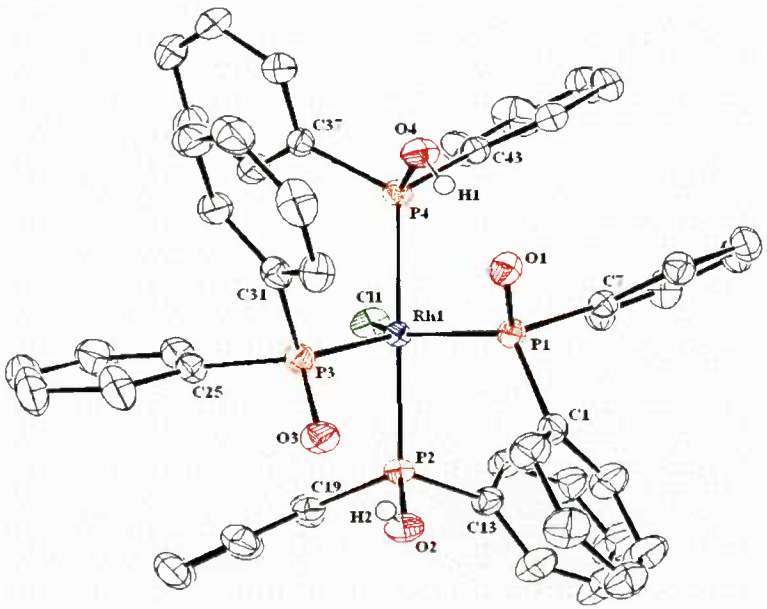


**Figure 2-1** Molecular structure of complex **VI.** Thermal ellipsoids are drawn at the 50% probability level. Most hydrogen atoms are excluded for clarity. Selected bond lengths (Å) and angles (deg): Rh-P(1) = 2.2668(6), Rh-P(2) = 2.4006(6), Rh-P(3) = 2.2880(5), Rh-P(4) = 2.3902(6), Rh-Cl = 2.4177(5), P(1)-O(1) = 1.5287(14), P(2)-O(2) = 1.5855(14), P(1)-Rh-P(3) = 88.457(19), P(1)-Rh-Cl = 128.907(19), P(3)-Rh-Cl = 142.626(19), P(2)-Rh-P(4) = 175.228(17).

Complex **VI** is the apparent product of exchange of cod ligand for diphenylphosphine oxide **1**. There are both tautomers of diphenylphosphine oxide present in the structure, $Ph_2P(O)$-H and $Ph_2P$-OH. Hydrogen bonding between P-O and O-H is evident from the distances between these groups. It is thought that this complex may be a precursor to the active catalyst.

The reaction of [Tp*Rh(PPh$_3$)$_2$] **III** with excess diphenylphosphine oxide **1** is shown in Scheme 2-2.[113] The crystalline product was analyzed by X-ray diffraction to reveal a dirhodium complex that has square planar geometry about both rhodium atoms. The solid-state structure of complex **VII** is shown in Figure 2-2.

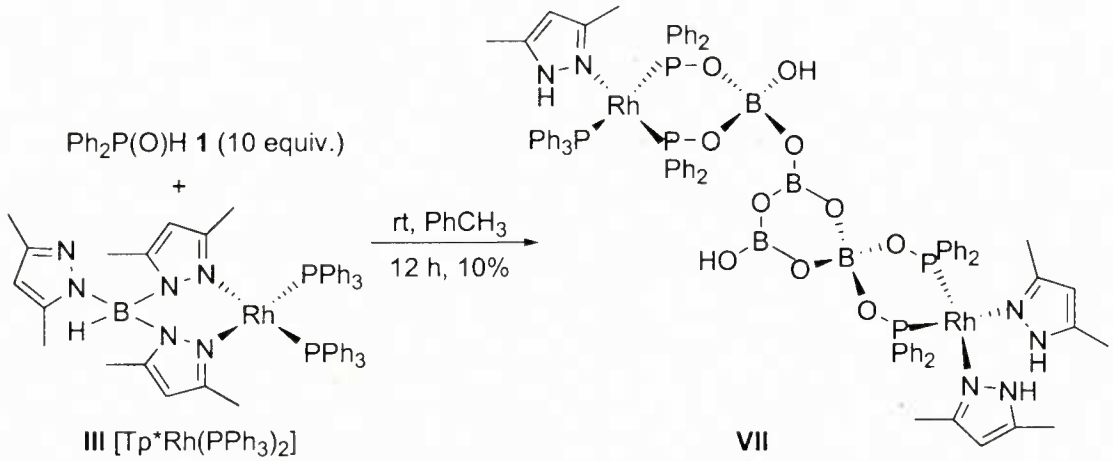


**Scheme 2-2** Synthesis of complex **VII**

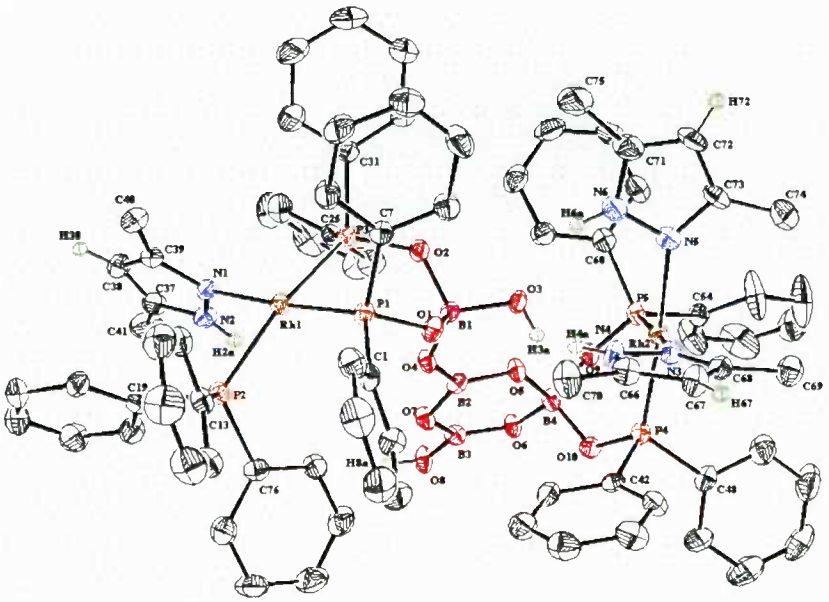

**Figure 2-2** Molecular structure of complex **VII.** Thermal ellipsoids are drawn at the 50% probability level. Hydrogen atoms are excluded for clarity. Selected bond lengths (Å) and angles (deg): Rh(1)-P(1) = 2.2299(11), Rh(1)-P(2) = 2.3369(11), Rh(1)-P(3) = 2.3007(11), Rh(1)-N(1) = 2.111(3), Rh(2)-P(4) = 2.2215(11), Rh(2)-P(5) = 2.2073(11), Rh(2)-N(3) = 2.136(3), Rh(2)-N(5) = 2.155(3), B(1)-O(1) = 1.487(5), B(1)-O(3) = 1.451(5), B(2)-O(5) = 1.359(5), B(4)-O(5) = 1.480(5), P(1)-Rh(1)-P(2) = 96.58(4), P(1)-Rh(1)-P(3) = 84.78(4), P(2)-Rh(1)-P(3) = 167.46(4), P(4)-Rh(2)-P(5) = 88.53(4), P(4)-

Rh(2)-N(3) = 93.33(9), P(4)-Rh(2)-N(5) = 173.66(9).

Complex **VII** is probably not an intermediate in the hydrophosphinylation pathway, but is more likely a decomposition product. There is evidence of fragmentation of the Tp* ligand, since complex **VII** contains no Tp* yet has four atoms of boron, probably from four molecules of Tp*. It appears that diphenylphosphine oxide **1** has exchanged with the B-N and B-H bonds in Tp*. Two of the boron atoms are four coordinate and the other two are three coordinate. Examples of fragmentation of pyrazolylborate ligands on rhodium complexes are known.[36] The formation of complex **VII** does indicate some instability of the catalyst. However, the yield of this decomposition product after 12 h was low (10%) and [Tp*Rh($PPh_3$)$_2$] **III** was shown to effect catalytic hydrophosphinylation in under 3 h.

### 2.3.2.1 Effect of catalyst decomposition on hydrophosphinylation

We suspected that other potentially catalytic species may be forming in solution since it is known that pyrazolylborate ligands can fragment under certain conditions.[36] Indeed, we have found evidence that Tp* can break apart, as shown by the formation of complex **VII**.[113] We wanted to investigate whether the Tp* fragments could contribute to active hydrophosphinylation catalysts forming with rhodium *in situ*. To test this, dimethylpyrazole and [ClRh(cod)]$_2$ **II** were combined in THF and stirred at room temperature overnight. $NaBPh_4$ was added to the solution and the solvent was reduced by vacuum. A fine yellow precipitate was collected by filtration. A sample of this product was added to a solution of $Ph_2P(O)H$ **1** and 1-octyne **2** in acetone-$d_6$ and monitored by $^1H$ NMR spectroscopy. The spectrum shows a small amount of the hydrophosphinylation product **3a** had formed.

Han *et al.* suggest that in alkyne hydrophosphinylation reactions catalyzed by either $[ClRh(PPh_3)_3]$ **I** or $[ClRh(cod)]_2$ **II**, the same active catalytic species forms in solution and results in similar yields and regioselectivity for these two catalysts (see Chapter 1: Section 1.2.4.3 and below: Section 2.3.4).[59] Perhaps the reason that we observe the same regioselectivity as was obtained for other rhodium catalysts is that the pyrazolylborate ligand is being removed from Rh and the same active species is generated. To further examine the reactivity of potential catalytic species that may be forming in solution, a comparison was made between three metal complexes. The complexes used were $[ClRh(cod)]_2$ **II**, $[Tp^*Rh(cod)_2]$ **III** prepared *in situ* from a mixture of $[ClRh(cod)]_2$ **II** and KTp*, and $[(OTf)Rh(pz^*)_3]$ prepared *in situ* from a mixture of $[ClRh(cod)]_2$ **II**, dimethylpyrazole, and silver triflate. Stoichiometric reactions of 1-octyne **1** with diphenylphosphine oxide **2** and one of three metal complexes were monitored by $^1H$ and $^{31}P$ NMR spectroscopy. The expected hydrophosphinylation product was observed in each of the $^1H$ NMR spectra, along with a corresponding disappearance of the starting materials. Based on the promising results of these initial test reactions, this set of experiments was repeated using catalytic conditions. For these catalytic reactions, the NMR data shows the disappearance of all starting diphenylphosphine oxide **1** and the appearance of (*E*)-1-(diphenylphosphinyl)-1-octene **3a** in 100% yield. This yield was achieved in less than 25 minutes for all three reactions. This result reveals that all three of these catalyst preparations seem to be equally active for hydrophosphinylation performed on a small scale.

## 2.3.3 Other P-H activation reactions

P-H sources other than diphenylphosphine oxide **1** were considered for reaction

with alkynes catalyzed by rhodium pyrazolylborate complexes. The other P-H bond sources that were considered included $Ph_2PH$ **14**, $(MeO)_2P(O)H$ **15**, and $(EtO)_2P(O)H$ **16**.

### 2.3.3.1 Reactions of [TpRh(cod)] with diphenylphosphine

A small-scale catalytic reaction was performed with diphenylphosphine **14** in combination with equimolar 1-octyne **2** and 3 mol % of [TpRh(cod)] **VIII** in toluene-$d_8$ in an NMR tube. A small amount of rhodium hydride formed immediately at room temperature, as observed by $^1H$ NMR spectroscopy (δ -13.8). After several days at room temperature, the reaction showed the formation of a trace amount of hydrophosphination product **3a**. The reaction mixture was heated for 2 h to 80 °C and monitored by $^1H$ NMR spectroscopy but no further product formed from this treatment. [TpRh(cod)] **VIII** was shown as a non-viable catalyst with low activity for the hydrophosphination of 1-octyne **2** with diphenylphosphine **14** for these reaction conditions.

The formation of a hydride in the above reaction suggests that [TpRh(cod)] **VIII** activated the diphenylphosphine P-H bond and this result inspired further study into the stoichiometric reaction of [TpRh(cod)] **VIII** with diphenylphosphine **14**, monitored by $^1H$ and $^{31}P$ NMR spectroscopy. The appearance of Rh-H peaks in the $^1H$ NMR spectrum suggests that P-H activation of diphenylphosphine **14** had occurred.

### 2.3.3.2 Reactions of [TpRh(cod)] with dialkylphosphites

Small-scale catalytic reactions were performed with dialkylphosphites ($(MeO)_2P(O)H$ **15** and $(EtO)_2P(O)H$ **16**) in combination with equimolar 1-octyne **2** and 3 mol % of [TpRh(cod)] **VIII** in toluene-$d_8$ in an NMR tube. The immediate formation of small amounts of rhodium hydrides (around -14 ppm) were observed by $^1H$ NMR spectroscopy at room temperature. Heating the reaction mixtures to 80 °C for 2 h had

produced no further product as observed by $^{1}H$ NMR spectroscopy. [TpRh(cod)] **VIII** was not shown to be an active catalyst for the hydrophosphorylation of 1-alkyne **2** with dialkylphosphites for these reaction conditions.

Again, the formation of hydrides suggests that [TpRh(cod)] **VIII** activated P-H bonds so stoichiometric reactions of [TpRh(cod)] **VIII** with dialkylphosphites were performed and monitored by $^{1}H$ and $^{31}P$ NMR spectroscopy. The stoichiometric reactions of [TpRh(cod)] **VIII** with dialkylphosphites ($(MeO)_2P(O)H$ **15** and $(EtO)_2P(O)H$ **16**) showed peaks in their $^{1}H$ NMR spectra indicative of the formation of Rh-H, suggesting P-H bond activation. These spectra have two very interesting features worth noting. First, they each have broad singlet peaks around 17 ppm, the exact location seems to vary depending on concentration and temperature. Second, they each have hydride peaks at around –14 ppm with very well-resolved splitting into a doublet of double doublets (ddd). For the product formed from $(MeO)_2P(O)H$ **15**, δ -14.3 (ddd, $^{1}J_{Rh\text{-}H}$ = 20.8 Hz, $^{2}J_{P\text{-}H}$ = 24.4 Hz, $^{2}J_{P\text{-}H}$ = 13.6 Hz, Rh-*H*). For the product formed from $(EtO)_2P(O)H$ **16**, δ -14.2 (ddd, $^{1}J_{Rh\text{-}H}$ = 20.9 Hz, $^{2}J_{P\text{-}H}$ = 24.3 Hz, $^{2}J_{P\text{-}H}$ = 13.3 Hz, Rh-*H*).

The broad singlets at 17 ppm are of interest because there are very few types of protons known to give peaks at such low field. Peaks found in this region are indicative of very strong hydrogen bonding resulting in an unusually highly deshielded proton. Molecules that are known to have proton peaks appear as high as 16 ppm include intermolecular hydrogen bonded alcohols and pyrroles.[117]

The well-resolved ddd hydrides indicate three strong couplings to the rhodium hydride proton. One of these splittings is due to direct coupling with $^{103}Rh$. The broad band $^{31}P\{^{1}H\}$ NMR spectrum shows the hydride peak has simplified to a doublet. The

other two splittings are almost certainly two-bond couplings with $^{31}P$. As there are two unique coupling constants, this indicates that there must be two different $^{31}P$ environments. Other features of the $^{1}H$ NMR spectra suggest that there are four distinct alkyl group environments of equivalent abundance.

A 2D COSY spectrum was collected of the diethyl phosphite **16** and [TpRh(cod)] **VIII** reaction mixture but did not reveal any new information since the species of interest forms in concentrations too low to be usable for this experiment. Attempts to isolate the complex and prepare more concentrated samples were unsuccessful. The $^{31}P\{^{1}H\}$ NMR spectrum shows two doublet of doublets (dd) of equivalent abundance at δ 113.9 ($J$ = 36.5, $J$ = 190.1) and δ 84.9 ($J$ = 35.9, $J$ = 163.9). When the $^{1}H$ decoupler is turned off for the $^{31}P$ NMR spectrum, these signals appear as poorly resolved doublets of double doublets.

In a similar experiment, Trzeciak and Ziólkowski react $[Rh(acac)(CO)_2]$ with excess diphenylphosphite to form the $Rh^{III}$ complex, $[HRh\{[P(OPh)_2O]_2H\}_2]$, shown in its two isomeric forms in Scheme 2-3.[116] These proposed structures were based on $^{1}H$ and $^{31}P$ NMR studies. $^{1}H$ NMR spectroscopy showed a doublet of quintets for the square pyramidal isomer and doublet of double quartets for the trigonal bipyramidal isomer. They suggest that the large $J_{(P\text{-}H)}$ (229 Hz) indicates that the hydride and a phosphorus are located trans to each other in the trigonal bipyramidal structure. The cyclic $[P(OPh)_2O]_2H$ ligand forms from the coordination of two molecules of diphenylphosphite, one of each tautomeric form represented. The isomerism of hydrogen phosphonates is shown in Scheme 2-4.[118] The tetracoordinated phosphorus tautomer (A) coordinates to Rh by oxidative addition, thereby providing the hydride ligand as well. The tricoordinated

phosphorus tautomer (B) coordinates datively from the lone pair on phosphorus. Hydrogen bonding stabilizes the resulting cyclic $[P(OPh)_2O]_2H$ ligand.

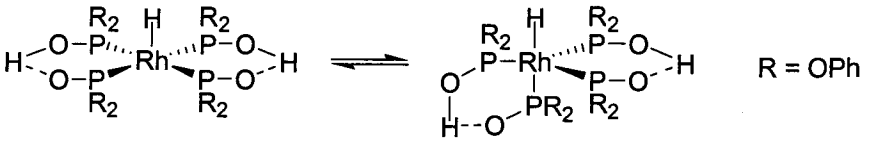


**Scheme 2-3** Isomerism of $[HRh\{[P(OPh)_2O]_2H\}_2]$

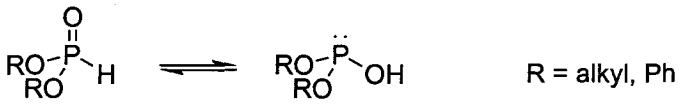


**Scheme 2-4** Tautomerism of hydrogen phosphonates

Figure 2-3 shows the general proposed structure that fits the NMR spectroscopic evidence found for the reactions of [TpRh(cod)] **VIII** with alkylphosphites ($(MeO)_2P(O)H$ **15** and $(EtO)_2P(O)H$) **16**. This proposed structure was inspired in part by the similarity of the Trzeciak and Ziólkowski experiment with the reactions presented here between [TpRh(cod)] **VIII** and dialkylphosphites. They observe a doublet of double quartets for their trigonal bipyramidal complex and one would expect a doublet of double doublets for the analogous structure with two fewer equatorial phosphorus nuclei, as in the proposed complexes **IX** and **X**. The approximately 17 ppm broad singlet peaks might be the signals for the O-H on $(RO)_2P(OH)$, hydrogen bonded to $(RO)_2P(O)^-$. A cyclic $[P(OR)_2O]_2H$ ligand is consistent with the Trzeciak and Ziólkowski example as well as with our result for complex **VI**. The structure shown in Figure 2-4 is based on the X-ray crystal structure that we obtained for complex **VI**.

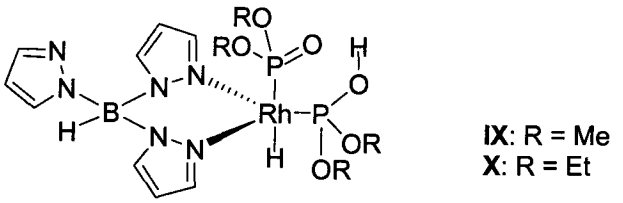


**IX**: R = Me
**X**: R = Et

**Figure 2-3** Structures of proposed complexes **IX** and **X**

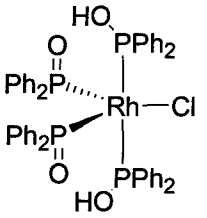


**Figure 2-4** Structure of complex **VI**

Trzeciak and Ziólkowski reported only the hydride peaks for their $^1$H NMR results; no low-field signals were reported for their complex, [HRh{[P(OPh)$_2$O]$_2$H}$_2$]. One might expect that such a structure could exhibit low-field peaks in the $^1$H NMR spectrum since its P-O-H-O-P moiety has much in common with that of intermolecular hydrogen bonded alcohols, known for their low-field peaks.

Several attempts were made to prepare high quality crystals of the products of reactions of [TpRh(cod)] **VIII** with dialkylphosphites in an effort to reveal the structures of these products by X-ray crystallography. For these reactions, a toluene solution of the reaction mixture was filtered through Celite then concentrated under vacuum. The concentrates were layered with hexanes and left to precipitate. Within minutes, a fine yellow precipitate crashed out of solution. Another technique to prepare crystals involved placing concentrated toluene solutions in small vials, inside of larger vials and adding pentane to the outer vials. The outer vials were capped and placed in a freezer inside the glovebox for several days. By this technique, no precipitates formed. These samples have been left in the glovebox over many months in the hope that crystals may form one day.

### 2.3.4 Mechanism of P-H bond activation reactions

Trzeciak and Ziólkowski observed two rhodium hydride species in the $^1$H NMR spectrum of their reaction of [Rh(acac)(CO)$_2$] with excess diphenylphosphite, discussed above and shown in Scheme 2-3.[116] Similarly in their mechanistic investigations on hydrophosphinylation, Han *et al.* observed two Rh-H species, one with a doublet of double quartets and one with a doublet of quintets in the $^1$H NMR spectrum (see Chapter 1, Section 1.2.4.3).[59] The doublet of quintets suggests that the hydride is coupled to rhodium and to four identical phosphorus nuclei. The doublet of double quartets suggests that in addition to the rhodium coupling, there are four phosphorus nuclei but one of these is in a unique environment from the other three. In the reaction between [TpRh(cod)] **VIII** and excess dialkylphosphites performed by our group, a Rh-H species is observed as a doublet of double doublets in the $^1$H NMR spectrum. This suggests that there are just two phosphorus nuclei on rhodium, each in unique environments. Presumably only two phosphorus ligands add to rhodium in this example because Tp remains attached as well. The results of three research groups (Trzeciak and Ziólkowski, Han *et al.*, and our group) seem to consistently show that when certain Rh complexes are combined with an excess of secondary phosphine oxides or dialkylphosphites (both P-H sources) that P-H activation occurs to yield rhodium hydrides ligated by phosphine oxides or dialkylphosphites. Since oxidative addition of P-H to the rhodium complex occurs immediately for each of these examples, it is likely that this is a common initial step in the mechanism of P-H activation reactions catalyzed by pyrazolylborate rhodium complexes or by [ClRh(cod)]$_2$ **II** or ClRh(PPh$_3$)$_3$ **I** and that the overall mechanisms for these reactions are likely very similar to that proposed by Han *et al.* for rhodium-catalyzed hydrophosphinylation of alkynes discussed in Chapter 1.[59] A proposed general

mechanism for P-H bond activations catalyzed by rhodium complexes is shown in Scheme 2-5. In this generalized mechanism, oxidative addition of a P-H bond to the Rh complex forms a Rh-H species in the first step. The next step is a migratory insertion of the alkyne into the Rh-H bond. Finally, reductive elimination yields the product and regeneration of the catalyst.

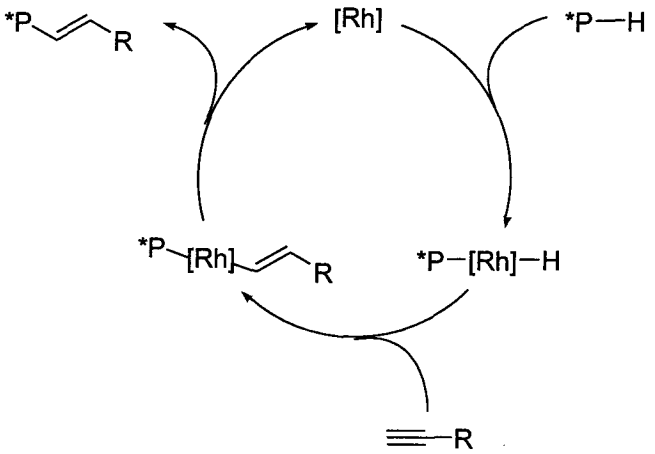


*P—H = a secondary phosphine oxide or dialkylphosphite

**Scheme 2-5** Generalized mechanism of P-H activation reactions catalyzed by rhodium complexes

## 2.4 Conclusions

[Tp*Rh(cod)] **IV** and [Tp*Rh($PPh_3$)$_2$] **III** have now been shown to catalyze hydrophosphinylation of 1-octyne **2** with diphenylphosphine oxide **1**, adding to our knowledge of rhodium pyrazolylborate reactivity. The yields for catalytic hydrophosphinylation by these two rhodium pyrazolylborates were moderate and not as high as the yields for these reactions with Wilkinson's catalyst **I**. [Tp*Rh($PPh_3$)$_2$] **III** was further shown to catalyze hydrophosphinylation of a range of alkyne substrates, all of which provided exclusively the vinylphosphine oxide resulting from *syn*-addition of P-H across the alkyne bond. This regioselectivity contrasts with results for hydrothiolation reactions, where these Tp*RhL$_n$ complexes mainly provided the branched products.[41]

Aliphatic alkynes provided higher yields than aromatic alkynes. An internal aliphatic alkyne provided the highest yield in the group. It appears that product formation may be directed by the steric bulk of the ligands on rhodium. We propose that hydrophosphinylation catalyzed by rhodium pyrazolylborate complexes follows an analogous mechanism to that proposed by Han *et al.* for hydrophosphinylation by $[ClRh(PPh_3)_3]$ **I** or $[ClRh(cod)]_2$ **II**. There is evidence that related P-H bond activation reactions probably also follow a similar mechanism.

## 2.5 Experimental Procedures

### 2.5.1 General Methods

Manipulation of metallic compounds was performed using standard Schlenk techniques under an atmosphere of dry nitrogen or in a nitrogen-filled Vacuum Atmospheres or MBraun glovebox ($[O_2] < 2$ ppm). NMR spectra were recorded on Bruker Avance 300 or Bruker Avance 400 spectrometers. Toluene and THF were dried by passage through solvent purification columns.[119] $CDCl_3$ was vacuum-transferred from $P_2O_5$ and degassed prior to use. Acetone-$d_6$ and 1,2-dichloroethane were distilled and degassed prior to use. Toluene-$d_8$ was degassed prior to use. All other reagents and solvents were obtained from commercial sources and used as received. $^1H$ and $^{31}P\{^1H\}$ NMR spectra are reported in parts per million and were referenced to residual solvent. Coupling constant values were extracted assuming first-order coupling. $^{31}P\{^1H\}$ NMR spectra were referenced to an external 85% $H_3PO_4$ standard. All spectra were obtained at 25 °C, unless otherwise stated. GC chromatographs were recorded on a Varian CP-3800 or an HP 5890 Series II gas chromatograph. Mass spectra were recorded on a Kratos MS-50 mass spectrometer.

### 2.5.1.1 Preparation of Tp*Rh(PPh$_3$)$_2$ III

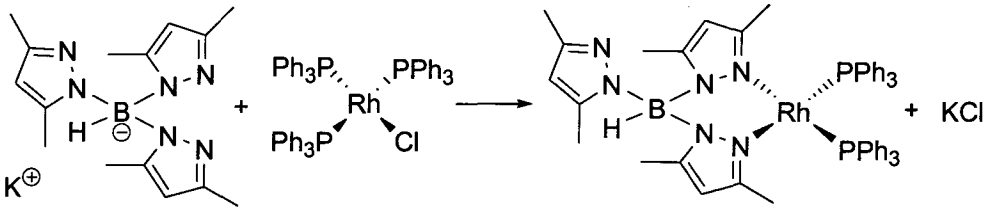


17 I III

A suspension of [ClRh(PPh$_3$)$_3$] **I** (1.00 g, 1.08 mmol) and KTp* **17** (potassium hydrotris{3,5-dimethylpyrazolyl}borate) (0.364 g, 1.08 mmol) in THF (15 mL) was placed in a 50 mL Schlenk flask equipped with a magnetic stir bar and was stirred at room temperature inside a glovebox for 2 h. The suspension dissolved fully and turned from dark red to orange within 1 h. After 2 h, most of the THF was removed by vacuum. Toluene was added and the resultant slurry was filtered through Celite to remove KCl. The solvent was removed by vacuum via Schlenk line from the crude product. To improve the purity, the product was redissolved in a minimal quantity of toluene and then hexane was added to the toluene solution and the product precipitated. The precipitate was collected and washed 5 times with 1 – 2 mL hexane to ensure that no residual starting material remained, as confirmed by the $^{31}$P NMR spectrum. Yield of crude product: 0.92 g (92%). The product identity was confirmed by comparing the $^{31}$P NMR spectrum with reported data.[28]

### 2.5.1.2 Preparation of [Tp*Rh(cod)] IV

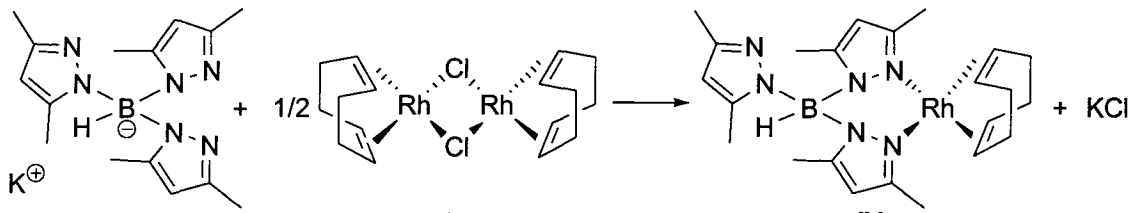


17 II IV

A suspension of [ClRh(cod)]$_2$ **II** (0.083 g, 0.166 mmol) and KTp* **17** (0.11 g,

0.333 mmol) in 15 mL THF was placed in a small Schlenk flask equipped with a magnetic stir bar and stirred at room temperature inside a glovebox overnight. Most of the THF was removed by vacuum. Toluene was added and the resultant slurry was filtered through Celite to remove KCl. The solvent was removed by vacuum. Yield: 0.11 g (65%). The product identity was confirmed by comparing the $^1$H NMR spectrum with reported data.[22]

### 2.5.1.3 Preparation of (*E*)-1-(diphenylphosphinyl)-1-octene 3

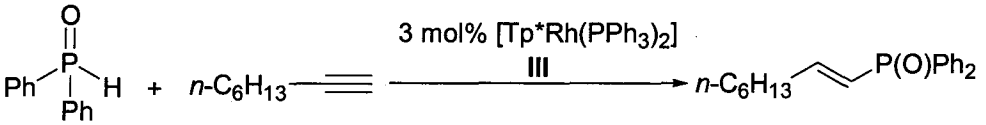


**1** **2** **3**

Tp*Rh(PPh$_3$)$_2$ **III** (28 mg, 0.030 mmol, 3 mol%), toluene (1 mL), diphenylphosphine oxide **1** (207 mg, 1.0 mmol) and 1-octyne **2** (147 μL, 1.0 mmol) were combined in the glove box in a 15 mL Schlenk flask equipped with a magnetic stir bar and a glass stopper. The flask was removed from the glove box and heated in an oil bath at 110 °C for 3 h. After the reaction was completed, the resulting mixture was concentrated under Schlenk line vacuum. Flash chromatography ($SiO_2$ and a 1:1 mixture of hexanes and ethyl acetate as eluent) provided the product as a white solid. Yield: 0.161 g (51%). The product identity was confirmed by comparing the $^1$H and $^{31}$P NMR spectra with reported data.[59]

### 2.5.1.4 General small-scale catalytic hydrophosphinylation procedure

Trimethylsilane (TMS) (0.1 mmol, internal standard), [ClRh(cod)]$_2$ (0.015 mmol, 3 mol% Rh), toluene-$d_8$ (500 μL), diphenylphosphine oxide **1** (21 mg, 0.1 mmol) and 1-octyne **2** (15 μL, 0.1 mmol) were combined in the glove box in an NMR tube. The NMR tube was sealed and shaken to mix the contents. The reactions were maintained at room

temperature. $^{1}H$ and $^{31}P$ NMR spectra were obtained as soon as possible after combining reagents (15 to 25 minutes) and repeated after approximately 1 h, and 3 days.

### 2.5.1.5 Preparation of (*E*)-1-(diphenylphosphinyl)-3,3-dimethyl-1-butene 8

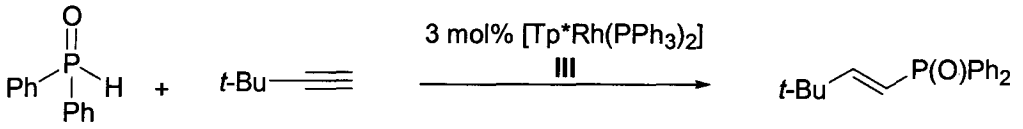


**1** **4** **8**

$Tp^{*}Rh(PPh_3)_2$ **III** (28 mg, 0.030 mmol, 3 mol%), toluene (1 mL), diphenylphosphine oxide **1** (207 mg, 1.0 mmol) and 3,3-dimethyl-1-butyne **4** (12 μL, 1.0 mmol) were combined in the glove box in a 15 mL Schlenk flask equipped with a magnetic stir bar and a glass stopper. The flask was removed from the glove box and heated in an oil bath at 110 °C for 3 hours. After the reaction was completed, the resulting mixture was concentrated under Schlenk line vacuum. Flash chromatography ($SiO_2$ and a 1:1 mixture of hexanes and ethyl acetate as eluent) provided the product as a white solid. Yield: 0.118 g (41%). The product identity was confirmed by comparing the $^{1}H$ and $^{31}P$ NMR spectra with reported data.[59]

### 2.5.1.6 Preparation of (*E*)-1-(diphenylphosphinyl)-2-phenylethene 9

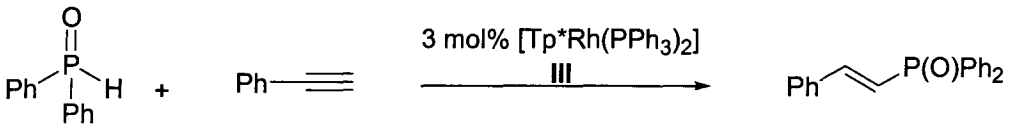


**1** **5** **9**

$Tp^{*}Rh(PPh_3)_2$ **III** (28 mg, 0.030 mmol, 3 mol%), toluene (1 mL), diphenylphosphine oxide **1** (207 mg, 1.0 mmol) and phenylacetylene **5** (11 μL, 1.0 mmol) were combined in the glove box in a 15 mL Schlenk flask equipped with a magnetic stir bar and a glass stopper. The flask was removed from the glove box and heated in an oil

bath at 110 °C for 3 hours. After the reaction was completed, the resulting mixture was concentrated under Schlenk line vacuum. Flash chromatography ($SiO_2$ and a 1:1 mixture of hexanes and ethyl acetate as eluent) provided the product as a white solid. Yield: 0.0529 g (17%). The product identity was confirmed by comparing the $^1H$ and $^{31}P$ NMR spectra with reported data.[59]

### 2.5.1.7 Preparation of (*E*)-1-(diphenylphosphinyl)-2-(4-methoxyphenyl)ethane 10

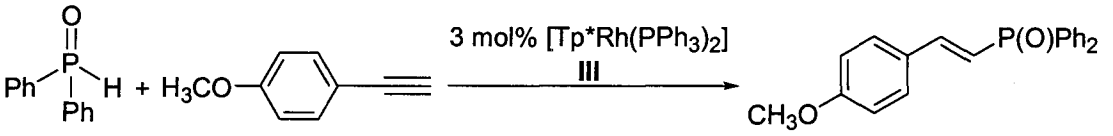


1 6 10

· $Tp^*Rh(PPh_3)_2$ **III** (28 mg, 0.030 mmol, 3 mol%), toluene (1 mL), diphenylphosphine oxide **1** (207 mg, 1.0 mmol) and 1-ethynyl-4-methoxybenzene **6** (13 μL, 1.0 mmol) were combined in the glove box in a 15 mL Schlenk flask equipped with a magnetic stir bar and a glass stopper. The flask was removed from the glove box and heated in an oil bath at 110 °C for 3 hours. After the reaction was completed, the resulting mixture was concentrated under Schlenk line vacuum. Flash chromatography ($SiO_2$ and a 1:1 mixture of hexanes and ethyl acetate as eluent) provided the product as a white solid. Yield: 0.0927 g (28%). $^{31}P$ NMR ($CDCl_3$, 121 MHz) δ 30.44. The product identity was confirmed by comparing the $^1H$ NMR spectrum with reported data.[115]

### 2.5.1.8 Preparation of (*E*)-3-(diphenylphosphinyl)-3-hexene 11

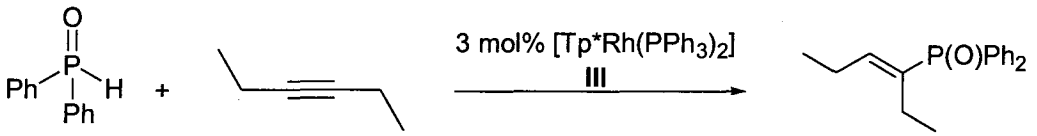


1 7 11

$Tp^*Rh(PPh_3)_2$ **III** (28 mg, 0.030 mmol, 3 mol%), toluene (1 mL), diphenylphosphine oxide **1** (207 mg, 1.0 mmol) and 3-hexyne **7** (11 μL, 1.0 mmol) were

combined in the glove box in a 15 mL Schlenk flask equipped with a magnetic stir bar and a glass stopper. The flask was removed from the glove box and heated in an oil bath and at 110 °C for 3 hours. After the reaction was completed, the resulting mixture was concentrated under Schlenk line vacuum. Flash chromatography ($SiO_2$ and a 1:1 mixture of hexanes and ethyl acetate as eluent) provided the product as a white solid. Yield: 0.172 g (61%). $^1$H NMR ($C_6D_6$, 300 MHz) δ 7.91 - 7.83 (m, 4 H, Ph), 7.24 – 7.16 (m, 6 H, Ph), 6.22 (dt, $J_{P\text{-}H}$ = 21.0 Hz, $J$ = 7.20 Hz, 1 H, C-*H*), 2.38 - 2.30 (m, 2 H), 1.99 - 1.94 (m, 2 H), 0.99 (t, 3 H), 0.79 (t, 3 H). $^{13}$C NMR ($C_6D_6$, 75 MHz) δ 147.51 (d, 1 C), 136.35 (d, 2 C, Ph), 132.69 (d, 4 C, Ph), 131.84 (d, 2 C, Ph), 128.88 (d, 4 C, Ph), 22.51 (br s, 1 C), 21.83 (br s, 1 C), 15.20 (br s, 1 C), 13.86 (br s, 1 C). $^{31}$P NMR ($C_6D_6$, 121 MHz) δ 29.17. HRMS (EI) m/z calcd for $C_{18}H_{21}OP$: 284.1330; found: 284.1335.

### 2.5.1.9 Background reaction procedure

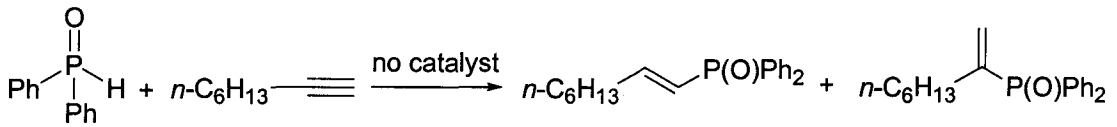


**1** **2** **3a** < 1% **3b** < 1%

Toluene (1 mL), diphenylphosphine oxide **1** (207 mg, 1.0 mmol) and 1-octyne **2** (147 μL, 1.0 mmol) were combined in the glove box in a 15 mL Schlenk flask equipped with a magnetic stir bar and a glass stopper. The flask was removed from the glove box and heated in an oil bath at 110 °C for 3 h. The resulting mixture was concentrated under Schlenk line vacuum. A sample of the crude reaction mixture was dissolved in $C_6D_6$ in an NMR tube. The $^1$H NMR spectrum showed a trace (< 1%) amount of each isomer of hydrophosphinylation product had formed. The product identity was confirmed by comparing the $^1$H and $^{31}$P NMR spectra with reported data.[59]

### 2.5.1.10 Background reaction of diphenylphosphine oxide with triphenylphosphine

$Ph_2P(O)H$ + $Ph_3P$ ⟶ no reaction

**1** **12**

A 1:1 mixture of triphenylphosphine **12** and diphenylphosphine oxide **1** in $CDCl_3$ was monitored by $^{31}P$ NMR in comparison to standards of the two reagents made up to the same concentration in separate NMR tubes. The concentration of the two reagents did not change and no new peaks formed as monitored by $^{31}P$ NMR spectroscopy over 2 hours. After 3 days at room temperature the $^{31}P$ NMR spectrum still showed no evidence of any reaction.

### 2.5.1.11 Preparation of [TpRh(cod)] VIII

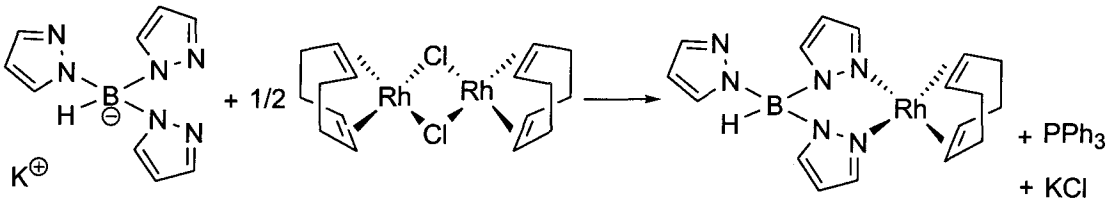


**18** **II** **VIII**

A suspension of $[ClRh(cod)]_2$ **II** (0.083 g, 0.166 mmol) and KTp **18** (potassium hydrotris{pyrazolyl}borate) (0.084 g, 0.333 mmol) in 15 mL THF was placed in a small Schlenk flask equipped with a magnetic stir bar and stirred at room temperature inside a glovebox overnight. Most of the THF was removed by vacuum. Toluene was added and the resultant slurry was filtered through Celite to remove KCl. The solvent was removed by vacuum. Yield: 0.10 g (70%). The product identity was confirmed by comparing the $^1H$ NMR spectrum with reported data.[22]

### 2.5.1.12 Preparation of complex IX

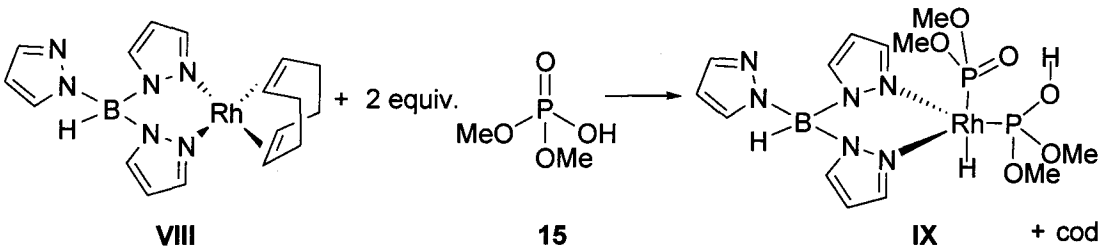


**VIII** **15** **IX** + cod

TpRh(cod) **VIII** (9 mg, 0.02 mmol), toluene-$d_8$ (600 μL), dimethylphosphite **15** (9 μL, 0.1 mmol) were combined in the glove box in an NMR tube. A trace amount of complex **IX** was observed by NMR spectroscopy in the reaction mixture. $^1$H NMR (toluene-$d_8$, 400 MHz) δ 17.2 (br s), -14.3 (ddd, $^1J_{Rh\text{-}H}$ = 20.8 Hz, $^2J_{P\text{-}H}$ = 24.4 Hz, $^2J_{P\text{-}H}$ = 13.6 Hz, Rh-*H*). $^{31}$P NMR (toluene-$d_8$, 162 MHz) δ 116.4 (dd, $J$ = 207 Hz, $J$ = 37.3 Hz), 86.99 (dd, $J$ = 37.9 Hz, $J$ = 165 Hz).

### 2.5.1.13 Preparation of complex X

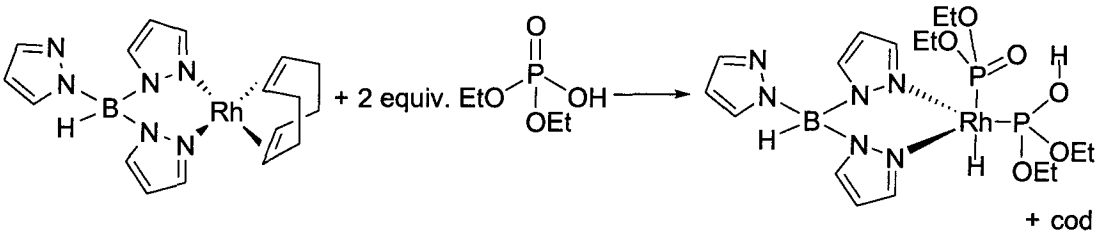


**VIII** **18** **X** + cod

TpRh(cod) **VIII** (9 mg, 0.02 mmol), toluene-$d_8$ (600 μL), diethylphosphite **18** (13 μL, 0.1 mmol) were combined in the glove box in an NMR tube. A trace amount of complex **X** was observed in the reaction mixture by NMR spectroscopy. $^1$H NMR (toluene-$d_8$, 400 MHz) δ 17.3 (br s), 4.5 – 3.5 (4 m, 4 x 2 H, O$CH_2$CH$_3$), 1.35, 1.12, 1.05, 0.89 (4 t, 4 x 3 H, Me), -14.2 (ddd, $^1J_{Rh\text{-}H}$ = 20.9 Hz, $^2J_{P\text{-}H}$ = 24.3 Hz, $^2J_{P\text{-}H}$ = 13.3 Hz, Rh-*H*). $^{31}$P NMR (toluene-$d_8$, 162 MHz) δ 113.0 (dd, $J$ = 190 Hz, $J$ = 36.2 Hz), 84.2 (dd, $J$ = 164 Hz, $J$ = 36.6 Hz).

# 3 Direct functionalization of olefins via 2-rhodaoxetanes

## 3.1 Introduction

The field of metal-mediated olefin functionalizations encompasses a vast range of possible reactions that follow various different mechanisms. This project focuses on reactions that are all expected to proceed along analogous mechanisms via a common intermediate, a 2-metallaoxetane. 2-Metallaoxetanes can theoretically undergo β-H elimination, ring-opening and reductive elimination reactions, shown in Scheme 3-1. Any of these reactions might potentially be incorporated into a catalytic cycle, enabling a wide range of possible products. We postulated that metallaoxetanes could be utilized as reactive intermediates for catalytic functionalizations of olefins. The reactions chosen for study in this project included oxidation, aminohydroxylation and arylhydroxylation of olefins via metallaoxetanes. Scheme 3-2 shows examples of these reactions via a 2-metallaoxetane intermediate of the simplest olefin, ethylene.

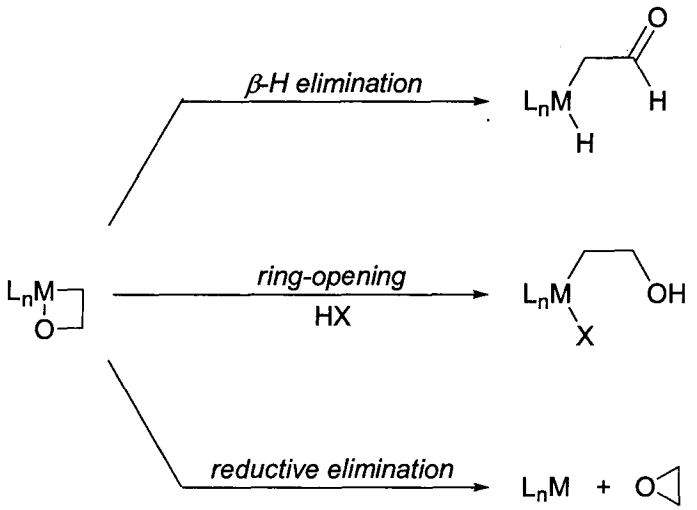


**Scheme 3-1** Reactivity of 2-metallaoxetanes

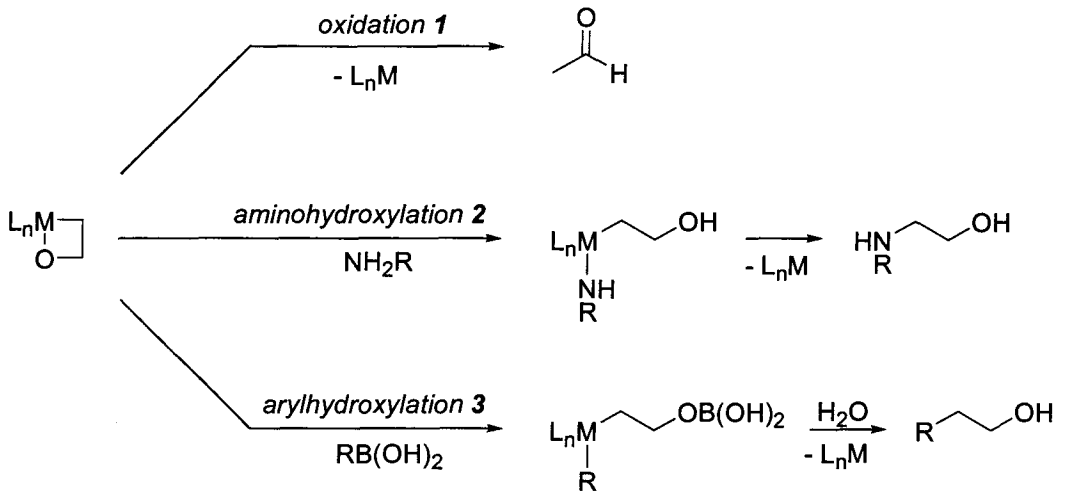


**Scheme 3-2** Oxidation, aminohydroxylation and arylhydroxylation of ethylene, via a 2-metallaoxetane intermediate

The metallaoxetane chosen for the basis of this study was a 2-rhodaoxetane, $[(TPA)Rh^{III}(\kappa^2\text{-C,O-2-oxyethyl})]^+ BPh_4^-$ **XIII**, developed by Gal and coworkers, shown in Figure 3-1.[78] This specific 2-rhodaoxetane complex can be readily generated and isolated, and has shown interesting reactivity[79] that could be exploited for use in potentially catalytic reactions, including oxidation, aminohydroxylation and arylhydroxylation of olefins.

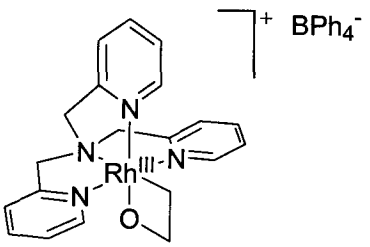


**Figure 3-1** $[(TPA)Rh^{III}(\kappa^2\text{-C,O-2-oxyethyl})]^+ BPh_4^-$ **XIII**

## 3.2 Research goals

### 3.2.1 Catalysis involving a 2-rhodaoxetane intermediate

Reactions of 2-rhodaoxetanes could potentially be incorporated into catalytic

cycles that would lead to a range of products from a common intermediate, as shown in Scheme 3-3. The use of rhodaoxetanes in these reactions would present a mechanistically novel approach to olefin functionalization. Initially we planned to focus on the stoichiometric reactivity of rhodaoxetanes, with the ultimate goal of developing these reactions as catalytic processes. It was important that these reactions eventually be catalytic because of the expense associated with any rhodium compounds. These reactions could make economical sense only if tiny quantities of rhodium are used. Importantly, catalytic turnover would also lessen the environmental impact of these reactions.

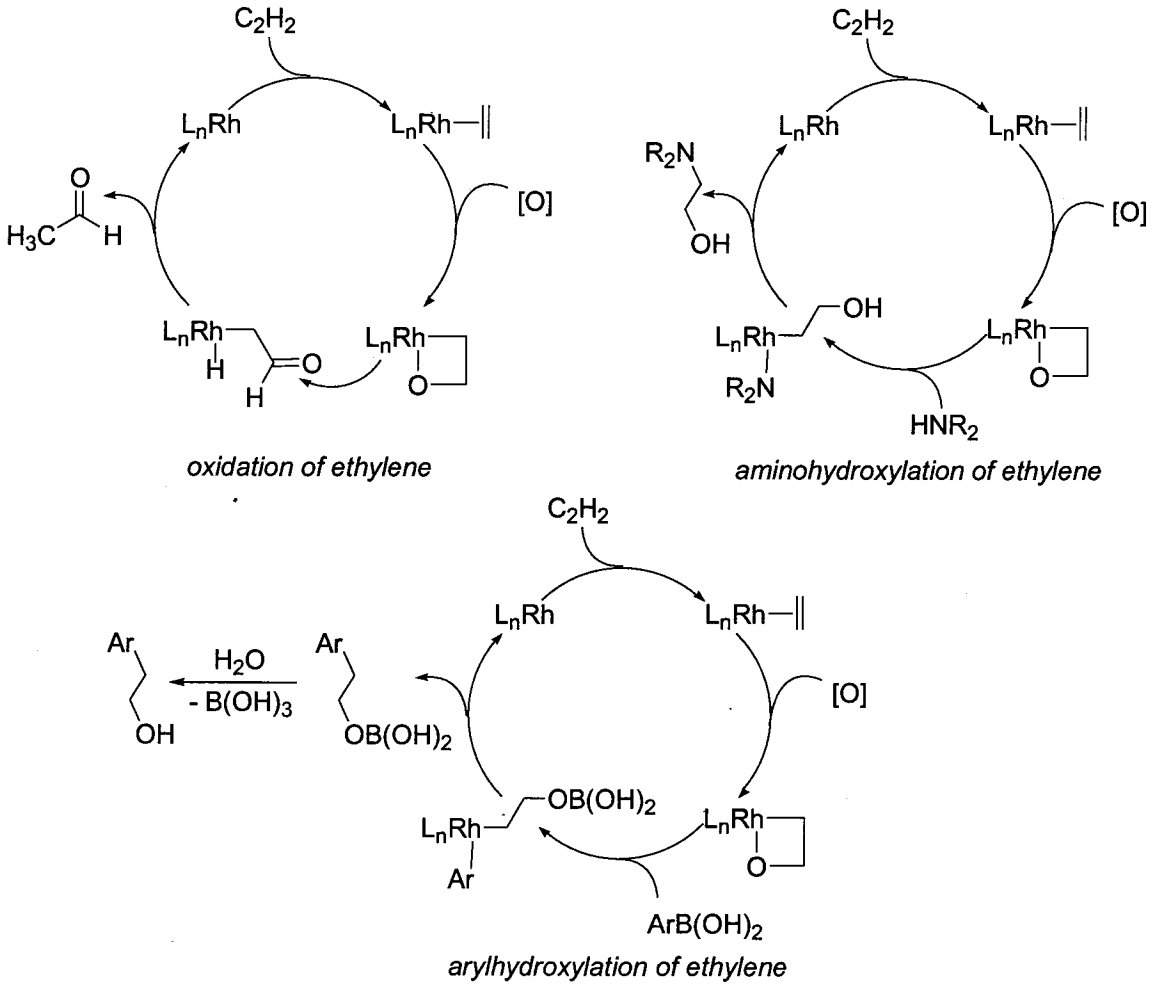


**Scheme 3-3** Proposed catalytic cycles involving a 2-rhodaoxetane intermediate

We planned to first develop catalytic reactions with ethylene and later expand the scope of olefin substrates. If metallaoxetanes could be readily generated from olefins, these catalytic cycles would be very useful.

Gal and coworkers attempted to develop a variation of the catalytic oxidation of ethylene involving a reactive '$N_3$'-rhodaoxetane shown in Scheme 1.13 of the introductory chapter.[80] As previously discussed, catalytic turnover was unsuccessful for this reaction sequence in one pot although the individual steps were achieved separately. They suggest that $H_2O_2$ may be interfering in one or more ways that compete with the desired reactions. One possibility is that coordination by $H_2O_2$ is faster than ethylene and this leads to poisoning of the active catalyst. Additionally, $H_2O_2$ may be further oxidizing the 2-rhodaoxetane intermediate to a formylmethyl-hydroxy complex. Perhaps an alternative oxidant could be found that would be more successful, for instance, nitrous oxide.

TPA-rhodaoxetane and other related metallaoxetanes are isolable, which means that certain reaction steps of the potentially catalytic cycles can be studied individually. This feature provides the investigators with more control over the many aspects of this research. Hopefully it should be possible to fine-tune the catalyst and conditions in order to achieve catalytic turnover for these reactions.

### 3.2.2 Regioselectivity of olefin functionalization reactions via 2-rhodaoxetanes

Once the proposed olefin functionalization reactions have been achieved with ethylene, the next step of this project would be to develop the regioselectivity of these transformations by exploring a range of possible unsymmetrical olefin substrates.

Working with the simplest olefin, ethylene, there are no regiochemistry issues with which to contend. Scheme 3-4 shows how the use of unsymmetrical olefins could lead to two possible regioisomers of 2-rhodaoxetanes.

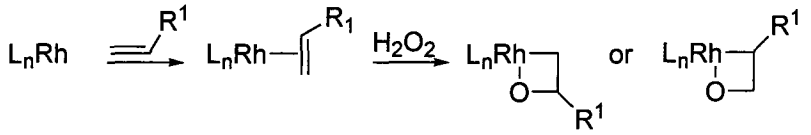


**Scheme 3-4** Possible regioisomers of 2-rhodaoxetanes formed from a mono-substituted olefin

This regioselectivity would be explored for a number of unsymmetrical olefins and for different ligands on the rhodium center. Scheme 3-5 shows the possible outcomes of using monosubstituted olefins in each of the three types of reactions we planned to pursue for this project.

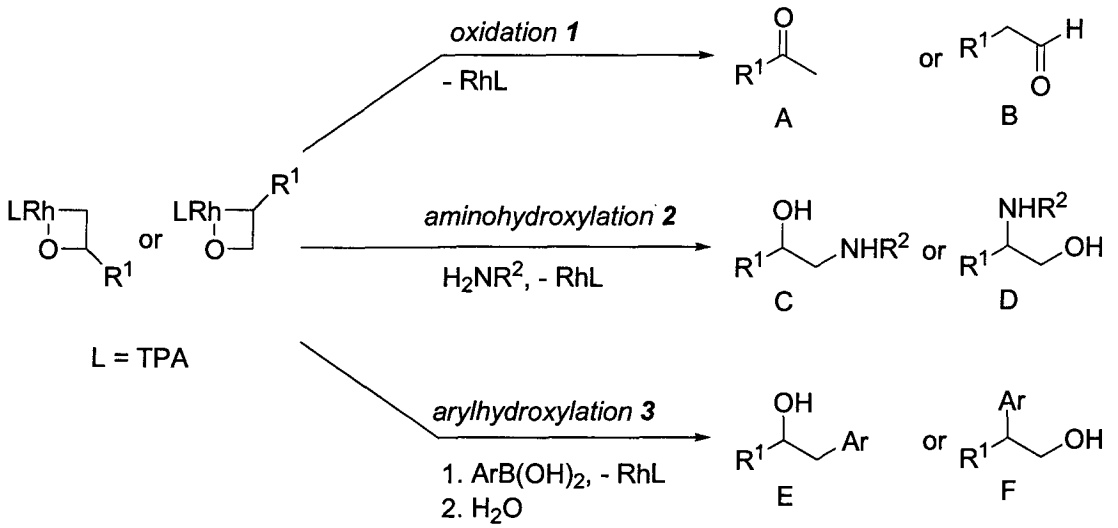


**Scheme 3-5** Possible outcomes of the proposed functionalization reactions with monosubstituted olefins

Regioselectivity of rhodaoxetane formation would determine whether Markovnikov or *anti*-Markovnikov product formation would be favored. Our approach involves setting the stereochemistry at the oxidation step, when discrete Rh-C and Rh-O

bonds are formed in close proximity to the other ligands on the metal center. Changes made to the auxiliary ligands will alter the sterics and electronics of the complex, which should affect the regiocontrol of these reactions. A range of ligands will be explored in an effort to improve the regioselectivity of these reactions for various olefinic substrates.

### 3.2.3 Oxidation via TPA-rhodaoxetane

Gal and coworkers have demonstrated that 2-rhodaoxetanes can eliminate acetaldehyde either by heating to 65 °C or by activation with the non-coordinating acid $[H(OEt_2)_2]B(C_6H_3(CF_3)_2)_4$, $HBAr^f_4$.[79,80] A catalytic version of this reaction remains to be developed. We eventually plan to explore a range of substituted olefinic substrates for the potential development of regio- and enantioselective versions of this reaction. Equation 1 of Scheme 3-5 shows the two possible regioisomeric products of the oxidation of mono-substituted olefins, methyl ketones (A) or aldehydes (B). The aldehyde product (B) would be of particular interest since the Wacker reaction provides the opposite regioisomer (A).

### 3.2.4 Aminohydroxylation and arylhydroxylation via TPA-rhodaoxetane

The aminohydroxylation of olefins provides vicinal amino alcohols by the simultaneous incorporation of both a nitrogen and an oxygen. Aminohydroxylation of olefins via 2-rhodaoxetanes (Scheme 3-5, Eq. 2) would be an improvement over existing methods that involve expensive and toxic osmium reagents or radicals, both of which lack regiocontrol.[120,121] There are numerous other methods for producing vicinal amino acids from olefins, most significant among them are ring-opening reactions of either epoxides or aziridines.[122] Each of these transformations involves two reactions: first the epoxidation or aziridination of the appropriate olefin, then nucleophilic ring opening by a nitrogen or oxygen nucleophile, respectively. Regioselectivity is the dominant issue for

both of these ring-opening reactions since either of the two carbons in the epoxide or aziridine can be targeted by the nucleophile. Aminohydroxylation via 2-rhodaoxetanes would be mechanistically different from existing methods and is expected to yield vicinal amino alcohols chemoselectively. Changes made to the auxiliary ligands may effect regiocontrol over these reactions since the regiochemistry is determined at the oxidation step. The eventual use of chiral ligands for this reaction has the potential to provide greater stereocontrol over the products.

Arylhydroxylation of olefins via 2-rhodaoxetane intermediates (Scheme 3-5, Eq. 3) would constitute a novel method for simultaneous incorporation of a hydroxyl and an aryl group and potentially also vinyl and alkyl moieties.

Scheme 3-6 shows a proposed mechanism of the insertion reaction of acetone into TPA-rhodaoxetane **XIII**, followed by analogous mechanisms for the addition reactions we planned to develop with amines and organometallic reagents. The reactivity of TPA-rhodaoxetane **XIII** towards electrophiles has been demonstrated and is driven by the strongly nucleophilic character of the 2-rhodaoxetane oxygen.[79] We plan to exploit this reactivity for the development of two new reactions, aminohydroxylation and arylhydroxylation of olefins via metallaoxetanes. These transformations will require the successful ring-opening of the 2-rhodaoxetane by a chosen substrate followed by reductive elimination of the product from rhodium.

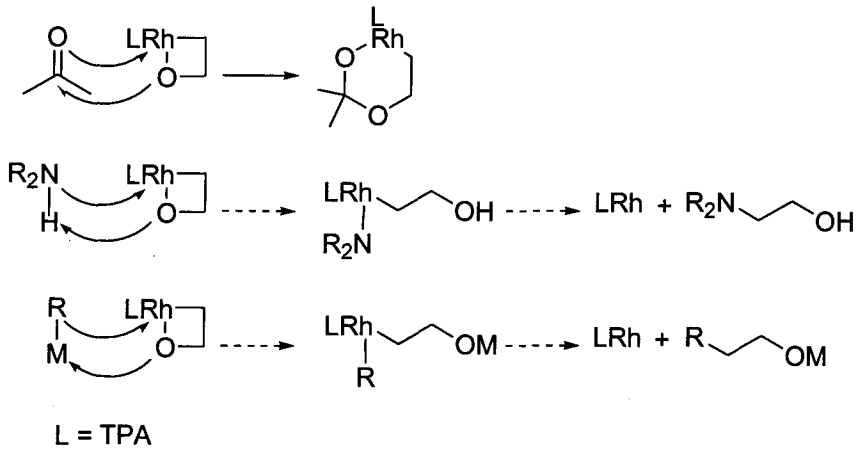


**Scheme 3-6** Mechanisms for the reactions of TPA-rhodaoxetane **XIII** with acetone, amines and organometallics

Hayashi and coworkers have achieved the Rh-catalyzed 1,4-addition of aryl and alkenylboronic acids to enones and certain other α,β-unsaturated compounds, shown in Scheme 3-7.[123-125] This highly successful transformation involves the transmetalation of the aryl or alkenylboronic acid with a Rh-O bond (both rhodium hydroxides and alkoxides). This transmetalation step is mechanistically analogous to the first step shown of our proposed reaction of TPA-rhodaoxetane **XIII** with an organometallic substrate in Scheme 3-6 above.

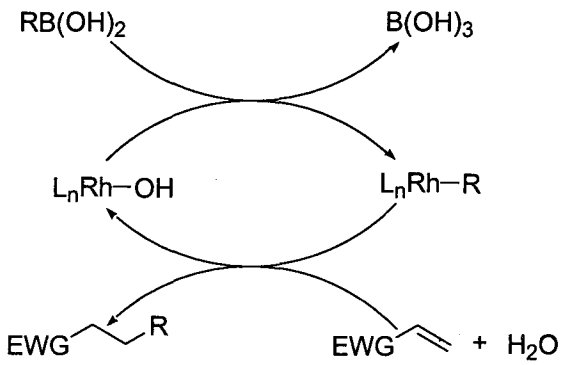


**Scheme 3-7** Rh-catalyzed 1,4-addition reaction

## 3.3 Results and Discussion

TPA-rhodaoxetane **XIII** is of central importance to this study. All of our proposed reactions for study involve TPA-rhodaoxetane **XIII** or possibly a related rhodaoxetane species. Our initial plan was to first prepare TPA-rhodaoxetane **XIII** according to known methods, then use this complex to explore the proposed olefin functionalization reactions, as described in Section 3.2.

### 3.3.1 Preparation of TPA

Tris[(2-pyridyl)methyl]amine (TPA) **21** was prepared following the literature method.[126] In the literature procedure TPA **21** was purified by distillation under vacuum. Our attempts to purify TPA **21** by this method were unsuccessful, perhaps because the strength of the vacuum available to us was much higher than the one used in the literature procedure and this made the distillation difficult to control. An alternative method was developed using an unusual extraction method with water and acetone. The crude TPA **21** was dissolved in a minimal quantity of acetone. The concentrated acetone solution was decanted off of any undissolved material. Sufficient distilled water was added to the concentrated acetone solution to approximately double the total volume. The mixture formed two layers; the top layer was pale yellow and cloudy and the bottom layer was tarry orange-brown. The upper layer was decanted and dried to yield pure TPA crystals. The bottom layer contained TPA **21** and impurities. This extraction could be repeated on the dried bottom layer to yield several batches of highly pure TPA **21**, as determined by $^1$H NMR spectroscopy.

### 3.3.2 Preparation of $[(\eta^2\text{-ethene})(\kappa^4\text{-TPA})Rh^I]^+ BPh_4^-$

The rhodium ethylene complex, $[(\eta^2\text{-ethene})(\kappa^4\text{-TPA})Rh^I]^+ BPh_4^-$ **XII**, was

prepared following the procedure published by de Bruin *et al.*[78] De Bruin reports a yield of 59% for this complex and our best yield was 53%. They filter the solution away from the precipitated product but otherwise do not report any purification steps.

### 3.3.3 Preparation of TPA-rhodaoxetane

Three methods for preparing TPA-rhodaoxetane **XIII** were explored. The first two methods were published by de Bruin *et al.*[78,80] and involve the use of hydrogen peroxide to oxidize the TPA-rhodium ethylene complex **XII**. The third method uses nitrous oxide as the oxidant. None of these methods produced TPA-rhodaoxetane **XIII** reliably and in all three cases the yields were very low. Attempts to isolate TPA-rhodaoxetane **XIII** invariably led to a loss of the product, presumably due to decomposition.

#### 3.3.3.1 Preparation of TPA-rhodaoxetane by hydrogen peroxide oxidation

De Bruin *et al.* report two methods for the preparation of TPA-rhodaoxetane **XIII** by oxidation of $[(\eta^2\text{-ethene})(\kappa^4\text{-TPA})Rh^I]^+$ **XII** with hydrogen peroxide. The first method uses isolated $[(\eta^2\text{-ethene})(\kappa^4\text{-TPA})Rh^I]^+$ **XII** that was prepared previously.[78] The second method involves the direct preparation of TPA-rhodaoxetane **XIII** from $[(\eta^2\text{-ethene})(\kappa^4\text{-TPA})Rh^I]^+$ **XII** prepared *in situ* and directly oxidized by hydrogen peroxide.[80]

By the first method we prepared $[(TPA)Rh^{III}(\kappa^2\text{-}C,O\text{-2-oxyethyl})]^+ BPh_4^-$ **XIII** from $[(\eta^2\text{-ethene})(\kappa^4\text{-TPA})Rh^I]^+ BPh_4^-$ **XII**. According to the published procedure, $[(\eta^2\text{-ethene})(\kappa^4\text{-TPA})Rh^I]^+ BPh_4^-$ **XII** is used as it was prepared, with no additional purification steps. Our reaction was done on a very small scale in an NMR tube. The product was immediately analyzed by $^1H$ NMR spectroscopy, which matched the data published by de Bruin *et al.*[78] Attempts to isolate the product were unsuccessful so this

technique was used to prepare fresh TPA-rhodaoxetane **XIII** samples to be used directly in other reactions of interest. Attempts to prepare TPA-rhodaoxetane **XIII** by this method on the larger scale, as published, were wholly unsuccessful for us.

TPA-rhodaoxetane **XIII** was also prepared directly from TPA **21** and [{Rh(μ-Cl)(ethene)$_2$}$_2$] **XI** starting materials according to the second protocol published by de Bruin *et al.*[80] In this case the ethylene complex **XII** was not isolated but was directly oxidized by $H_2O_2$ to TPA-rhodaoxetane **XIII**. The rhodaoxetane precipitated with $NaBPh_4$ or $KPF_6$ to give yellow powder. Analysis of this product by $^1H$ NMR spectroscopy showed that a small amount of the desired product formed in low purity. To isolate TPA-rhodaoxetane **XIII**, attempts were made to recrystallize the product from a $CH_2Cl_2$ solution layered with pentane. Only a fine yellow precipitate formed by this method and analysis of this precipitate and the solution by $^1H$ NMR spectroscopy showed no remaining TPA-rhodaoxetane **XIII**.

### 3.3.3.2 Background reaction of TPA with hydrogen peroxide

A reaction between TPA **21** and hydrogen peroxide was performed in order to determine whether these two species underwent any side reaction during the oxidation of [($\eta^2$-ethene)($\kappa^4$-TPA)Rh$^I$]$^+$ **XI**. If any such reaction between TPA **21** and $H_2O_2$ were to occur it would compete with the desired oxidation reaction and it might also contribute to the decomposition of the rhodium complexes in solution. TPA **21** (50 mg) and $H_2O_2$ (10.0 μL of a 35% aqueous solution) were combined with $CDCl_3$ (0.6 mL) in an NMR tube. A $^1H$ NMR spectrum of the reaction mixture showed no evidence of any reaction occurring.

#### 3.3.3.3 Preparation of TPA-rhodaoxetane by nitrous oxide oxidation

A third protocol for preparing rhodaoxetane was inspired by the work of Hillhouse and coworkers where nitrous oxide was used to prepare an oxanickelacycle by oxygen insertion into a nickelacyclopentane ring.[108] In a 25 mL Schlenk flask equipped with a stir bar and a septum, 0.070 g of $[(\eta^2\text{-ethene})\text{-}(\kappa^4\text{-TPA})Rh^I]^+$ $BPh_4^-$ **XII** was dissolved in approximately 20 mL of dry benzene. Nitrous oxide was bubbled through the solution for 10 minutes while stirring. The benzene was removed by Schlenk line vacuum and the crude product was dissolved in approximately 0.5 mL of acetone-$d_6$ and placed in an NMR tube. A $^1$H NMR spectrum showed peaks corresponding to TPA-rhodaoxetane **XIII**.

Although small amounts of TPA-rhodaoxetane **XIII** were observed by $^1$H NMR spectroscopy, none of the aforementioned techniques were reliable. On many occasions these procedures yielded no observable TPA-rhodaoxetane **XIII** product. When TPA-rhodaoxetane **XIII** was prepared successfully the yield was very low and the product could not be isolated.

### 3.3.4 Reactions of TPA-rhodaoxetane

Test reactions were performed using samples of TPA-rhodaoxetane **XIII**, generated *in situ* in an NMR tube from $[(\eta^2\text{-ethene})(\kappa^4\text{-TPA})Rh^I]^+$ **XII** and $H_2O_2$ in acetone-$d_6$. Each of these samples was prepared in an NMR tube equipped with a septum so that $H_2O_2$ could be added by syringe and later a solution of a chosen substrate could be added by syringe to the fresh TPA-rhodaoxetane **XIII**. The substrates chosen for study were aniline **23**, toluenesulfonamide **24**, phenylboronic acid **25** and benzaldehyde **22**. In every case, the sample was observed by $^1$H NMR spectroscopy over a number of days. For all cases, $^1$H NMR peaks corresponding to TPA-rhodaoxetane **XIII** are observed to

grow in for approximately the first 2 h. After that time, these peaks steadily decline over the next hours and up to several days, until none is observable in the spectra. For all of these examples, the $^1$H NMR signals for the chosen substrates remain steady over the duration of the experiment. In each case, $^1$H NMR signals of unknown species develop over time. The amounts of these products are very small in each case and it was not possible to identify or isolate these products.

### 3.3.4.1 Background reaction of benzaldehyde with hydrogen peroxide

It is known that TPA-rhodaoxetane **XIII** reacts with acetone, however this reaction occurs relatively slowly, taking approximately 2 weeks at room temperature.[79] It was thought that benzaldehyde **22** might react with the residual $H_2O_2$ in solution since over time benzaldehyde **22** reacts with air to form benzoic acid. To test whether such a reaction might be occurring, small amounts of benzaldehyde **22** and $H_2O_2$ were combined with $CDCl_3$ in an NMR tube. The reaction mixture was monitored by $^1$H NMR spectroscopy for 8 h and showed no evidence of any reaction occurring.

The main difficulty with the trial reactions with TPA-rhodaoxetane **XIII** was that the method for generation of TPA-rhodaoxetane **XIII** was not reliable. The quantity of TPA-rhodaoxetane **XIII** in the sample was very small and probably not the same for each sample. The amount of each substrate that was added was much greater than the amount of TPA-rhodaoxetane **XIII** in the sample. If the substrate was reacting with TPA-rhodaoxetane **XIII**, the amount was not sufficient to be observable with any significance. It was our intention to repeat these reactions with more rigorous experimental technique when the generation of TPA-rhodaoxetane **XIII** became more reliable. In the meantime, these reactions do not lead us to any conclusion about the reactivity of TPA-rhodaoxetane

**XIII**.

## 3.4 Summary

TPA-rhodaoxetane **XIII** was prepared according to two procedures published by de Bruin *et al.*[78,80] with limited success. A third preparation method was explored involving the use of $N_2O$ as oxidant; however, only trace amounts of TPA-rhodaoxetane **XIII** formed by this method. Despite great time and effort directed towards this goal we never achieved adequate purity or quantity of TPA-rhodaoxetane **XIII**. Our difficulty producing TPA-rhodaoxetane **XIII** limited our ability to explore the scope of the reactivity of this complex. A few test reactions were performed using trace amounts of impure TPA-rhodaoxetane **XIII** combined with a selection of substrates. The large amount of impurity in the samples obscured our analysis, making any results difficult to interpret. It was apparent that TPA-rhodaoxetane **XIII** was disappearing from the samples, possibly because it reacted with the introduced substrate in each case. We are continuing our pursuit of this research into TPA-rhodaoxetane **XIII** reactivity.

## 3.5 Experimental Procedures

### 3.5.1 General Methods

Manipulation of metallic compounds was performed using standard Schlenk techniques under an atmosphere of dry nitrogen or in a nitrogen-filled Vacuum Atmospheres or MBraun glovebox ($[O_2] < 2$ ppm). NMR spectra were recorded on Bruker Avance 300 or Bruker Avance 400 spectrometers. Benzene was dried by passage through solvent purification columns.[119] $CDCl_3$ was vacuum-transferred from $P_2O_5$ and degassed prior to use. Acetone-$d_6$ was distilled from $CaSO_4$ and degassed prior to use. Toluene-$d_8$ was degassed prior to use. All other reagents and solvents were obtained from

commercial sources and used as received. $^{1}H$ and $^{31}P\{^{1}H\}$ NMR spectra are reported in parts per million and were referenced to residual solvent. Coupling constant values were extracted assuming first-order coupling. All spectra were obtained at 25 °C, unless otherwise stated.

### 3.5.1.1 Preparation of tris[(2-pyridyl)methyl]amine (TPA) 21

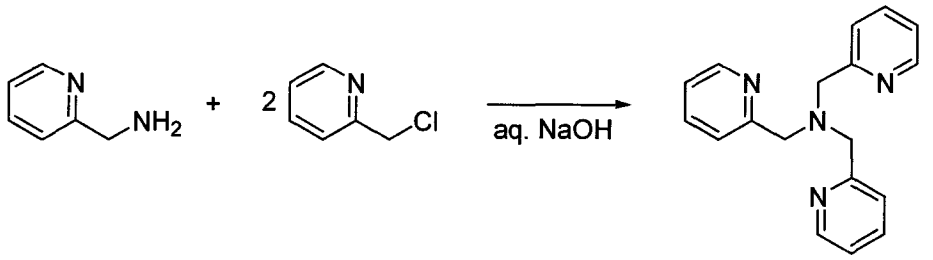


**19** **20** **21**

TPA **21** was prepared following a modified literature method.[126] 2-(Aminomethyl)pyridine **19** (8 mL, 80 mmol) was added dropwise to a solution of 2-picolyl chloride **20** (25.6 g, 160 mmol) in distilled water (40 mL) in a 250 mL round bottom flask equipped with a magnetic stir bar and a stopper, under a flow of $N_2$. The reaction mixture turned red after several minutes of stirring. Sodium hydroxide (31.0 mL of a 10 M solution, 320 mmol) was added at a rate of approximately 5 drops/minute, controlled by an addition funnel. The flask was placed in an oil bath set to 70 °C for 30 minutes. The flask was removed from the heat source and cooled to room temperature. The resulting dark red oily suspension was extracted with $CH_2Cl_2$ (3 x 125 mL) using a separatory funnel. The combined extracts were dried over $Na_2SO_4$. The mixture was filtered and the solvent removed by Schenk line vacuum. The crude product was placed in a vial and partially dissolved in a very small quantity of acetone to form a viscous layer of solution over the tarry sediment. This solution was decanted away from any undissolved material. An approximately equal volume of distilled water was added to the

decanted solution. The resultant mixture formed two layers. The cloudy yellow top layer was decanted and dried to yield pure TPA **21** crystals. The orange-brown bottom layer contained TPA **21** and impurities. This extraction could be repeated on the dried bottom layer to yield several batches of highly pure TPA **21**. Yield: 3.60 g (16%). $^1$H NMR ($CDCl_3$, 300 MHz) δ 8.52 – 8.50 (m, 3 H), 7.66 – 7.54 (m, 6 H), 7.14 – 7.10 (m, 3 H), 3.87 (s, 3 x 2 H, $CH_2$). The product identity was confirmed by comparing the $^1$H NMR spectrum with reported data.[126]

### 3.5.1.2 Preparation of $[(\eta^2\text{-ethene})(\kappa^4\text{-TPA})Rh^I]^+ BPh_4^-$ XII

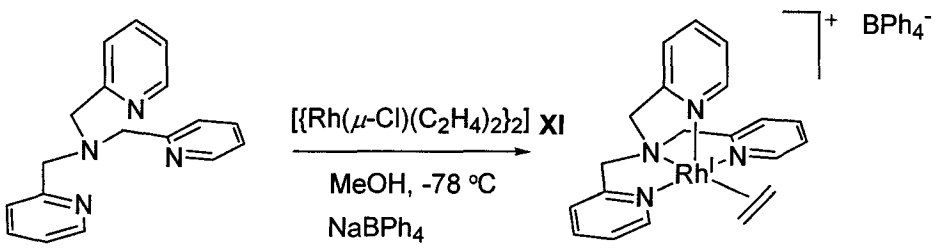


TPA **21** (30 mg, 0.104 mmol) and [{Rh(μ-Cl)(ethene)$_2$}$_2$] **XI** (20 mg, 0.05 mmol) were placed together in a 15 mL Schlenk flask equipped with a magnetic stir bar and stopper under $N_2$ in a glovebox. The flask was removed from the glovebox and placed on a $N_2$ filled Schlenk line, following standard Schlenk techniques to avoid contamination with air or moisture. Anhydrous methanol (5 mL) was added to the flask by cannula. The mixture was cooled to -78 °C in a $CO_2$/acetone bath and stirred for 1 h. The solution was added to a second 15 mL Schlenk flask containing $NaBPh_4$ (164 mg, 0.48 mmol). Some of the solvent was removed by vacuum and a fine yellow-green precipitate formed. The mixture was filtered through a sintered glass funnel and the yellow-green powder was dried under vacuum. Yield: 0.034 g (53%). The product identity was confirmed by comparing the $^1$H NMR spectrum with reported data.[78]

### 3.5.1.3 Preparation of $[(TPA)Rh^{III}(\kappa^2\text{-C,O-2-oxyethyl})]^+ BPh_4^-$ XIII (by oxidation of $[(\eta^2\text{-ethene})(\kappa^4\text{-TPA})Rh^I]^+ BPh_4^-$ XII with $H_2O_2$)

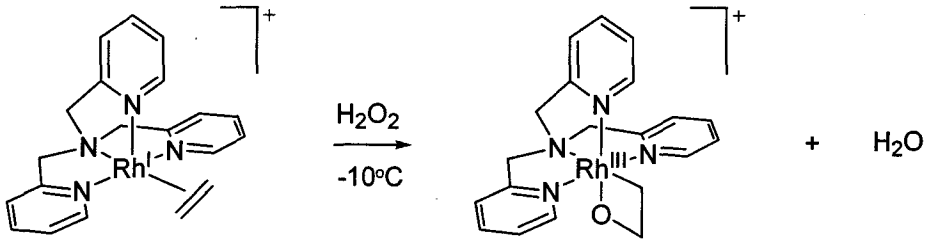


XII XIII

$[(\eta^2\text{-ethene})(\kappa^4\text{-TPA})Rh(I)]^+ BPh_4^-$ **XII** (0.034 g, 0.0053 mmol) and acetone-$d_6$ (0.6 mL) were placed in an NMR tube equipped with a septum under $N_2$ in a glovebox. The tube was removed from the glovebox. Hydrogen peroxide (5.0 μL of a 35% aqueous solution) was added through the septum by syringe. The NMR tube was inverted repeatedly to mix the contents. The solution was cooled to -10 °C in an ice bath for 1 h before collecting the NMR data. The product identity was confirmed by comparing the $^1H$ NMR spectrum with reported data.[78]

### 3.5.1.4 Preparation of $[(TPA)Rh^{III}(\kappa^2\text{-C,O-2-oxyethyl})]^+ BPh_4^-$ XIII (by oxidation of $[(\eta^2\text{-ethene})(\kappa^4\text{-TPA})Rh^I]^+ BPh_4^-$ XII with $N_2O$)

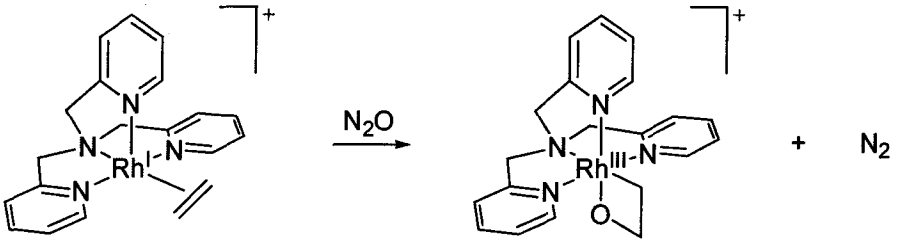


XII XIII

$[(\eta^2\text{-Ethene})(\kappa^4\text{-TPA})Rh^I]^+ BPh_4^-$ **XII** (70 mg, 0.11 mmol) and benzene (approximately 20 mL) were placed in 25 mL Schlenk flask equipped with a septum and a magnetic stir bar. The Schlenk flask was removed from the glovebox. Nitrous oxide was bubbled through the solution for 10 minutes using a needle inserted through the septum. A second needle was inserted through the septum to provide an exhaust for

excess pressure. The benzene was removed by Schlenk line vacuum and the crude product was redissolved in acetone-$d_6$ (approximately 0.5 mL) and placed in an NMR tube for analysis. The $^1$H NMR spectrum showed the appearance of new peaks indicating a trace amount of product. The product was not identified and further attempts at this reaction were no more successful.

### 3.5.1.5 Background reaction of TPA 21 with $H_2O_2$

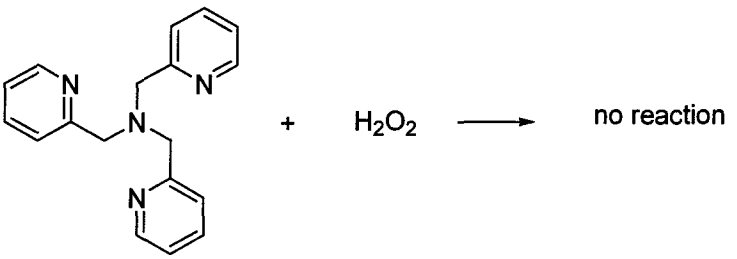


**21**

TPA **21** (50 mg, 0.17 mmol) and $CDCl_3$ (0.6 mL) were placed in an NMR tube equipped with a septum. A syringe was used to add $H_2O_2$ (10.0 μL of a 35% aqueous solution) and the tube was inverted repeatedly to mix the contents. A $^1$H NMR spectrum of the mixture was obtained and showed no evidence of any reaction occurring.

### 3.5.1.6 Background reaction of benzaldehyde 22 with $H_2O_2$

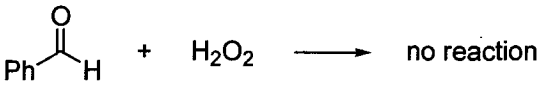


**22**

Small amounts of benzaldehyde **22** (a drop) and hydrogen peroxide (a few drops of a 35% aqueous solution) were combined in an NMR tube with approximately 0.5 mL $CDCl_3$. The reaction mixture was monitored by $^1$H NMR spectroscopy for 8 h and showed no evidence of any reaction occurring.

### 3.5.1.7 Reaction of [(TPA)Rh$^{III}$($\kappa^2$-C,O-2-oxyethyl)]$^+$ XIII with aniline 23

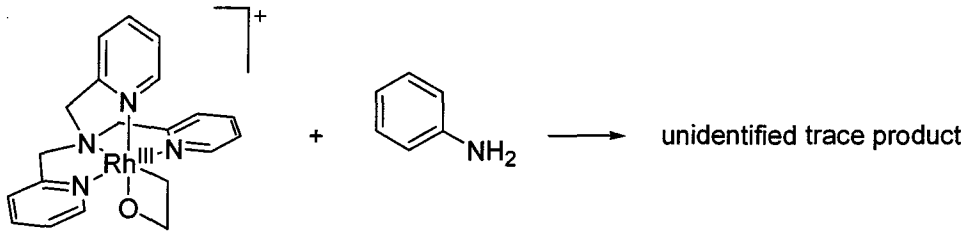


XIII 23

A fresh sample of [(TPA)Rh$^{III}$($\kappa^2$-C,O-2-oxyethyl)]$^+$ **XIII** was prepared in an NMR tube by dissolving a small quantity of [($\eta^2$-ethene)($\kappa^4$-TPA)Rh$^I$]$^+$ **XII** in approximately 0.5 mL of acetone-$d_6$. $H_2O_2$ (5.0 μL of a 35% aqueous solution) was then added by syringe through a septum in the NMR tube cap. The formation of [(TPA)Rh$^{III}$($\kappa^2$-C,O-2-oxyethyl)]$^+$ **XIII** was confirmed by comparing the $^1$H NMR spectrum with reported data.[78] A small amount of aniline **23** (5.0 μL, 0.055 mmol) was added to the TPA-rhodaoxetane **XIII** sample by syringe. The sample was kept cool in an ice water bath for 30 minutes prior to analysis. The solution was monitored by $^1$H NMR spectroscopy over 3 days. Trace reaction was observed in the $^1$H NMR spectra and no products were identified.

### 3.5.1.8 Reaction of [(TPA)Rh$^{III}$($\kappa^2$-C,O-2-oxyethyl)]$^+$ XIII with toluenesulfonamide 24

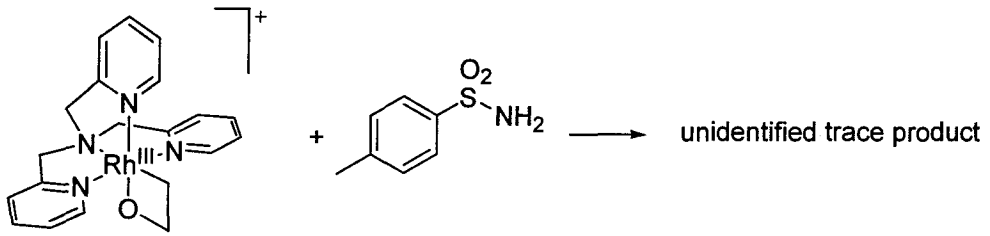


XIII 24

A fresh sample of [(TPA)Rh$^{III}$($\kappa^2$-C,O-2-oxyethyl)]$^+$ **XIII** was prepared in an NMR tube by dissolving a small quantity of [($\eta^2$-ethene)($\kappa^4$-TPA)Rh$^I$]$^+$ **XII** in approximately 0.5 mL of $CD_2Cl_2$. $H_2O_2$ (5.0 μL of a 35% aqueous solution) was then

added by syringe through a septum in the NMR tube cap. The formation of $[(TPA)Rh^{III}(\kappa^2\text{-C,O-2-oxyethyl})]^+$ **XIII** was confirmed by comparing the $^1H$ NMR spectrum with reported data.[78] A small amount of toluenesulfonamide **24** (10.0 μL of an approximately 100 g/L $CD_2Cl_2$ solution) was added to the TPA-rhodaoxetane **XIII** sample by syringe. The sample was kept cool in an ice water bath for 20 minutes prior to analysis. The solution was monitored by $^1H$ NMR spectroscopy over 3 days. Trace reaction was observed in the $^1H$ NMR spectra and no products were identified.

### 3.5.1.9 Reaction of $[(TPA)Rh^{III}(\kappa^2\text{-C,O-2-oxyethyl})]^+$ XIII with phenylboronic acid 25

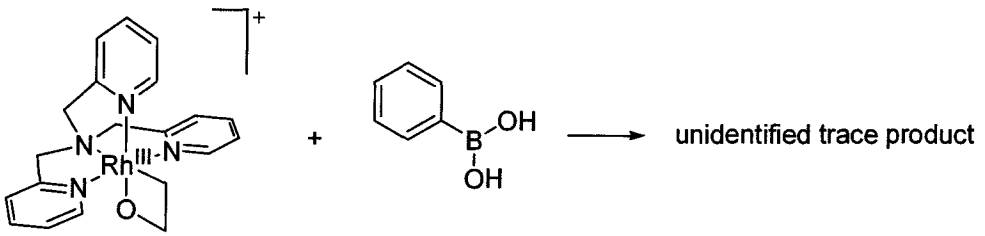


**XIII** **25**

A fresh sample of $[(TPA)Rh^{III}(\kappa^2\text{-C,O-2-oxyethyl})]^+$ **XIII** was prepared in an NMR tube by dissolving a small quantity of $[(\eta^2\text{-ethene})(\kappa^4\text{-TPA})Rh^I]^+$ **XII** in approximately 0.5 mL of $CD_2Cl_2$. $H_2O_2$ (5.0 μL of a 35% aqueous solution) was then added by syringe through a septum in the NMR tube cap. The formation of $[(TPA)Rh^{III}(\kappa^2\text{-C,O-2-oxyethyl})]^+$ **XIII** was confirmed by comparing the $^1H$ NMR spectrum with reported data.[78] A small amount of phenylboronic acid **25** (10.0 μL of an approximately 100 g/L $CD_2Cl_2$ solution) was added to the rhodaoxetane sample by syringe. The sample was kept cool for 1 h prior to analysis. The solution was monitored by $^1H$ NMR spectroscopy over 3 days. Trace reaction was observed in the $^1H$ NMR spectra and no products were identified.

### 3.5.1.10 Reaction of $[(TPA)Rh^{III}(\kappa^2\text{-C,O-2-oxyethyl})]^+$ XIII with benzaldehyde 22

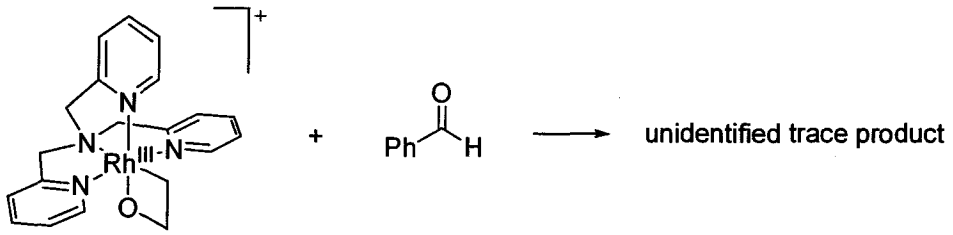


XIII 22

A fresh sample of $[(TPA)Rh^{III}(\kappa^2\text{-C,O-2-oxyethyl})]^+$ **XIII** was prepared in an NMR tube by dissolving a small quantity of $[(\eta^2\text{-ethene})(\kappa^4\text{-TPA})Rh^I]^+$ **XII** in approximately 0.5 mL of acetone-$d_6$. $H_2O_2$ (5.0 μL of a 35% aqueous solution) was then added by syringe through a septum in the NMR tube cap. The formation of $[(TPA)Rh^{III}(\kappa^2\text{-C,O-2-oxyethyl})]^+$ **XIII** was confirmed by comparing the $^1H$ NMR spectrum with reported data.[78] A small amount of benzaldehyde **22** (10.0 μL of a 100 μL/g acetone solution) was added to the TPA-rhodaoxetane **XIII** sample by syringe. The solution was monitored by $^1H$ NMR spectroscopy at 15 min, 30 min, and 1 h. Trace reaction was observed in the $^1H$ NMR spectra and no products were identified.

# 4 Summary, conclusions and future work

## 4.1 Summary

The development of reactions that lead to selectively functionalized products from simple and readily available olefins and alkynes is an active area of research. Much of the focus of study is directed toward transition metal complexes for their potential as catalysts for these reactions. The research presented in this thesis regards the reactivity of Rh-P and Rh-O bonds in rhodium complexes with multidentate nitrogen donor ligands. This thesis is comprised of two subprojects: one exploring P-H bond activation by pyrazolylborate rhodium complexes and the other on developing olefin functionalization reactions via 2-rhodaoxetane intermediates.

### 4.1.1 Hydrophosphinylation catalyzed by pyrazolylborate rhodium complexes

The pyrazolylborate rhodium complexes [Tp*Rh($PPh_3$)$_2$] **III** and [Tp*Rh(cod)]$_2$ **IV** were compared with known catalysts for their activity in the hydrophosphinylation of 1-alkyne **2** with diphenylphosphine oxide **1**. These Tp*Rh$L_n$ complexes demonstrated moderate activity and high regioselectivity for the *E*-linear vinylphosphine oxide product from this reaction; however, they were not as active as the known catalysts [ClRh($PPh_3$)$_2$] **I** and [ClRh(cod)]$_2$ **II**. The activity of [Tp*Rh($PPh_3$)$_2$] **III** was then evaluated for hydrophosphinylation of a range of alkyne substrates. In each case, the *E*-linear vinylphosphine oxide resulting from *syn*-addition of P-H across the alkyne bond formed as the exclusive product. Higher yields were provided by aliphatic alkynes than aromatic alkynes and the highest yield was obtained for an internal aliphatic alkyne. Product formation may be directed by the steric bulk of the ligands on rhodium. An investigation

was made into the mechanism of hydrophosphinylation catalyzed by $Tp^{R}RhL_n$ complexes. $^{1}H$ and $^{31}P$ NMR spectroscopic evidence suggests that hydrophosphinylation catalyzed by pyrazolylborate rhodium complexes follows an analogous mechanism to that proposed by Han *et al.* for hydrophosphinylation by $[ClRh(PPh_3)_3]$ **I** or $[ClRh(cod)]_2$ **II**.

### 4.1.2 Direct functionalization of olefins via 2-rhodaoxetanes

TPA-rhodaoxetane **XIII** has been shown to be readily generated and isolable, yet reactive toward a number of substrates.[79] TPA-rhodaoxetane **XIII** could potentially be used as an intermediate for a number of mechanistically novel olefin functionalization reactions. Three methods for preparing TPA-rhodaoxetane were pursued with limited success. Two published procedures were followed that each provided small quantities of impure TPA-rhodaoxetane.[78,80] A third method involved oxidation of $[(\eta^2\text{-ethene})(\kappa^4\text{-TPA})Rh^{I}]^{+}$ $BPh_4^-$ **XII** by $N_2O$; however, only trace amounts of TPA-rhodaoxetane **XIII** formed as observed by $^{1}H$ NMR spectroscopy. Test reactions were performed with what little amount of TPA-rhodaoxetane **XIII** was available combined with a selection of substrates. These test reactions do not lead to any conclusions about the reactivity of TPA-rhodaoxetane since the large amount of impurity in the samples interfered with the analysis of any results.

## 4.2 Future work

Metal-heteroatom reactivity, including reactions involving Rh-P and Rh-O bonds, will continue to be explored through many ongoing research projects in the Love group. In particular regard to this thesis work, the project involving the development of olefin functionalization reactions via 2-rhodaoxetanes is being continued by a Ph.D. student,

Alexander Dauth.

### 4.2.1 P-H bond activation reactions catalyzed by pyrazolylborate rhodium complexes

In this thesis the ability of pyrazolylborate rhodium complexes to catalyze the hydrophosphinylation of alkynes has been established. Future investigations will endeavor to provide more reactive $Tp^{R}RhL_{n}$ catalysts for this reaction. Substituents on the pyrazolyl groups of $Tp^{R}$ ligands can be varied such that the steric and electronic features of the resulting complexes might bring about more efficient catalysis. Efforts will be made to further expand the scope of this reaction to other types of P-H sources and a wider range of alkyne substrates.

### 4.2.2 Functionalization reactions of olefins via 2-rhodaoxetanes

Finding a reliable method for generating TPA-rhodaoxetane **XIII** will be a crucial initial goal for the future success of this project. Once TPA-rhodaoxetane **XIII** is available in reasonable yield and purity, the development of the reactions proposed in this thesis will be pursued. Any reactions that are developed can then be explored for their potential regio- and enantioselectivities when substituted olefins are used in place of simple ethylene.

#### 4.2.2.1 Enantioselectivity of olefin functionalization reactions via 2-rhodaoxetanes

2-Rhodaoxetane intermediates with chiral ligands could be used to develop enantioselective versions of oxidation, aminohydroxylation, and carbohydroxylation. The metal center should strongly influence the enantioselectivity-determining step of these reactions. Scheme 4-1 shows examples of how 2-rhodaoxetane intermediates might be used for enantioselective syntheses. Equation 1 in Scheme 4-1 shows how chiral aldehydes might be prepared from 1,1-disubstituted olefins. Equation 2 would likely lead

to a stable β-disubstituted rhodaoxetane since at least one β-hydrogen would be necessary for the elimination of a carbonyl-containing compound from this complex. 1,2-Disubstituted olefins would lead to products with two stereocenters. Equation 3 depicts the potential formation of enantiomers by aminohydroxylation and likewise, Equation 4 would potentially provide enantiomers from aryl or alkylhydroxylation.

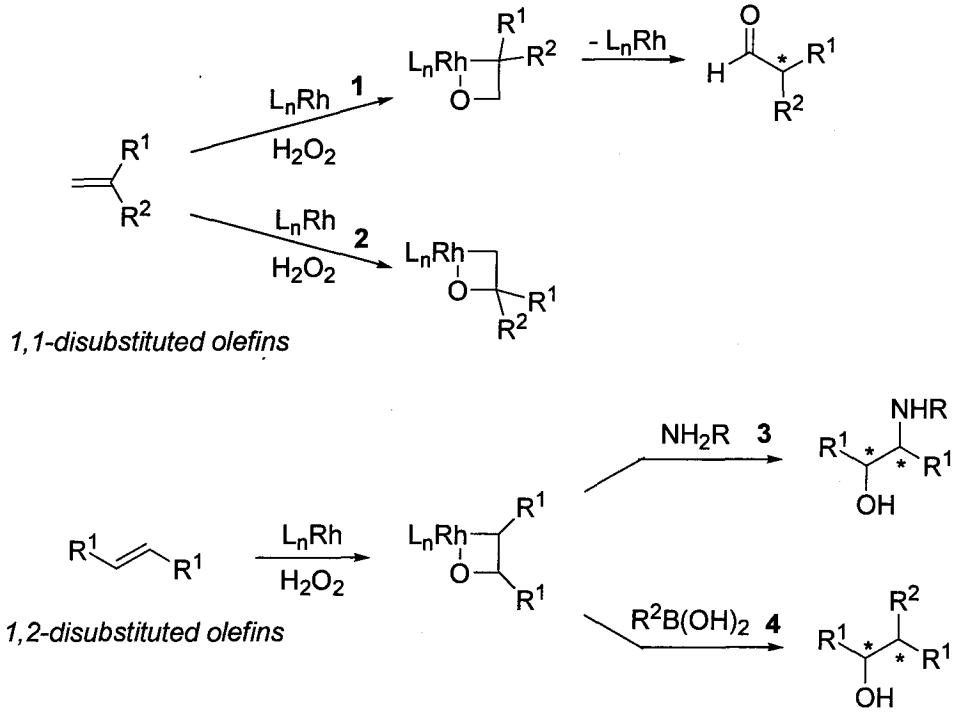


**Scheme 4-1** Possible outcomes of the proposed functionalization reactions with either 1,1- or 1,2-disubstituted olefins

# References


(1) Lautens, M.; Roy, A.; Fukuoka, K.; Fagnou, K.; Martin-Matute, B. *J. Am. Chem. Soc.* **2001**, *123*, 5358-5359.

(2) Heck, R. F.; Nolley, J. P., Jr. *J. Org. Chem.* **1972**, *37*, 2320-2322.

(3) RajanBabu, T. V. *Chem. Rev.* **2003**, *103*, 2845-2860.

(4) Caballero, A.; Sabo-Etienne, S. *Organometallics* **2007**, *26*, 1191-1195.

(5) Hegedus, L. S.; Williams, R. E.; McGuire, M. A.; Hayashi, T. *J. Am. Chem. Soc.* **1980**, *102*, 4973-4979.

(6) Lachaize, S.; Sabo-Etienne, S.; Donnadieu, B.; Chaudret, B. *Chem. Comm.* **2003**, *2*, 214-215.

(7) Miyaura, N.; Suzuki, A. *Chem. Rev.* **1995**, *95*, 2457-2483.

(8) Morrill, C.; Grubbs, R. H. *J. Org. Chem.* **2003**, *68*, 6031-6034.

(9) Beller, M.; Seayad, J.; Tillack, A.; Jiao, H. *Angew. Chem. Int. Ed.* **2004**, *43*, 3368-3398.

(10) Beletskaya, I. P.; Ananikov, V. P. *Pure Appl. Chem.* **2007**, *79*, 1041-1056.

(11) Hintermann, L.; Labonne, A. *Synthesis* **2007**, *8*, 1121-1150.

(12) de Bruin, B.; Budzelaar, P. H. M.; Gal, A. W. *Angewandte Chemie, International Edition* **2004**, *43*, 4142-4157.

(13) Trofimenko, S. *J. Am. Chem. Soc.* **1966**, *88*, 1842-1844.

(14) Trofimenko, S. *Chemical Reviews (Washington, DC, United States)* **1993**, *93*, 943-980.

(15) Trofimenko, S. *Scorpionates – The Coordination Chemistry of Polypyrazolylborate Ligands;* Imperial College Press: London, 2005.

(16) Bergman, R. G.; Cundari, T. R.; Gillespie, A. M.; Gunnoe, T. B.; Harman, W. D.; Klinckman, T. R.; Temple, M. D.; White, D. P. *Organometallics* **2003**, *22*, 2331-2337.

(17) Chauby, V.; Serra-Le Berre, C.; Kalck, P.; Daran, J-.C.; Commenges, G. *Inorg. Chem.* **1996**, *35*, 6354-6355.

(18) Slugovc, C.; Padilla-Martinez, I.; Sirol, S.; Carmona, E. *Coord. Chem. Rev.* **2001**, *213*, 129-157.

(19) Jones, W. D.; Hessell, E. T. *Inorg. Chem.* **1991**, *30*, 778-783.

(20) Ghosh, C. K. Ph. D. Thesis, University of Alberta, 1988.

(21) Ball, R. G.; Ghosh, C. K.; Hoyano, J. K.; McMaster, A. D.; Graham, W. A. G. *J. Chem. Soc., Chem. Commun.* **1989**, 341-342.

(22) Bucher, U. E.; Currao, A.; Nesper, R.; Rüegger, H.; Venanzi, L. M.; Younger, E. *Inorg. Chem.* **1995**, *34*, 66-74.

(23) Ruman, T.; Ciunik, Z.; Trzeciak, A. M.; Wolowiec, S.; Ziólkowski, J. J. *Organometallics* **2003**, *22*, 1072-1080.

(24) Oldham, W. J., Jr.; Heinekey, D. M. *Organometallics* **1997**, *16*, 467-474.

(25) Webster, C. E.; Hall, M. B. *Inorg. Chim. Acta* **2002**, *330*, 268-282.

(26) Fraser, L. R. M.Sc. Thesis, University of British Columbia, Aug. 2007.

(27) Fraser, L. R.; Bird, J.; Wu, Q.; Cao, C.; Patrick, B. O.; Love, J. A. *Organometallics in press.*

(28) Connelly, N. G.; Emslie, D. J. H.; Geiger, W. E.; Hayward, O. D.; Linehan, E. B.; Orpen, A. G.; Quayle, M. J.; Rieger, P. H. *J. Chem. Soc., Dalton Trans.* **2001**, 670-683 (29) Ghosh, C. K.; Graham, W. A. G. *J. Am. Chem. Soc.* **1987**, *109*, 4726-4727.

(30) Lian, T.; Bromberg, S. E.; Yang, H.; Proulx, G.; Bergman, R. G.; Harris, C. B. *J. Am. Chem. Soc.* **1996**, *118*, 3769-3770.

(31) Ghosh, C. K.; Rodgers, D. P. S.; Graham, W. A. G. *J. Chem. Soc. , Chem. Commun.* **1988**, 1511-1512.

(32) Hessell, E. T.; Jones, W. D. *Organometallics* **1992**, *11*, 1496-1505.

(33) Jones, W. D.; Hessell, E. T. *J. Am. Chem. Soc.* **1992**, *114*, 6087-6095.

(34) Cîrcu, V.; Fernandes, M. A.; Carlton, L. *Inorg. Chem.* **2002**, *41*, 3859-3865.

(35) Cao, C.; Wang, T.; Patrick, B. O.; Love, J. A. *Organometallics* **2006**, *25*, 1321-1324.

(36) Cîrcu, V.; Fernandes, M. A.; Carlton, L. *Polyhedron* **2003**, *22*, 3293-3298.

(37) Katayama, H.; Yamamura, K.; Miyaki, Y.; Ozawa, F. *Organometallics* **1997**, *16*, 4497-4500.

(38) Alvarado, Y.; Busolo, M.; Lopez-Linares, F. *J. Mol. Cat. A: Chem.* **1999**, *142*, 163-167.

(39) Trujillo, M. Ph. D. Thesis, University of Sevilla, 1999.

(40) Ogawa, A.; Ikeda, T.; Kimura, K.; Hirao, T. *J. Am. Chem. Soc.* **1999**, *121*, 5108-5114.

(41) Cao, C.; Fraser, L. R.; Love, J. A. *J. Am. Chem. Soc.* **2005**, *127*, 17614-17615.

(42) Burling, S.; Field, L. D.; Messerle, B. A.; Vuong, K. Q.; Turner, P. *Dalton Transactions* **2003**, 4181-4191.

(43) Kuniyasu, H.; Ogawa, A.; Sato, K.; Ryu, I.; Kambe, N.; Sonoda, N. *J. Am. Chem. Soc.* **1992**, *114*, 5902-5903.

(44) Bäckvall, J.-E.; Ericsson, A. *J. Org. Chem.* **1994**, *59*, 5850-5851.

(45) Han, L.; Zhang, C.; Yazawa, H.; Shimada, S. *J. Am. Chem. Soc.* **2004**, *126*, 5080-5081.

(46) Singer, H.; Wilkinson, G. *J. Chem. Soc. A* **1968**, *10*, 2516-2520.

(47) Teuma, E.; Loy, M.; Serra-Le Berre, C.; Etienne, M.; Daran, J.; Kalck, P. *Organometallics* **2003**, *22*, 5261-5267.

(48) Alonso, F.; Beletskaya, I. P.; Yus, M. *Chem. Rev.* **2004**, *104*, 3079-3159.

(49) Maj, A. M.; Pietrusiewicz, K. M.; Suisse, I.; Agbossou, F.; Mortreux, A. *Tetrahedron* **1999**, *10*, 831-835.

(50) Inoue, H.; Nagaoka, Y.; Tomioka, K. *J. Org. Chem.* **2002**, *67*, 5864-5867.

(51) Oliana, M.; King, F.; Horton, P. N.; Hursthouse, M. B.; Hii, K. K. *J. Org. Chem.* **2006**, *71*, 2472-2479.

(52) Braga, A. L.; Rhoden, C. R. B.; Zeni, G.; Silveira, C. C.; Andrade, L. H. *J. Organomet. Chem.* **2003**, *682*, 35-40.

(53) Haynes, R. K.; Vonwiller, S. C.; Hambley, T. W. *J. Org. Chem.* **1989**, *54*, 5162-5170.

(54) Haynes, R. K.; Loughlin, W. A.; Hambley, T. W. *J. Org. Chem.* **1991**, *56*, 5785-5790.

(55) Keglevich, G.; Gaumont, A.-C.; Denis, J.-M. *Heteroatom Chem.* **2001**, *12*, 161-167.

(56) Wąsek, T.; Olczak, J.; Janecki, T. *Synlett* **2006**, *10*, 1507-1510.

(57) Han, L.-B.; Choi, N.; Tanaka, M. *Organometallics* **1996**, *15*, 3259-3261.

(58) Han, L.-B.; Hua, R.; Tanaka, M. *Angew. Chem., Int. Ed.* **1998**, *37*, 94-96.

(59) Han, L.-B.; Zhao, C. Q.; Tanaka, M. *J. Org. Chem.* **2001**, *66*, 5929-5932.

(60) JØrgensen, K. A.; SchiØtt, B. *Chem. Rev.* **1990**, *90*, 1483-1506.

(61) Molinaro, C.; Jamison, T. F. *J. Am. Chem. Soc.* **2003**, *125*, 8076-8077.

(62) Linic, S.; Barteau, M. A. *J. Am. Chem. Soc.* **2002**, *124*, 310-317.

(63) Gable, K. P.; Phan, T. N. *J. Am. Chem. Soc.* **1994**, *116*, 833-839.

(64) Norrby, P.-O.; Kolb, H. C. K.; Sharpless, B. *Organometallics* **1994**, *13*, 344-347.

(65) Corey, E. J.; Noe, M. C. *J. Am. Chem. Soc.* **1996**, *118*, 11038-11053.

(66) Hamada, T.; Fukuda, T.; Imanishi, H.; Katsuki, T. *Tetrahedron* **1996**, *52*, 515-530.

(67) Norrby, P.-O.; Becker, H.; Sharpless, K. B. *J. Am. Chem. Soc.* **1996**, *118*, 35-42.

(68) Schroder, M.; Constable, E. C. *J. Chem. Soc. , Chem. Commun.* **1982**, *13*, 734-736.

(69) Freeman, F.; Fuselier, C. O.; Armstead, C. R.; Dalton, C. E.; Davidson, P. A.; Karchesfski, E. M.; Krochman, D. E.; Johnson, M. N.; Jones, N. K. *J. Am. Chem. Soc.* **1981**, *103*, 1154-1159.

(70) Lee, D. G.; Noureldin, N. A. *J. Am. Chem. Soc.* **1983**, *105*, 3188-3191.

(71) Rappe, A. K.; Goddard, W. A. *J. Am. Chem. Soc.* **1982**, *104*, 3287-3294.

(72) Norrby, P.-O.; Linde, C.; Åakermark, B. *J. Am. Chem. Soc.* **1995**, *117*, 11035-11036.

(73) Blum, J.; Zinger, B.; Milstein, D.; Buchman, O. *J. Org. Chem.* **1978**, *43*, 2961-2967.

(74) Linic, S.; Barteau, M. A. *J. Am. Chem. Soc.* **2003**, *125*, 4034-4035.

(75) Bakos, J.; Orosz, A.; Cserepi, S.; Toth, I.; Sinou, D. *J. Mol. Catal. A* **1997**, *116*, 85-97.

(76) Read, G.; Urgelles, M.; Galas, A. M. R.; Hursthouse, M. B. *J. Chem. Soc. , Dalton Trans.* **1983**, *5*, 911-913.

(77) Chen, X.; Zhang, X.; Chen, P. *Angew. Chem. Int. Ed.* **2003**, *42*, 3798-3801.

(78) de Bruin, B.; Boerakker, M. J.; Donners, J. J. J. M.; Christiaans, B. E. C.; Schlebos, P. P. J.; de Gelder, R.; Smits, J. M. M.; Spek, A. L.; Gal, A. W. *Angew. Chem., Int. Ed.* **1997**, *36*, 2064-2067.

(79) de Bruin, B.; Boerakker, M. J.; Verhagen, J. A. W.; de Gelder, R.; Smits, J. M. M.; Gal, A. W. *Chem. Eur. J.* **2000**, *6*, 298-312.

(80) de Bruin, B.; Verhagen, J. A. W.; Schouten, C. H. J.; Gal, A. W.; Feichtinger, D.; Plattner, D. A. *Chem. Eur. J.* **2001**, *7*, 416-422.

(81) Hudlicky, M. *Oxidations in Organic Chemistry;* ACS Monograph series; American Chemical Society: Washington, DC, 1990; pp 357.

(82) Beller, M. *Adv. Synth. Catal.* **2004**, *346*, 107-108.

(83) Tejel, C.; Ciriano, M. A. *Top. Organomet. Chem.* **2007**, *22*, 97-124.

(84) Collman, J. P.; Hegedus, L. S.; Norton, J. R.; Finke, R. G. *Principles and Applications of Organotransition Metal Chemistry;* University Science Books: Mill Valley, California, 1987; pp 989.

(85) Zlota, A. A.; Frolow, F.; Milstein, D. *J. Am. Chem. Soc.* **1990**, *112*, 6411-6413.

(86) Meurer, E. C.; da Rocha, L. L.; Pilli, R. A.; Eberlin, M. N.; Santos, L. S. *Rapid Commun. Mass Spectrom.* **2006**, *20*, 2626-2629.

(87) Calhorda, M. J.; Galvão, A. M.; Ünaleroglu, C.; Zlota, A. A.; Frolow, F.; Milstein, D. *Organometallics* **1993**, *12*, 3316-3325.

(88) Anderegg, G.; Wenk, F. *Helv. Chim. Acta* **1967**, *50*, 2330-2332.

(89) Blackman, A. G. *Polyhedron* **2005**, *24*, 1-39.

(90) Budzelaar, P. H. M.; Blok, A. N. J. *Eur. J. Inorg. Chem.* **2004**, *11*, 2385-2391.

(91) de Bruin, B.; Boerakker, M. J.; De Gelder, R.; Smits, J. M. M.; Gal, A. W. *Angew. Chem., Int. Ed.* **1999**, *38*, 219-222.

(92) Dudley, C. W.; Read, G.; Walker, P. J. C. *J. Chem. Soc. , Dalton Trans.* **1974**, *17*, 1926-1931.

(93) Read, G.; Walker, Peter J. C. *J. Chem. Soc. , Dalton Trans.* **1977**, *9*, 883-888.

(94) Tsuji, J. *New J. Chem.* **2000**, *24*, 127-135.

(95) Tsuji, J. *Palladium Reagents and Catalysts; John Wiley & Sons: Chichester, 1995, Chapters 2and 3.*

(96) van Leeuwen, P. W. N. M. *The Wacker Reaction;* Homogeneous Catalysis; Kluwer Academic Publishers: Dordrecht, Netherlands, 2004; pp 320-324.

(97) Smith, M. B.; March, J. *March's Advanced Organic Chemistry;* John Wiley: New York, 2001; pp 2083.

(98) Tacaks, J. M.; Jiang, X.-t. *Curr. Org. Chem.* **2003**, *7*, 369-396.

(99) Bäckvall, J. E.; Åakermark, B.; Ljunggren, S. O. *J. Am. Chem. Soc.* **1979**, *101*, 2411-2416.

(100) Krom, M.; Peters, T. P. J.; Coumans, R. G. E.; Sciarone, T. J. J.; Hoogboom, J.; ter Beek, S. I.; Schlebos, P. P. J.; Smits, J. M. M.; de Gelder, R.; Gal, A. W. *Eur. J. Inorg. Chem.* **2003**, *6*, 1072-1087.

(101) Krom, M.; Coumans, R. G. E.; Smits, J. M. M.; Gal, A. W. *Angew. Chem. Int. Ed.* **2001**, *40*, 2106-2108.

(102) Krom, M.; Coumans, R. G. E.; Smits, J. M. M.; Gal, A. W. *Angew. Chem. Int. Ed.* **2002**, *41*, 575-579.

(103) Gorelsky, S. I.; Ghosh, S.; Solomon, E. I. *J. Am. Chem. Soc.* **2006**, *128*, 278-290.

(104) Vaughan, G. A.; Rupert, P. B.; Hillhouse, G. L. *J. Am. Chem. Soc.* **1987**, *109*, 5538-5539.

(105) Cooper, N. J.; Green, M. L. H.; Couldwell, C.; Prout, K. *J. Chem. Soc. , Chem. Commun.* **1977**, 145-146.

(106) List, A. K.; Koo, K.; Rheingold, A. L.; Hillhouse, G. L. *Inorg. Chim. Acta* **1998**, *270*, 399-404.

(107) Vaughan, G. A.; Hillhouse, G. L.; Lum, R. T.; Buchwald, S. L.; Rheingold, A. L. *J. Am. Chem. Soc.* **1988**, *110*, 7215-7217.

(108) Matsunaga, P. T.; Hillhouse, G. L.; Rheingold, A. L. *J. Am. Chem. Soc.* **1993**, *115*, 2075-2077.

(109) Matsunaga, P. T.; Mavropoulos, J. C.; Hillhouse, G. L. *Polyhedron* **1995**, *14*, 175-185.

(110) Koo, K.; Hillhouse, G. L.; Rheingold, A. L. *Organometallics* **1995**, *14*, 456-460.

(111) Vaughan, G. A.; Sofield, C. D.; Hillhouse, G. L.; Rheingold, A. L. *J. Am. Chem. Soc.* **1989**, *111*, 5491-5493.

(112) Vaughan, G. A.; Hillhouse, G. L.; Rheingold, A. L. *J. Am. Chem. Soc.* **1990**, *112*, 7994-8001.

(113) Van Rooy, S.; Cao, C.; Patrick, B. O.; Lam, A.; Love, J. A. *Inorg. Chim. Acta* **2006**, *359*, 2918-2923.

(114) Krossing, I.; Raabe, I. *Angew. Chem. Int. Ed.* **2004**, *43*, 2066-2090.

(115) Bartels, B.; Clayden, J.; Martin, C. G.; Nelson, A.; Russell, M. G.; Warren, S. *J. Chem. Soc., Perkin Trans.* **1999**, 1807-1822.

(116) Trzeciak, A. M.; Ziólkowski, J. J. *Pol. J. Chem.* **2003**, *77*, 749-756.

(117) Williams, D. H.; Fleming, I. *Spectroscopic methods in organic chemistry, Fifth Edition;* McGraw-Hill: Berkshire, England, 1995; pp 63-169.

(118) Roundhill, D. M.; Sperline, R. P.; Beaulieu, W. B. *Coord. Chem. Rev.* **1978**, *26*, 263-279.

(119) Pangborn, A. B.; Giardello, M. A.; Grubbs, R. H.; Rosen, R. K.; Timmers, F. J. *Organometallics* **1996**, *15*, 1518-1520.

(120) Bodkin, J. A.; McLeod, M. D. *J. Chem. Soc. , Perkin Trans. 1* **2002**, 2733-2746.

(121) Noack, M.; Goettlich, R. *Chem. Comm.* **2002**, *5*, 536-537.

(122) Bergmeier, S. C. *Tetrahedron* **2000**, *56*, 2561-2576.

(123) Hayashi, T. *Russ. Chem. Bull. , Int. Ed.* **2003**, *52*, 2595-2605.

(124) Duan, W. L.; Iwamura, H.; Shintani, R.; Hayashi, T. *J. Am. Chem. Soc.* **2007**, *129*, 2130-2138.

(125) Kina, A.; Yasuhara, Y.; Nishimura, T.; Iwamura, H.; Hayashi, T. *Chem. Asian J.* **2006**, *1*, 707-711.

(126) Canary, J. W.; Wang, Y.; Roy, R., Jr.; Que, L., Jr.; Miyake, H. *Inorg. Synth.* **1998**, *32*, 70-75.

# Appendix I: NMR spectra

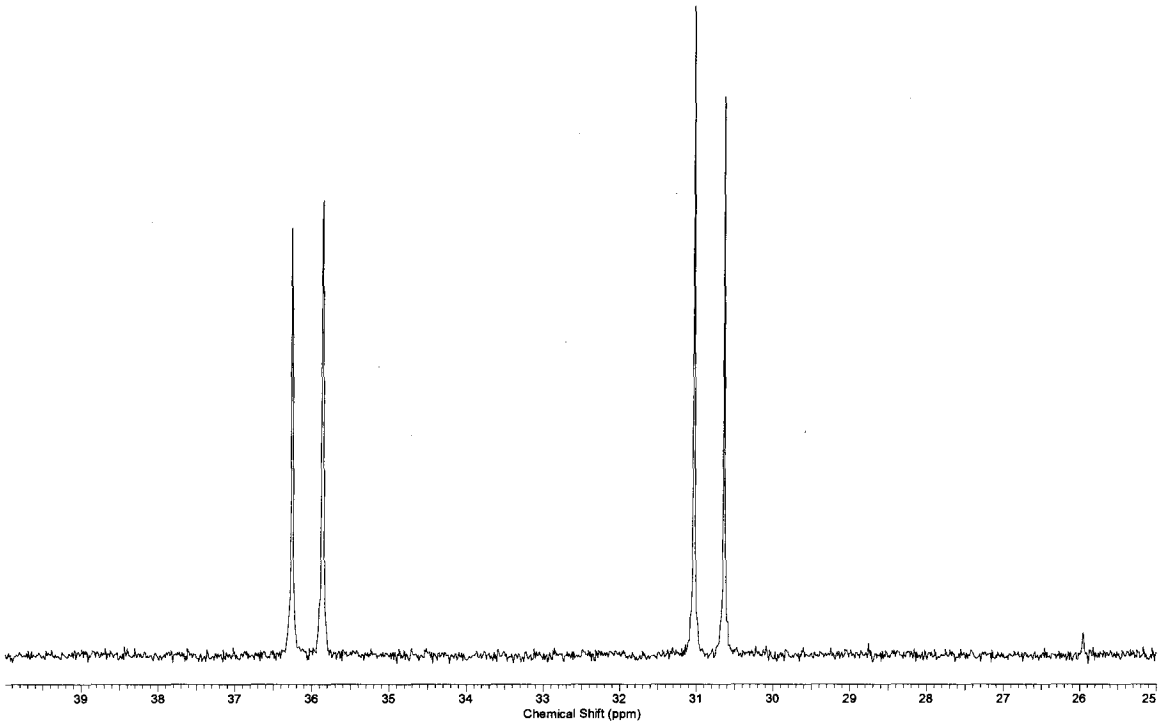


$^{31}P\{^{1}H\}$ NMR ($C_6D_6$, 121 MHz) spectrum of (*E*)-1-(diphenylphosphinyl)-2-(4-methoxyphenyl)ethene **10**

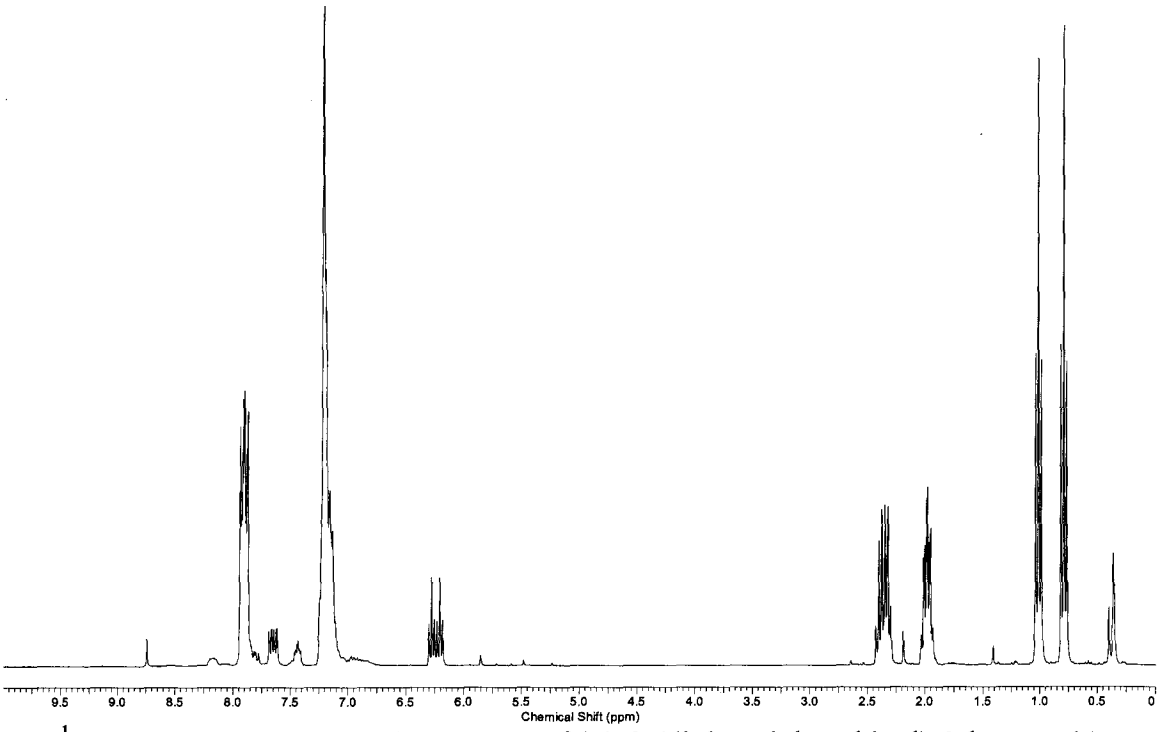


$^{1}$H NMR ($C_6D_6$, 300 MHz) spectrum of (*E*)-3-(diphenylphosphinyl)-3-hexene **11**

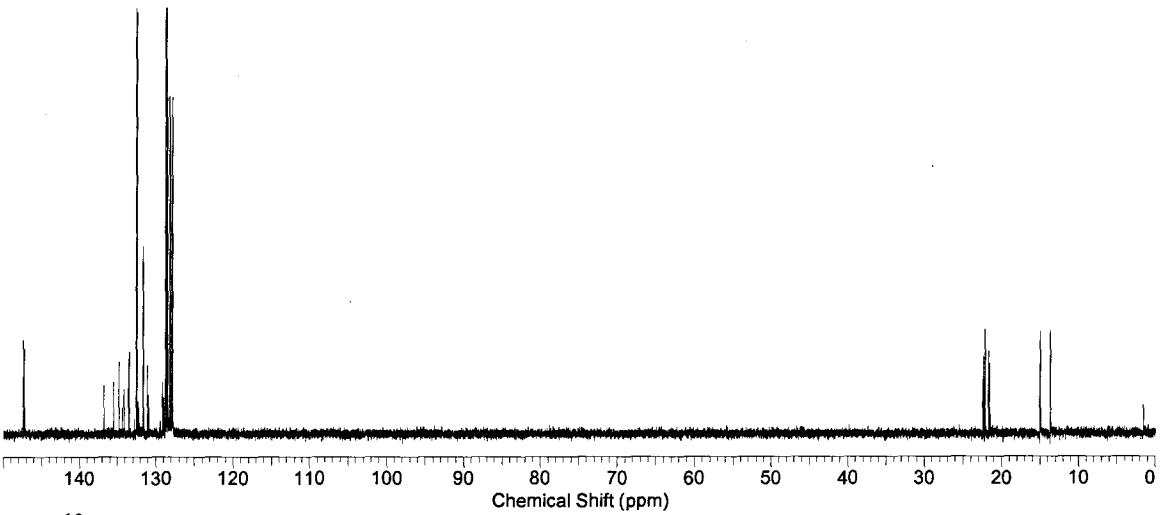


$^{13}$C NMR ($C_6D_6$, 75 MHz) spectrum of (*E*)-3-(diphenylphosphinyl)-3-hexene **11**

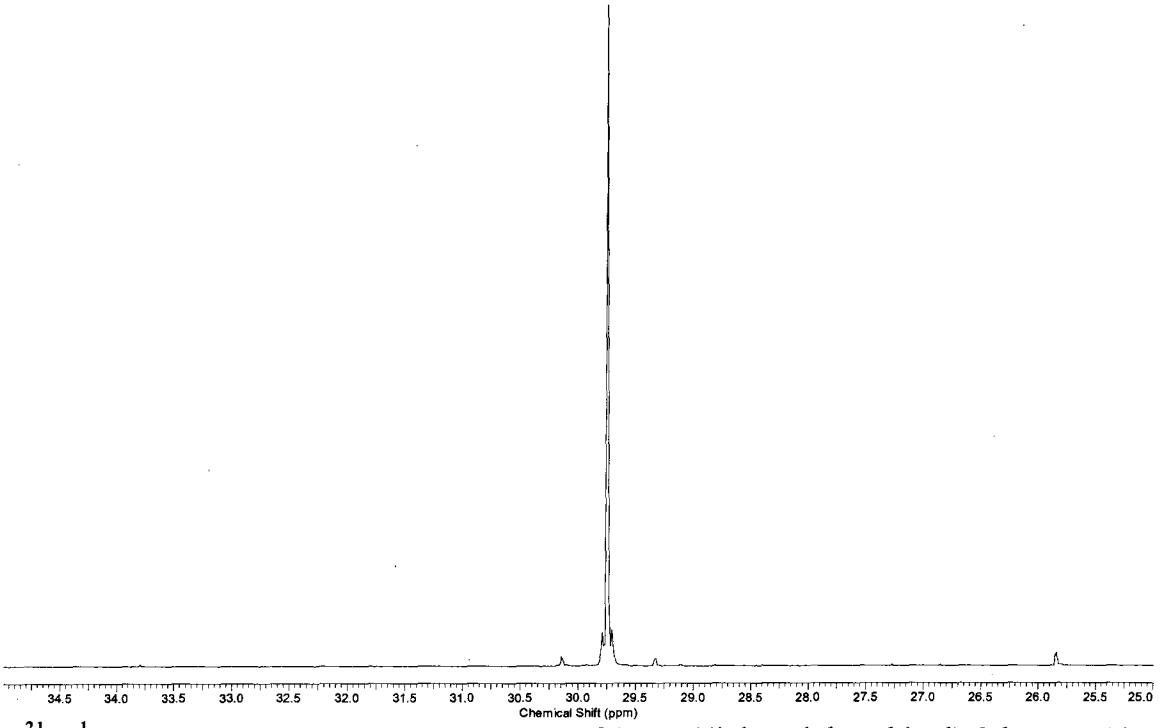


$^{31}P\{^{1}H\}$ NMR ($C_6D_6$, 121 MHz) spectrum of (*E*)-3-(diphenylphosphinyl)-3-hexene **11**

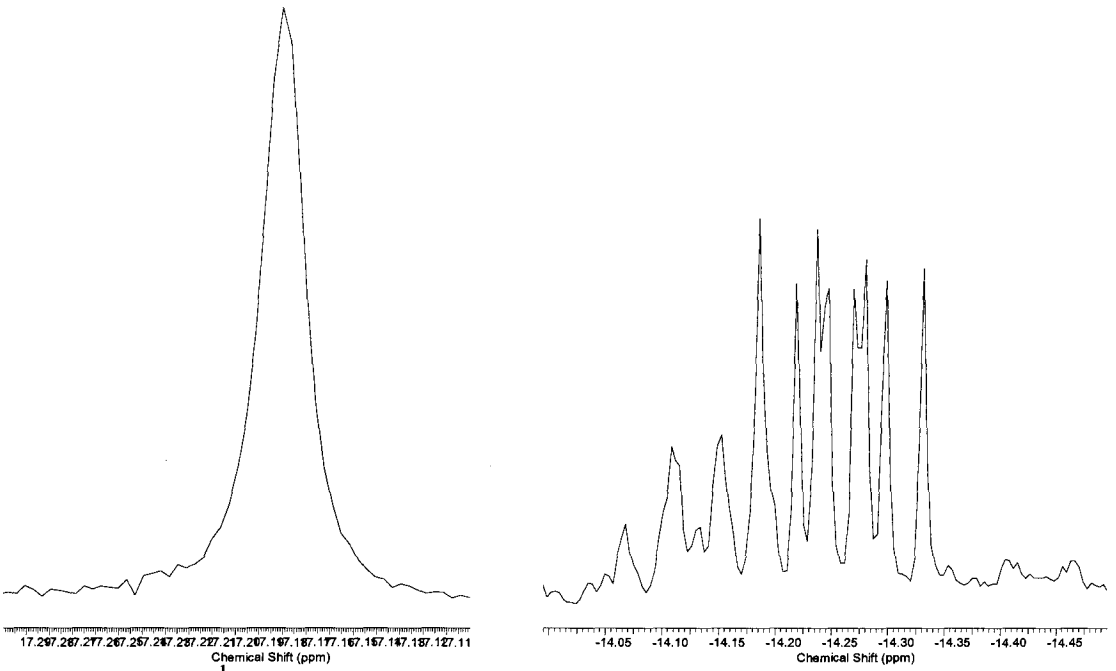


$^{1}H$ NMR ($C_6D_6$, 400 MHz) spectrum of complex **IX**

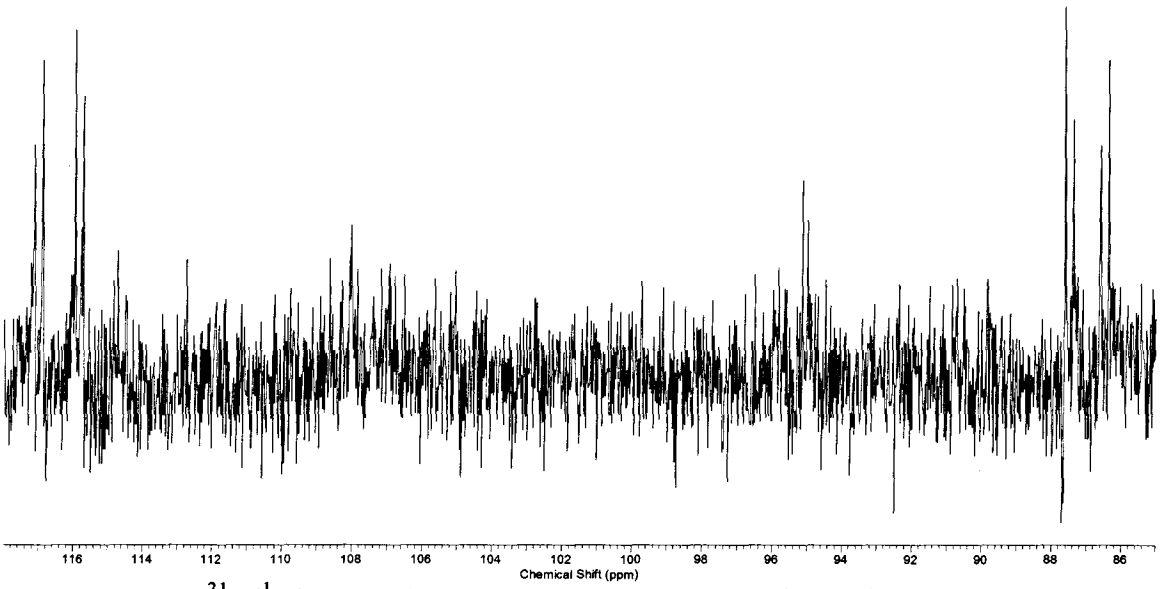


$^{31}P\{^{1}H\}$ NMR ($C_6D_6$, 162 MHz) spectrum of complex **IX**

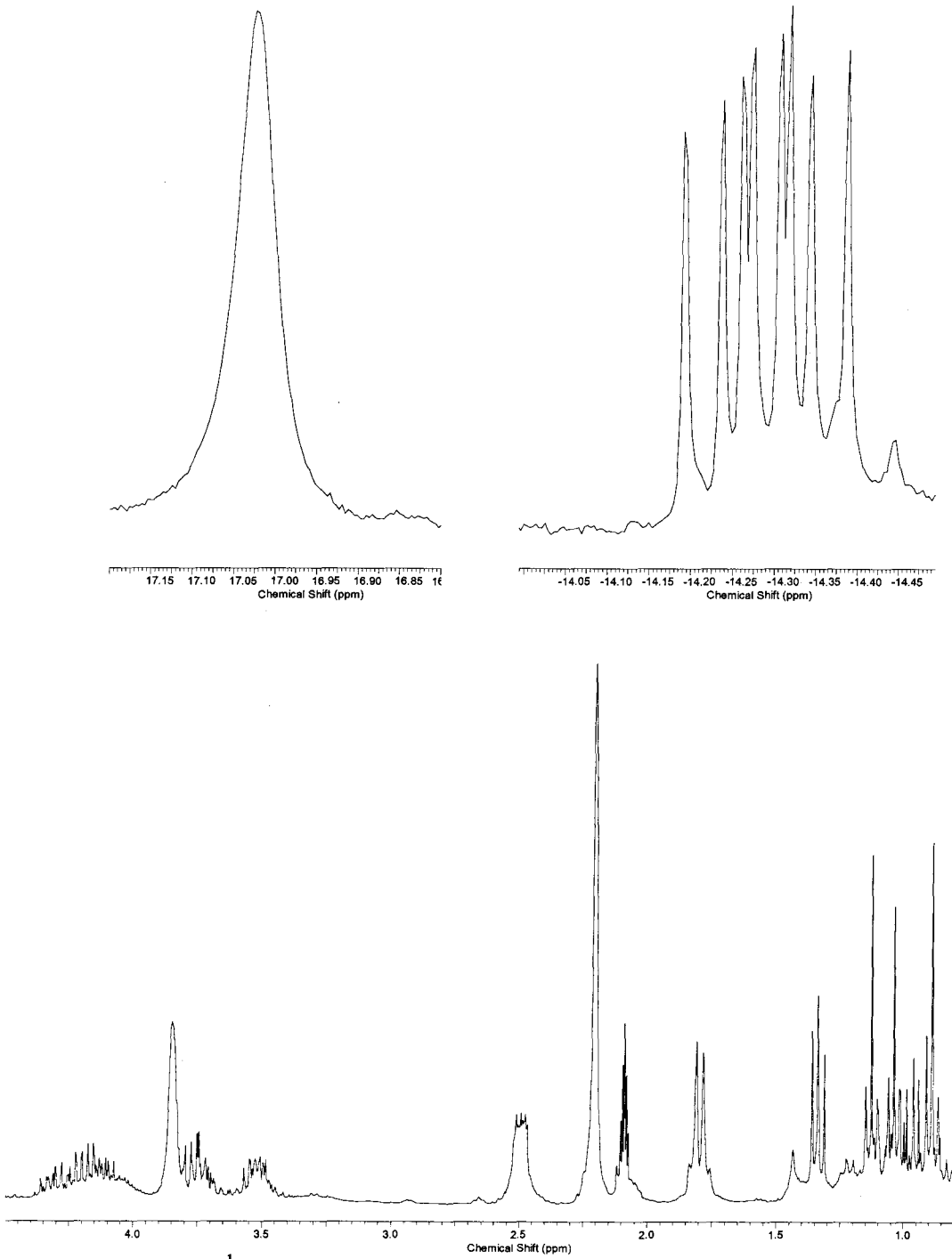


$^1$H NMR ($C_6D_6$, 400 MHz) spectrum of complex **X**

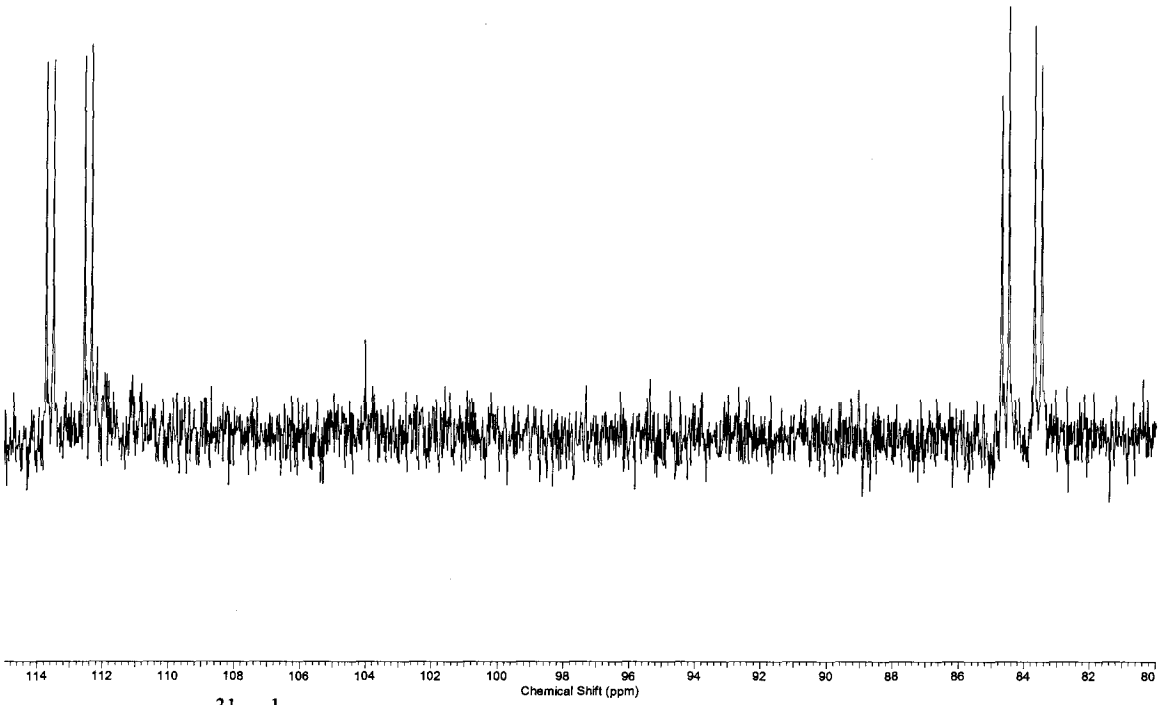


$^{31}P\{^{1}H\}$ NMR ($C_6D_6$, 162 MHz) spectrum of complex **X**

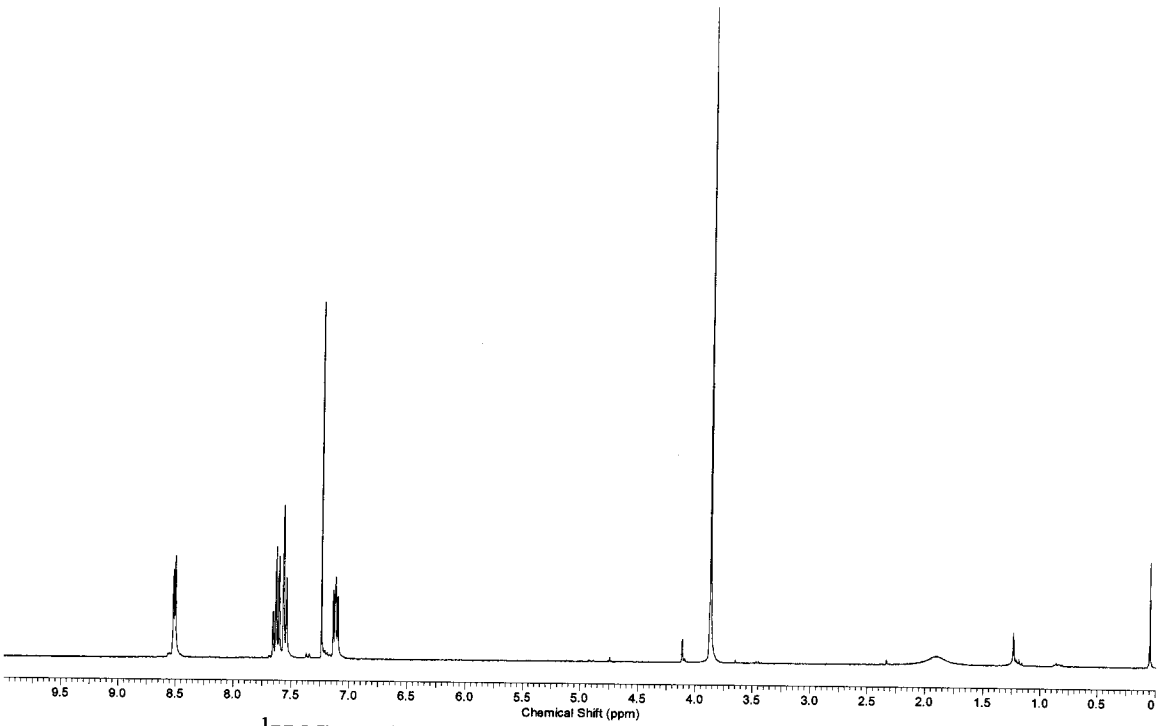


$^1$H NMR ($CDCl_3$, 300 MHz) spectrum of TPA **21**